Multipurpose Separation and Purification Facility

By

Reshan Sewnarain

[BSc. (Eng.)]
University of Natal, Durban

Submitted in fulfillment of the academic requirements for the degree of Master of Science in Engineering in the School of Chemical Engineering, University of Natal

Durban
2001

ABSTRACT

A waste acid stream is being produced by a local petrochemical company (SASOL) at a rate of 10 000 –12 000 tons per annum and contains approximately 44-mole % butyric acid, 20 % isobutyric acid and 10 % valeric acid. Whilst this stream is currently being incinerated, SASOL has requested an investigation into the possibility of separating and purifying butyric acid and isobutyric acid from this waste acid stream.

The goal of this project was to determine a separation and purification route for butyric acid and isobutyric acid from SASOL'S waste acid stream. In order to achieve this, vacuum distillation and freeze crystallization were chosen for the recovery and purification of the acids respectively.

Vapour-liquid equilibrium data for key component pairs present in the waste acid stream (propionic acid + butyric acid, isobutyric acid + butyric acid, butyric acid + isovaleric acid and butyric acid + hexanoic acid) were experimentally determined in a dynamic VLE still. The measured VLE data was successfully correlated using the gamma-phi approach, with the NRTL activity coefficient model representing the liquid phase and the virial equation of state describing the vapour phase. Using these equations, the VLE data obtained from the experimental work was then regressed to provide interaction coefficients for the NRTL model, which were then used in the *Hysys* process simulator to explore a range of design alternatives for distillation.

Hysys simulations showed that greater than 80 % butyric acid and isobutyric acid can be recovered from the waste acid stream in a single distillation column containing 18 theoretical stages and an optimum reflux ratio of 3.8. The simulation was performed at a pressure of 58kPa and a maximum operating temperature of 150^{0}C.

Batch distillation experiments performed in a batch rectification column at 250kPa recovered more than 90 % of both the butyric acid and isobutyric acid from a 450ml sample of the waste acid stream. A subsequent batch experiment concentrated the recovered acids into a distillate containing more than 95 % butyric acid and isobutyric acid combined.

To investigate freeze crystallization as a suitable operation for purifying butyric acid and isobutyric acid a solid-liquid phase equilibrium curve for the system was generated using the Van Hoft equation. The generated curve showed that butyric acid and isobutyric acid could be theoretically

purified (>98%) by operating two crystallizers at -20^{0}C and -55^{0}C respectively. A simple freeze crystallization experiment produced butyric acid with greater than 94% purity.

An economic feasibility study conducted on the process showed that separation and purification of the acids by this process (distillation and crystallization) could create a business opportunity with revenue of approximately R47 million per annum. Preliminary estimates for capital investment amounted to approximately R5.4 million, for which the payback period was estimated at less than one year.

PREFACE

The work presented in this thesis was performed at the University of Natal, Durban from January 2000 to December 2001. The work was supervised by Professor D Ramjugernath and Professor D.R Arnold.

This thesis is presented as full requirement for the degree M.Sc. in Chemical Engineering. All the work presented in this thesis is original unless otherwise stated and has not (in whole or part) been submitted previously to any tertiary institute as part of a degree.

_____

R.Sewnarain

As the candidate's supervisor I have approved this thesis for submission

Signed: _____

Name: _____

Date: _____

ACKNOWLEDGEMENTS

I would like to acknowledge the following people for their contribution to this work:

- My supervisors, Professor D. Ramjugernath and Professor D.R Arnold for guiding my research and myself over the past two years. Without their knowledge, help and ideas this project could not have been completed.

- Professor J.D Raal for his ideas and assistance in this project.

- Marc Joseph, Bava Pillay and Pierre Van Edeen from SASOL for the effort they put into this project.

- SASOL and DATACHEM (Raal and Ramjugernath) for financial support during my degree.

- My colleagues, Ezekiel, Kasuren, Tyrone, Daniel, Roland, Roger, Prathieka, Kleantha, Vernon, Randhir and Prathisha from the School of Chemical Engineering for their ideas and friendship.

- Devina Tashmira Gungadeen for love, encouragement and assistance.

- On a personal note, my family, Manilal, Ganga, Vishen, Ushen and Monica for years of support and motivation.

TABLE OF CONTENTS

Abstract i

Preface iii

Acknowledgements iv

List of Figures x

List of Tables xv

Nomenclature xvii

Chapter One **Introduction** 1

Chapter Two **Literature Review** 4

2.1 Characteristics of Separation Processes 4

2.1.1 Separation by phase addition or creation 5

2.1.2 Separation by barriers or fields 9

2.2 Chemistry of Carboxylic Acids 9

2.2.1 Synthesis of carboxylic acids 10

2.2.2 Properties of carboxylic acids 11

2.2.3 Reactions of carboxylic acids 12

2.3 Factors affecting the choice of separation processes 12

2.3.1 Feasibility 13

2.3.2 Scale of operation 13

2.3.3 Design reliability 14

2.3.4 Separation Factor 15

2.3.5 Number of steps required 16

2.3.6 Energy requirements 17

2.4 Selection of Separation Processes 17

2.4.1 Establishing feed and product conditions 18

2.4.2 Present day separation and purification processes for carboxylic acids 20

2.4.3 Property differences 20

2.4.4 Classification of unit operations 21

2.4.5 Selection of a base case 21

2.4.6 Process flowsheets 22

Chapter Three Vapour-Liquid Equilibrium 27

3.1 Relative Volatility **30**

3.2 Theoretical Aspects of VLE **33**

3.2.1 Evaluation of fugacity coefficients 34

3.2.2 Evaluation of activity coefficients 36

3.2.2.1 The NRTL model 37

3.2.2.2 The UNIFAC method 37

3.3 Equipment **38**

3.3.1 Vapour-liquid equilibrium still 40

3.3.2 Temperature and pressure measurement 42

3.3.3 Pressure control 42

3.3.4 Composition analysis 42

3.4 Experimental Procedure **43**

3.4.1 Detection of leaks 43

3.4.2 Pressure calibration 43

3.4.3 Temperature control 44

3.4.4 Calibration of gas chromatograph 44

3.4.5 Procedure for measurement of isobaric VLE data 47

TABLE OF CONTENTS

3.5	Experimental Results		48
3.6	Discussion		55
Chapter Four	**Distillation**		**62**
4.1	VLE Unit Diagrams		63
4.2	Numerical Short Cut Methods		66
4.3	Rigorous Distillation Calculations		69
4.4	*Hysys* Simulation		71
4.5	Simulation Results		72
4.6	Analysis of Simulation Results		74
Chapter Five	**Batch Distillation**		**80**
5.1	Experimental Set-up		81
	5.1.1	Batch distillation apparatus	82
	5.1.2	Temperature and pressure measurement	85
	5.1.3	Pressure control	85
	5.1.4	Composition analysis	85
5.2	Experimental Procedure		86
	5.2.1	Start-up	86
	5.2.2	Heating of the fluid in the reboiler	86
	5.2.3	Sampling and analysis	86
5.3	Results and Discussion		88

Chapter Six **Freeze Crystallization** 92

6.1 The Basis of Freeze Separation 93

6.2 Evaluating Freeze Crystallization as a Separation Operation 94

6.3 Solid-liquid Equilibria 96

6.4 Experimental Set-up and Procedure 99

6.5 Results and Discussion 100

Chapter Seven **Economic Feasibility** 103

7.1 Market Evaluation and Forecasting 103

7.2 Capital Cost Estimation 106

7.3 Operating Cost Estimation 107

7.4 Evaluation of Project Profitability 107

Chapter Eight **Conclusions and Recommendations** 109

References 112

APPENDIX A 121

A.1 Details of Sasol Solvents' Acid Recovery Plant 121

A.2 Physical properties of components present in waste acid stream 123

APPENDIX B 128

B.1 Criterion for phase equilibrium 128

B.2 Program for calculation of fugacity coefficients 130

B.3 The UNIFAC method 135

B.4 Calibration Curves 137

B.5 Thermodynamic consistency tests 142

APPENDIX C 145

C.1 Capital cost estimation 145

C.2 Operating cost estimation 147

C.3 Evaluation of project profitability 148

LIST OF FIGURES

Figure 2-1	Simple representation of a separation process	4
Figure 2-2	Reaction map for the synthesis of carboxylic acids	10
Figure 2-3	Carboxylic acids exist as monomers and dimers in the vapour phase	12
Figure 2-4	Flowsheet 1	24
Figure 2-5	Flowsheet 2	25
Figure 2-6	Flowsheet 3	25
Figure 2-7	Flowsheet obtained from *Hysys* simulation	26
Figure 3-1	Outline for starting distillation simulations	29
Figure 3-2	x-y diagrams for (a) concentration of more volatile component in liquid and (b) effect of relative volatility on the concentration of the more volatile component	31
Figure 3-3	T-x-y diagram	32
Figure 3-4	x-y curve for an azeotropic system	32
Figure 3-5	Schematic diagram of the VLE apparatus set-up	39
Figure 3-6	Dynamic VLE still of Raal (Raal & Mühlbauer [1998])	41
Figure 3-7	Gas chromatograph (Varian 3000) calibration for isobutyric acid (1) + butyric acid (2)	46
Figure 3-8	Gas chromatograph (Varian 3000) calibration for isobutyric acid (1) + butyric acid (2)	47

LIST OF FIGURES

Figure 3-9	x-y diagram for cyclohexane (1) + ethanol (2) at 40 kPa	49
Figure 3-10	T-x-y diagram for cyclohexane (1) + ethanol (2) at 40 kPa	49
Figure 3-11	x-y diagram for propionic acid (1) + butyric acid (2) at 14 kPa	51
Figure 3-12	T-x-y diagram for propionic acid (1) + butyric acid (2) at 14 kPa	51
Figure 3-13	x-y diagram for isobutyric acid (1) + butyric acid (2) at 14 kPa	52
Figure 3-14	T-x-y diagram for isobutyric acid (1) + butyric acid (2) at 14 kPa	52
Figure 3-15	x-y diagram for butyric acid (1) + isovaleric acid (2) at 14 kPa	53
Figure 3-16	T-x-y diagram for butyric acid (1) + isovaleric acid (2) at 14 kPa	53
Figure 3-17	x-y diagram for butyric acid (1) + hexanoic acid (2) at 14 kPa	54
Figure 3-18	T-x-y diagram for butyric acid (1) + hexanoic acid (2) at 14 kPa	54
Figure 3-19	Fit of NRTL model to x-y diagram of isobutyric acid (1) + butyric acid (2) at 14kPa	58
Figure 3-20	Fit of NRTL model to T-x-y diagram of isobutyric acid (1) + butyric acid (2) at 14kPa	58
Figure 3-21	Fit of NRTL model to x-y diagram of propionic acid (1) + butyric acid (2) at 14kPa	59
Figure 3-22	Fit of NRTL model to T-x-y diagram of propionic acid (1) + butyric acid (2) at 14kPa	59

Figure 3-23	Fit of NRTL model to x-y diagram of butyric acid (1) + isovaleric acid (2) at 14kPa	60
Figure 3-24	Fit of NRTL model to T-x-y diagram of butyric acid (1) + isovaleric acid (2) at 14kPa	60
Figure 3-25	Fit of NRTL model to x-y diagram of butyric acid (1) + hexanoic acid (2) at 14kPa	61
Figure 3-26	Fit of NRTL model to T-x-y diagram of butyric acid (1) + hexanoic acid (2) at 14kPa	61
Figure 4-1	Sketch of a typical distillation column	63
Figure 4-2	McCabe Thiele diagram for separation of isobutyric acid and butyric acid	65
Figure 4-3	Vapour composition profile of distillation column	73
Figure 4-4	Liquid composition profile of distillation column	73
Figure 4-5	Temperature profile for distillation column	77
Figure 4-6	VLE curve obtained by Hengstebeck's method	78
Figure 5-1	Experimental set-up for batch distillation	81
Figure 5-2	Batch distillation (a) simple distillation, (b) batch rectifier, (c) batch stripper, (d) middle vessel column	83
Figure 5-3	Batch distillation apparatus	84
Figure 5-4	Distillate composition profiles for batch distillation of waste acid stream – batch 1	90

Figure 5-5	Distillate composition profiles for batch distillation of waste acid stream – batch 2	91
Figure 6-1	Binary solid-liquid equilibrium diagram	93
Figure 6-2	Solid-liquid equilibrium curve for 1,3-xylene (1) + 1,2-xylene (2)	98
Figure 6-3	Experimental set-up for crystallization experiment	99
Figure 6-4	Solid-liquid equilibrium curve for ethylene glycol (1) + water (2)	100
Figure 6-5	Predicted solid-liquid equilibrium curve for isobutyric acid (1) + butyric acid (2)	100
Figure 7-1	U.S consumption figures for the acids for the past years	105
Figure A-1	Simplified flowsheet for acid recovery plant at Secunda	122
Figure B-1	Calibration curve for the Fischer pressure transducer	137
Figure B-2	PT-100 calibration	137
Figure B-3	Gas chromatograph (Shimadzu) calibration for cyclohexane (1) + ethanol (2)	138
Figure B-4	Gas chromatograph (Shimadzu) calibration for cyclohexane (1) + ethanol (2)	138
Figure B-5	Gas chromatograph (Varian 3000) calibration for propionic acid (1) + butyric acid (2)	139
Figure B-6	Gas chromatograph (Varian 3000) calibration for propionic acid (1) + butyric acid (2)	139

Figure B-7 Gas chromatograph (Varian 3000) calibration for butyric acid (1) + isovaleric acid (2) 140

Figure B-8 Gas chromatograph (Varian 3000) calibration for butyric acid (1) + isovaleric acid (2) 140

Figure B-9 Gas chromatograph (Varian 3000) calibration for butyric acid (1) + hexanoic acid (2) 141

Figure B-10 Gas chromatograph (Varian 3000) calibration for butyric acid (1) + hexanoic acid (2) 141

LIST OF TABLES

Table 2-1	Liquid separation processes	6
Table 2-2	Names of simplest carboxylic acids	10
Table 2-3	Technological maturity vs. use maturity	14
Table 2-4	Design reliability of separation processes and the need for pilot plant operation	15
Table 2-5	Details of waste acid stream as supplied by SASOL	19
Table 3-1	Gas chromatograph operating conditions	45
Table 3-2	Vapour-liquid equilibria for test system cyclohexane (1) + ethanol (2) at 40kPa	48
Table 3-3	Experimental vapour-liquid equilibrium data for the acids	50
Table 3-4	Refractive index and purity of chemicals	55
Table 3-5	Activity coefficient model parameters for NRTL equation and calculated RMS values for consistency test	56
Table 4-1	Results obtained by shortcut distillation using *Hysys*	68
Table 4-2	The eight basic methods for rigorous distillation calculations	70
Table 4-3	*Hysys* simulation results	72
Table 4-4	Feed and product flowrate for main components	72
Table 4-5	Volatility of main components	74

Table 4-6	Limiting compositions for nonkey components	76
Table 5-1	Gas chromatograph operating conditions	87
Table 5-2	Operating conditions for distillation of first batch	88
Table 5-3	Material balances for distillation of first batch	89
Table 5-4	Material balance for distillation of second batch	91
Table 6-1	Results of crystallization experiment	102
Table 7-1	Specifications for the production of butyric and isobutyric acids	104
Table 7-2	Production figures for butyric and isobutyric acids	104
Table A-1	Composition of waste acid stream	121
Table A-2	Properties of components present in waste acid stream	124
Table B-1	Consistency index for direct test of Van Ness [1995]	144
Table C-1	Costing of equipment using published equipment data	145
Table C-2	Estimation of fixed capital investment as suggested by Timmerhaus et al [1980]	146
Table C-3	Estimation of operating cost as suggested by Brennan [1998]	147
Table C-4	Cash flow statement	148

NOMENCLATURE[a]

f	Fugacity
H_3O^+	Acidic solution
L	Liquid flowrate
P	Pressure
P_c	Critical pressure (bar)
P_i^{sat}	Saturated vapour pressure of component i
R	Universal gas constant (8.314 J/mol. K)
T	Temperature
T_c	Critical temperature
V	Vapour phase
V_c	Critical volume (cm^3/mol)
x	Liquid mole fraction
y	Vapour mole fraction
ϕ	Fugacity coefficient
δ_{ij}	Term used in equation 3-11
τ_{ij}	Term used in equation 3-14
G_{ij}	Term used in equation 3-15

Abbreviations

calc.	Calculated
C_3	Propionic acid
C_4	Butyric acid
C_5	Valeric acid
C_6	Hexanoic acid (Carboxylic acids containing 6 carbon atoms)
C_7	Heptanoic acid
C_{20}	Carboxylic acids containing 20 carbon atoms
exp.	Experimental
i-C_4	Isobutyric acid
i-C_5	Isovaleric acid

[a] All equations and variables are in SI units unless otherwise stated.

IUPAC	International Union of Pure and Applied Chemistry
$KMnO_4$	Potassium permanganate
LLE	Liquid-liquid extraction
NaCN	Sodium cyanide
n-C_4	Butyric acid
n-C_3	Propionic acid
n-C_5	Valeric acid
n-C_6	Hexanoic acid
n-C_7	Heptanoic acid
SS	Stainless steel
tpa	Tons per annum
VLE	Vapour-liquid equilibria

Subscripts

1	component 1
2	component 2
i	component *i*
j	component *j*
ij	component *i* relative to component *j*
ji	component *j* relative to component *i*
B	Bottoms flow
D	Distillate flow
F	Feed flow
HK	Heavy key component
LK	Light key component

Superscripts

F	"Free" contribution to second virial coefficient
D	Dimerization contribution to second virial coefficient

CHAPTER ONE

INTRODUCTION

The fact that naturally occurring processes are inherently mixing processes has been recognized over a hundred years, and has led to the reverse procedure of "unmixing" or separation processes becoming one of the most challenging categories of engineering problems (King [1971]).

The application of separation processes in the chemical industry is becoming increasingly important. This is especially so in the chemical industry, where waste streams containing valuable chemicals are produced during the production of high value products. For pollution control purposes recovery of the valuable products from waste streams is becoming increasingly favored over incineration of the waste streams because of the expense of the added fuel required for incineration.

A local petrochemical company, SASOL (South African Coal & Oil Limited) is currently producing a waste acid stream, which is formed during the production of high value petroleum products. This stream, emanating from SASOL Solvents' acid recovery plant, is produced at a rate of 10 000-12 000 tons per annum and contains approximately 44% butyric acid, 20% isobutyric acid and 10% valeric acid on a molar basis. Whilst the stream is presently being incinerated, SASOL has requested an investigation into the possibility of separating and purifying the acids. This will in turn benefit SASOL by:

- Adding value to this waste stream
- Freeing up capacity in the existing acid recovery incinerator
- Reducing the company's environmental emissions

The above mentioned acids have many uses either directly (e.g. butyric acid in plastics) or indirectly for the intermediate uses of their numerous derivatives (e.g. butyl acetate in perfumes). Currently butyric acid, isobutyric acid and valeric acid are being globally traded at R9.80 per kg, R16.70 per kg and R11.29 per kg respectively (Bizzari et al [1999]). Based on these prices and 80% of extractable volumes from the waste acid stream, separation and purification of these acids could create a business opportunity with revenue of approximately R80 million per annum. However, due to the small volume nature of the project, Sasol has earmarked this project as potential for a small entrepreneurial business to process the stream.

The investigation into the possibility of separating and purifying the acids was given to the University of Natal's School of Chemical Engineering and was undertaken as a research topic towards an MSc degree. This project involved the following objectives:

- Perform an extensive literature survey on the components present in the waste acid stream and together with reviewing separation processes select a separation and purification route for the valuable acids.
- Undertake an economic study of the selected separation and purification route.

Most recovery processes begin with the collection of the valuable components from waste processing operations. Following collection, purification of the valuable components takes place. For this project distillation was selected for recovery of the valuable acids and crystallization was chosen for purifying the acids.

A flowsheeting program (*Hysys*) was used to simulate the distillation process for the recovery of the valuable acids from the waste acid stream. In screening distillation as a separation process for recovery of the acids, vapour-liquid equilibrium (VLE) data of the components present in the waste acid stream was required. This is because the most uncertainties in distillation applications generally arise from uncertainties in the vapour-liquid equilibrium data. Due to the scarcity of experimental VLE data in literature and the failure of the process simulator to correctly predict VLE data for the components present in the waste acid stream, VLE data for key component pairs present in the waste acid stream were measured using a dynamic VLE still developed by Raal (Raal & Mühlbauer [1998]). The measured data was then regressed to provide binary interaction coefficients for correlating models, which was then used in the process simulator to accurately predict the VLE data and explore a range of design alternatives.

After process simulation showed that recovery of the acids is possible, laboratory scale batch distillation tests were conducted on an actual sample of the waste acid stream to confirm that recovery of the valuable acids is possible.

For purification of butyric acid and isobutyric acid freeze crystallization was screened as a suitable operation. This involved conducting simple freeze crystallization laboratory tests to determine if the butyric acid and isobutyric acid could be separated from each other and thus purified.

Finally, an economic study of the selected separation and purification route (distillation and crystallization) was undertaken to determine the economic feasibility of the process.

CHAPTER
TWO

LITERATURE REVIEW

The separation of a mixture into its constituent chemical species is a non-spontaneous process, which requires an expenditure of energy. Much attention has been devoted to understanding separation processes including the characteristics and selection of separation processes. As the majority of the waste acid stream constitutes carboxylic acids, the chemistry of these acids is also reviewed.

2.1 Characteristics of separation processes

A simple representation of a separation process is shown below.

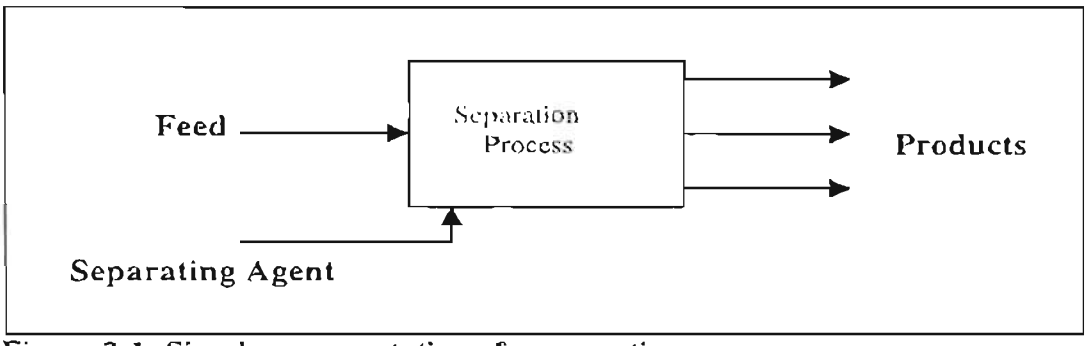

Figure 2-1: Simple representation of a separation process.

The feed may consist of one stream of matter, or of several streams. There must be at least two product streams, which are different in composition with respect to one another. Separation occurs by the addition of a separating agent, which can take the form of another stream of matter, or of

energy. This in turn forces the different chemical components of the feed into different spatial locations. Separation operations can be divided into two broad categories:

- Separation by phase addition or creation
- Separation by barrier or fields

Table 2-1 is a compilation of individual separation operations adopted from the five general separation techniques given by Seader & Henley [1998]. Only separation processes using liquid or vapour feed are considered in this project because of the nature of the feed stream. Although Table 2-1 may not include the latest technologies it does provide a range of alternatives.

To follow is a brief review of each of these techniques. The reader is referred to the excellent text of Seader & Henley [1998] for a detailed discussion on each of the techniques and individual operations.

2.1.1 Separation by phase addition or creation

The most common industrial technique involves the separation of a homogeneous single-phase solution (gas, liquid or solid) by the creation or addition of a second phase that is immiscible with the feed phase. This second phase can be created by an energy separating agent or a mass separating agent.

The energy-separating agent is in the form of energy (heat, shaft work or pressure reduction). Examples of processes using energy separating agents include distillation, evaporation and crystallization.

The mass separating agent takes the form of a second phase like a solvent that selectively dissolves some of the components in the feed. Examples include liquid-liquid extraction, absorption and stripping.

The mass separating agent may also be completely miscible with the mixture but may selectively alter species volatilities resulting in greater separation between certain species when used in conjunction with an energy separating agent, as in extractive distillation.

Table 2-1: Liquid Separation Processes

Name	Feed Phase	Separating Agent	Product Phases	Principles of Separation Process
a) Separation by Phase Addition or Creation				
1. Distillation	Liquid/Vapour	Heat	Liquid & Vapor	Difference in volatilities
2. Extractive Distillation	Liquid/Vapour	Liquid Solvent and Heat	Liquid & Vapor	Mass separating Agent increases volatility.
3. Liquid-liquid Extraction	Liquid	Immiscible Liquid	Two Liquids	Different Solubilities of different species in the two liquid phases.
4. Crystallization	Liquid	Cooling	Liquid & Solids	Difference in freezing tendencies.
5. Clathration ***	Liquid	Clathrating molecule and cooling	Liquid & Solid	Preferential participation in crystal structure.
6. Desublimation *	Vapour	Cooling	Solid & Vapor	Preferential Condensation
7. Foam Fractionation *, ***	Liquid	Rising air bubbles or complexing surfactants	Two liquids	Tendency of surfactant molecules to accumulate at gas-liquid interface and rise with air bubbles.
8. Reaction Distillation	Liquid	Heat + Reaction	Liquid	Difference in Volatilities

Table 2-1 ...continued

Name	Feed Phase	Separating Agent	Product Phases	Principles of Separation Process
b) Separation Operations Based on a Solid Agent				
9. Ion Exchange **	Liquid	Solid Resin	Liquid + Solid	Law of mass action applied to available anions and cations.
10. Adsorption **	Liquid	Solid Adsorbent	Fluid and Solid	Difference in adsorption potentials
11. Gel Filtration *, **	Liquid	Solid Gel	Gel phase + Liquid	Difference in molecular size and hence ability to penetrate swollen gel matrix.
12. Chromatography *, **	Liquid/Vapour	Solid or liquid adsorbent	Liquid + vapour	Preferential adsorption and desorption of species
c) Barrier Separations				
13. Osmosis **	Liquid	Non-porous membrane	Two liquids	Tendency to achieve uniform osmotic pressure
14. Ultrafiltration **	Liquid	Membrane	Two liquid phases	Different permeabilities
15. Dialysis **	Liquid	Selective Membrane	Liquids	Different rates of diffusional transport through membrane.
16. Liquid Membrane **	Liquid / Vapor	Liquid membrane with pressure gradient	Liquid / Vapor	Different combined solubilities and diffusivities of species in membrane.

Table 2-1 ...continued

Name	Feed Phase	Separating Agent	Product Phases	Principles of Separation Process
d) Separation Operations by Applied Field or Gradient				
17. Electrophoresis *	Liquid	Electric field	Two liquids	Different ionic mobilities of colloids
18. Electrolysis ***	Liquid	Electrical Energy	Liquids	Different rates of discharge of ions at electrode.
19. Electrodialysis ***	Liquid	Anionic and Cationic Membranes + Elecctric fields	Liquids	Tendency of anionic membranes to pass only anions etc.

Notes

* Small scale separation processes

** Separation processes that are generraly used to separate components present in dilute concentrations

*** Separation processes that cannot be readily designed from a mathematical model and/or scaled up from laboratory data

Another form, which a mass separating agent may take, is that of a solid agent. Examples of processes using solids as mass separating agents are ion exchange and gel filtration.

2.1.2 Separation by barriers or fields

The separation operations discussed in the previous section involved the addition or creation of another phase by the addition of an energy separating agent or a mass separating agent. Although these operations are more commonly applied in industrial applications, alternatives to the energy-intensive or material-intensive operations have been developed. Methods of accomplishing these separations are based on the application of barriers or fields to cause different components to diffuse at different velocities.

In barrier separation processes the separating agent takes the form of a barrier that restricts or enhances the movement of certain chemical components with respect to others. These types of separation processes are becoming increasingly common in industry due to an increase in the need for environmental protection from harmful industrial emissions. However they are limited to the removal of components present only in low concentrations. Examples of such processes include osmosis, ultrafiltration and dialysis.

Finally, processes such as electrolysis, which use external fields as separating agents to take advantage of the differing degrees of response of molecules and ions to forces and gradients.

2.2 Chemistry of carboxylic acids

Carboxylic acids are named systematically from their corresponding alkanes by changing the ending -ane to -oic acid. Methane thus gives rise to methanoic acid (HCOOH), while ethane gives rise to ethanoic acid. Many carboxylic acids (especially those containing six or fewer carbons) have been known for a long time and are commonly named after their sources rather than their chemical structures. For example: formic acid refers to the Latin for ant; acetic to wine; butyric to rancid butter, and caproic to goat fat. Common names for some of the simplest carboxylic acids (most of which are present in the waste acid stream) are given in Table 2-2 below. Isomers of carboxylic acids also exist and the isomers that are present in the waste acid stream are also shown in Table 2-2.

Table 2-2: Names of the simplest carboxylic acids

Common Name	IUPAC Name	Chemical Structure
Formic Acid	Methanoic Acid	HCOOH
Acetic Acid	Ethanoic Acid	CH_3COOH
Propionic Acid	Propanoic Acid	CH_3CH_2COOH
Isobutyric Acid	3-Methyl-Propionic Acid	$(CH_3)_2CHCOOH$
Butyric Acid	Butanoic Acid	$CH_3(CH_2)_2COOH$
Isovaleric Acid	3-Methyl-Butanoic Acid	$(CH_3)_2CH_2CHCOOH$
Valeric Acid	Pentanoic Acid	$CH_3(CH_2)_3COOH$
Caproic Acid	Hexanoic Acid	$CH_3(CH_2)_4COOH$
Enanthic Acid	Heptanoic Acid	$CH_3(CH_2)_5COOH$

2.2.1 Synthesis of carboxylic acids

Carboxylic acids can be prepared in the laboratory by several routes as shown in Figure 2-2.

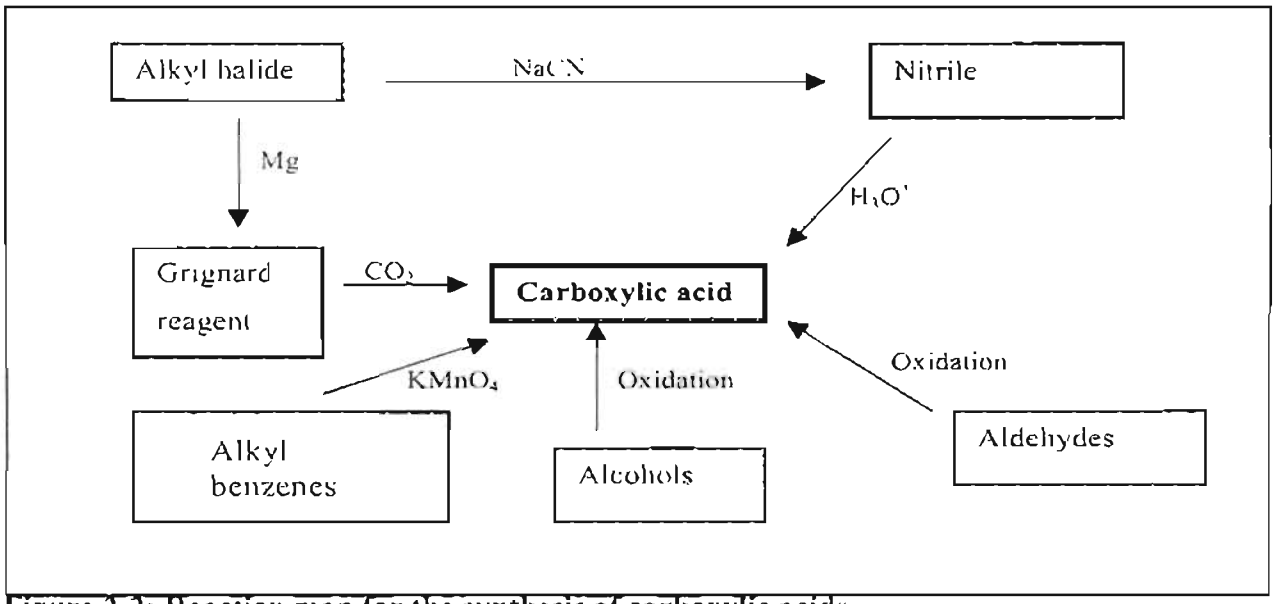

Figure 2-2: Reaction map for the synthesis of carboxylic acids.

Perhaps the most important reaction in Figure 2-2, is the oxidation of aldehydes to form carboxylic acids. This reaction is of importance as most carboxylic acids (especially butyric acid, isobutyric acid and valeric acid) are currently being produced via this reaction in industry. Butyric acid,

isobutyric acid and valeric acid are produced by the oxidation of n-butyraldehyde, iso-butyraldehyde and n-valeradehyde respectively.

2.2.2 Properties of carboxylic acids

The most important property of carboxylic acids, and the one that is responsible for naming them such, is their acidity. Carboxylic acids are able to donate a proton more readily than most other classes of organic compounds, so they are said to be stronger acids, even though they are much weaker than the most important mineral acids (sulphuric acid, nitric acid, and hydrochloric acid).

The first members of the carboxylic acid series are colorless liquids. The carboxylic acids with carbons 4 - 6 have very unpleasant odors (e.g. rancid butter, old used socks etc), and the higher carboxylic acids have little odor due to their low volatility.

The solubility of carboxylic acids in water is similar to that of alcohols, aldehydes, and ketones of the same number of carbon atoms. Acids with fewer than five carbon atoms dissolve in water: those with a higher molecular weight are insoluble owing to the larger alkyl portion, which is hydrophobic. Aqueous hydroxides readily convert carboxylic acids into their salts and aqueous mineral acids readily convert the salts back into the carboxylic acids. The sodium, ammonium, and potassium salts of the acids are generally quite soluble in water but insoluble in non-polar solvents. Thus, almost any carboxylic acid can be made to dissolve in water by converting it to such a salt.

Carboxylic acids are polar. Like alcohols, they form hydrogen bonds with themselves or with other molecules. Carboxylic acids have much higher boiling points than hydrocarbons, alcohols, ethers, aldehydes, or ketones of the same carbon number. They have higher boiling points than comparable alcohols. This is because two molecules of a carboxylic acid form two hydrogen bonds with each other. The two molecules can interact via a "head to tail" hydrogen bonding scheme in the vapour phase as shown in Figure 2-3. Thus, carboxylic acids exist as dimers (pairs of molecules) or trimers and boiling a carboxylic acid requires the addition of more heat than boiling the corresponding alcohol, because:

(1) if the dimer or trimer persists in the vapour state, the molecular weight is in effect doubled: and,
(2) if the dimer or trimer is broken upon boiling, extra energy is required to break the hydrogen bonds.

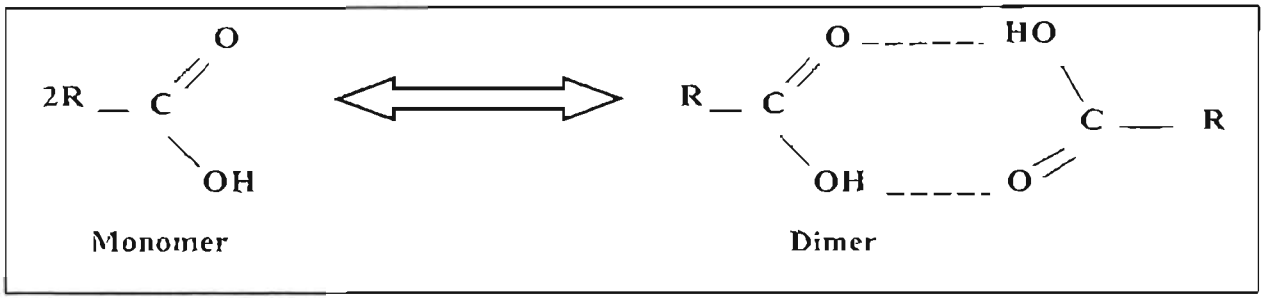

Figure 2-3: Carboxylic acids exist as a monomers and dimers in the vapour phase

2.2.3 Reactions of carboxylic acids

An extension of the property of carboxylic acid acidity is that they react with strong bases such as sodium hydroxide or potassium hydroxide to give water-soluble salts. They also react with ammonia to give ammonium salts. Thionyl chloride ($SOCl_2$) converts a carboxylic acid to a more reactive acyl halide by replacing the hydroxyl group with a chloride group. Carboxylic acids are also reduced by lithium tetrahydridoaluminate ($LiAlH_4$) to form alcohols.

Perhaps the most useful reaction of carboxylic acids in industry is the Fischer Esterification reaction. When a carboxylic acid is heated with an alcohol in the presence of a catalyst (usually hydrogen chloride or sulphuric acid), an equilibrium is established with the ester and water. This process is called Fischer Esterification. Although the reaction is an equilibrium, it can be used to make esters in high yield by shifting the equilibrium to the right. This can be easily accomplished by distilling the esters off as they form. This is because esters are much more volatile than the other compounds, and especially more volatile than the carboxylic acids.

2.3 Factors affecting the choice of a separation process

In this section, a brief review on the various major factors that should be considered when selecting a separation process for a particular application. Factors such as feed conditions also should be considered in process selection but this is discussed in Section 2-4. Much of the material in this section follows from the comprehensive presentations given by King [1971], Null [1987] and Seader & Henley [1998].

2.3.1 Feasibility

The most important consideration in choosing a separation process for any particular application is that the separation process must achieve the desired result. A large amount of screening for possible separation processes can be achieved by considering feasibility alone. As an example, King [1971] shows how the separation of two nonionic components (acetone and diethyl ether) cannot be achieved by ion exchange or electrophoresis due to the absence of anions or cations. Also, since these molecules do not differ enough in surface activity, processes such as foam or bubble fractionation can be immediately eliminated. However this method of elimination becomes increasingly difficult when the number of components being considered increases. For multi-component mixtures hybrid processes that use a combination of different processes have been suggested. Generally, for a mixture containing N components, N-1 process operations are required to isolate the N components. The problem then becomes which of the N components is to be separated first. Many authors including Seader & Westerberg [1977], Nath & Motard [1981] and most recently Nadgir & Liu [1983] discuss the generation of separation sequences. Each of the authors proposes slightly different heuristic rules for separation sequencing. This will not be discussed here, however the general rule is to perform the most difficult separations first or to remove the most plentiful components first.

2.3.2 Scale of operation

In many cases, the scale of operation is the main factor in choosing between alternative separation processes. Nowadays most mixtures are separated and analysed in laboratories by chemists using chromatographic separations. However, in large manufacturing plants chemical engineers use other separation processes such as distillation to achieve the same separation. Null [1987] further illustrates this point by showing how air separations on a very large scale are accomplished more economically by cryogenic separations whilst small scale air separations are accomplished more economically by other means such as pressure swing adsorption or hollow- fiber gas separation membranes.

2.3.3 Design reliability

Perhaps the most important factor in choosing one process in preference to the other is design reliability (Null [1987]). Above all considerations, the selected process must work when the plant is built. Also capital requirements are indirectly affected by design reliability in that larger safety factors are applied when the design methods are less reliable. A study by Keller [1987], shown in Table 2-3, reveals that the degree to which a separation is technologically mature correlates well with its commercial use. Table 2-4 lists a few separation processes together with their design reliability to illustrate this point. The need for pilot-plant operation is also considered for each operation.

Table 2-3: Technological maturity vs. use maturity

Process	Technological Maturity *	Use Maturity*
Distillation	87	87
Extractive Distillation	80	65
Solvent Extraction	73	61
Adsorption: Liquid Feed	50	40
Ion Exchange	60	60
Membranes: Liquid Feed	37	30
Chromatography	30	22
Crystallization	64	62
Field Induced Separations	24	13

* A score of 100 denotes that a given process has reached an asymptote

Table 2-4: Design reliability of separation processes and the need for pilot plant operation

Separation Method	Design reliability	Need for pilot plant
1. Distillation	Process can be reliably designed with the pertinent physical properties and VLE data	Occasionally required
2. Extraction	Process can be designed with the pertinent physical properties and phase-equilibrium relationships. However process design not as reliable as distillation.	Pilot plant recommended
3. Crystallization	Poor design reliability-process cannot be designed without bench-scale experiments.	Always necessary
4. Adsorption	Adsorption equipment can be reliably designed with properly measured isotherm data and mass transfer coefficients.	Occasionally required
5. Reverse osmosis	Poor design reliability	Always necessary
6. Ultrafiltration	Extensive testing required due to poor design reliability	Always necessary
7. Ion exchange	Process can be designed with a few laboratory tests	Always necessary

2.3.4 Separation Factor

Many indices are available to characterize separation power and to evaluate and compare the outcome of various separation processes. The separation of two components (*i* and *j*) is readily achievable if:

1. The concentration, c_i^{β} of component *i* in its preferred phase or region β well exceeds its concentration c_i^{π} in phase π, i.e. $c_i^{\beta} / c_i^{\pi} >> 1$
2. Component j partitions itself preferentially in phase π so that $c_i^{\beta} / c_i^{\pi} << 1$.

For separation processes the ratio $\alpha_{ij}^{'}$, which is referred to as the separation factor, must be much greater than unity for an effective separation to occur. The separation factor is defined as:

$$\alpha_{ij}^{'} = \frac{c_i^{\beta} / c_i^{\pi}}{c_j^{\beta} / c_j^{\pi}} \qquad (2\text{-}1)$$

Qualitatively, the separation factor is a measure of the extent of segregation of components between two phases (e.g. liquid-liquid extraction), regions (e.g. either side of a membrane filter), or product streams (e.g. distillation). For a single separation step or stage, the separation factor must be large for an effective separation. For certain multistage separation processes, a separation factor close to unity (e.g. $\alpha_{ij}^{'}$ = 1.3) in one stage can often be effectively increased by linking stages in series to achieve high separation levels in the product.

2.3.5 Number of steps required

Another important factor that affects the choice of a separation process is the number of processing steps required to accomplish the desired separation. An increase in the number of processing steps ultimately leads to an increase in the capital and operating expenses of the plant. However, this is not entirely true, as there are situations where it is more economical to install a separation sequence consisting of two or more steps in preference to a single-step process. A specific example is heavy water separation, which can be accomplished in a single distillation column with many stages and a very high reflux ratio but is accomplished more economically in a multicolumn chemical-exchange process involving hydrogen sulphide (Null [1987]). In most cases though, single-step processes are more economical than multi-step processes. To follow is a discussion on a few separation processes and their ability to accomplish complete separation in a single step.

- Distillation- Except for binary azeotropic mixtures, complete separation of most binary mixtures can be achieved in a single distillation column.
- Extraction- A second step is always required to separate the extracted component from the extracting solvent. Therefore, more than one step is always required for extraction processes.
- Crystallization- For those binary mixtures exhibiting no eutectic formation it is possible to separate the components in a single step. In most cases, however, a eutectic point is present and

a second step is required to break the eutectic. In melt crystallization a wash and filtration step is also required to remove occluded liquid from the pure solid.

- Adsorption- A regeneration step is always necessary to recover absorbed material.
- Reverse osmosis- Additional processing steps are required to obtain high recovery of solvent.
- Ultrafiltration- To obtain pure products additional processing steps are also required.
- Ion exchange- A regeneration step is required to recover the product and to reuse the bed.
- Dialysis and electrodialysis- If the transferred components are required in pure form, additional processing steps are required.

2.3.6 Energy requirements

Energy requirements of most separation processes generally contribute to most of the operating costs of a plant. Therefore, this factor must always be considered in choosing a separation process. It is very difficult to qualitatively discuss the energy requirements of the various separation processes as the energy requirements are dependent on many other factors and therefore require a thorough treatment. Nevertheless, Null [1980] suggests that barrier separations have a lower energy requirement than most other separation processes. However, barrier separations are limited to modest concentrations of very dilute solutions. Null [1980] also suggests that operations such as crystallization and extraction require less energy than distillation processes, which may require high reflux ratios. The reader is referred to the texts of King [1971] and Rousseau [1987] for a detailed discussion on the energy requirements of various separation processes.

2.4 Selection of separation processes

There is no established procedure by which separation processes are chosen (Null [1987]). However, there are certain guidelines, which assist in choosing a separation process for different applications. The selection of a separation and purification route depends on many factors, although the ultimate factor is based on economics. Selecting an optimum separation scheme also depends on the time and money allocated for process selection and analysis.

The steps taken in deciding which separation process would be suitable for the recovery and purification of the valuable acids will now be discussed.

2.4.1 Establishing feed and product conditions

The first step in the selection of a separation process is to establish the feed conditions, product recoveries and product purities. These conditions collectively define the separation problem.

For this project establishing the feed conditions involved identification of the various components of the waste acid stream and the temperature, pressure, flow rate and phase state of the waste stream. Details of these conditions were supplied by SASOL and are shown in Table 2-5. The most important feed conditions are composition and flow rate, because the other conditions (temperature, pressure and phase state) can be altered by pumps, compressors and heat exchangers. However this will add further costs to separation. From Table 2-5, it is evident that the bulk of the waste stream (feed mixture) consists of carboxylic acids containing between two carbon atoms (CH_3COOH-acetic acid) to seven carbon atoms ($CH_3(CH_2)_5COOH$-heptanoic acid). These acids make up 94.3% of the waste stream, with 2-cyclohexene-1-one and 4 butyrolactone being the only other components of note (i.e. > 1%).

A simplified flowsheet of the Solvents acid recovery plant at SASOL'S plant in Secunda is shown in Figure A-1 of the appendix. The waste acid stream being considered in this project emanates from the heavies column at a rate of 10 000-12 000 tons per annum. It is important to note that the composition of the acid water stream entering the Solvents acid recovery plant may fluctuate and therefore the compositions of the waste acid stream may also fluctuate. However, only the compositions given in Table 2-5 were used for design purposes.

Table 2-5: Details of waste acid stream as supplied by SASOL

Temperature : 179.1 °C
Pressure : 58.0 kPa (gauge)
Phase State : Liquid

Component Name (other name)	Flow (kg/h)	mol %
1.Butyric Acid	495.016	43.9
2.Iso-butyric acid	224.656	19.9
3.iso-Valeric Acid (3-methyl-butyric acid)	135.158	10.3
4. Valeric Acid (Pentanoic Acid)	135.158	10.3
5. Hexanoic Acid	67.079	4.5
6. Heptanoic acid	54.002	3.2
7. 2-cyclohexen.. 1-one	27.693	2.2
8. Propionic Acid	18.986	2
9. 4 Butyrolactone	13.616	1.2
10. Phenyl Acetate	12.154	0.7
11.Phenyl propionate (3-phenyl propionic acid)	9.693	0.5
12. 3-heptene-2-one trans	6.308.	0.4
13. Phenyl butyrate (3-phenyl butyric acid)	5.846	0.3
14. Cyclopentyl Acetae (Cyclopentanol acetate)	3.385	0.2
15. Cyclohexyl Acetate	3.385	0.2
16. Cyclopentanone	0.027	0.002486
17. Acetic acid	0.002	0.0003
18. 1M-2EBenzene	0.002	0.00012
Total Flow	**1212.165 kg/hr.**	

The most important product condition is the required product purity. The other conditions (e.g. phase state) can be altered once the desired separation has been successfully accomplished. When very pure products are required, either large differences in certain properties must exist or many stages must be used.

The valuable acids (butyric acid, isobutyric acid and valeric acid) were stipulated to be recovered with 80% extractable volumes and purities greater than 99%. These high purities are required for the use of the acids in food additives and pharmaceuticals. The acids are also stable liquids at atmospheric conditions.

Another important consideration of the project is that the selected separation and purification process should be flexible so that the techniques can be applied to the separation and purification of similar or related feed streams.

2.4.2 Present day separation and purification processes for carboxylic acids

An extensive literature survey was conducted on existing industrial separation processes that separate and purify carboxylic acids. All processes found involved the recovery of carboxylic acids present only in dilute concentrations. One example is the recovery of carboxylic acids with amine extractants. The process was developed by Kertes & King [1986]. Presently no process exists for the separation and purification of carboxylic acids (particularly those present in the waste acid stream) from each other.

2.4.3 Property differences

Once the feed conditions and product specifications have been established, the next essential step is to determine which separation methods are required to successfully separate and purify the acids. In order to separate two components, there must exist some difference in properties between them (Null [1987]). Since the principle of separation processes are based on the properties of the components involved, much time was spent finding these properties and are shown in Table A-3 of Appendix A. Many of these values were found in specialized reference books (Weast [1983], Prausnitz et al [1986] and Reid et al [1987]). Those that couldn't be found were estimated using the *Hysys* process simulator and checked by methods described by Reid et al [1987].

2.4.4 Classification of unit operations

Table 2-1 lists the most commonly used industrial separation methods. Although these operations often depend on several property differences, for their overall success, there is usually one property that forms the primary basis for separation. Therefore, Table 2-1 lists each unit operation together with its underlying principle of separation.

From the wide range of alternatives given in Table 2-1, those operations marked with asterisks were not considered in this project. These processes were eliminated after careful consideration of the factors discussed in the previous section and are summarized as follows:

- Due to the nature of the components present in the waste acid stream and the scale of operation, those operations marked with a single asterisk (*) were eliminated.
- The components to be recovered are not in dilute concentrations, thus barrier separations and separations based on solid agents which are usually more expensive to stage, were not considered (**).
- The remaining separation operations are not well understood and cannot be readily designed from a mathematical model and/or scaled up to a commercial size from laboratory data. This eliminated those marked with 3 asterisks (***).

This narrowed the list of operations down to distillation, liquid-liquid extraction, extractive distillation, reactive distillation and crystallization.

2.4.5 Selection of a base case

From the unit operations selected above one operation was chosen as a base case (i.e. an operation which was judged qualitatively as the most economical method that can be developed within the time and money constraints of the project).

Comparisons between the various separation processes discussed to this stage lead rather strongly to distillation being the most favorable separation process. Distillation has the most reliable design procedures, doesn't require any contaminating mass separating agent, involves no solid phases that make handling difficult and is easily staged in a single vessel. In fact, King [1971] suggests that the most sound approach to selecting a separation process is to begin by asking "Why not distillation?"

Distillation is and will remain the key separation method against which alternate methods must be judged (Fair [1987]). Distillation in general provides the cheapest and best method for separation of liquid mixtures. Kister [1992] lists the following factors, which most often operate against distillation:

- The difference of volatility is small, i.e. a separation factor too close to unity.
- A small quantity of high-boiling-point component is to be recovered from the feed. Distillation requires that the whole feed be vaporized in order to recover this small quantity.
- A compound is thermally unstable even under vacuum conditions.
- The mixture is extremely corrosive or highly fouling.

For this project, research conducted on the commercial production of fatty acids showed that acids ranging from C_6-C_{18} are currently being separated in the oleochemical industry by means of distillation (Aly & Ashour [1992]). It also became clearly evident that most experienced engineers and authors always chose distillation as an appropriate unit operation in the selection of an appropriate separation process. Therefore distillation was chosen as a base case in this project.

A flowsheeting program (*Hysys*) was used to simulate the distillation process for the fractionation of the waste acid stream. Atmospheric distillation was immediately disregarded because of carboxylic acids decomposing at their atmospheric boiling points (Ellerbe [1980]). Chapters 3 and 4 are devoted to the process followed for proper simulation. The simulation results showed that separation of the acids is possible by distillation.

2.4.6 Process flowsheets

From the few possible operations chosen in Section 2-4-4 and the separations obtained by the distillation simulations on *Hysys* three hypothetical hybrid processes were developed for separation and purification of the acids. These flowsheets are shown in Figures 2-4 to 2-6.

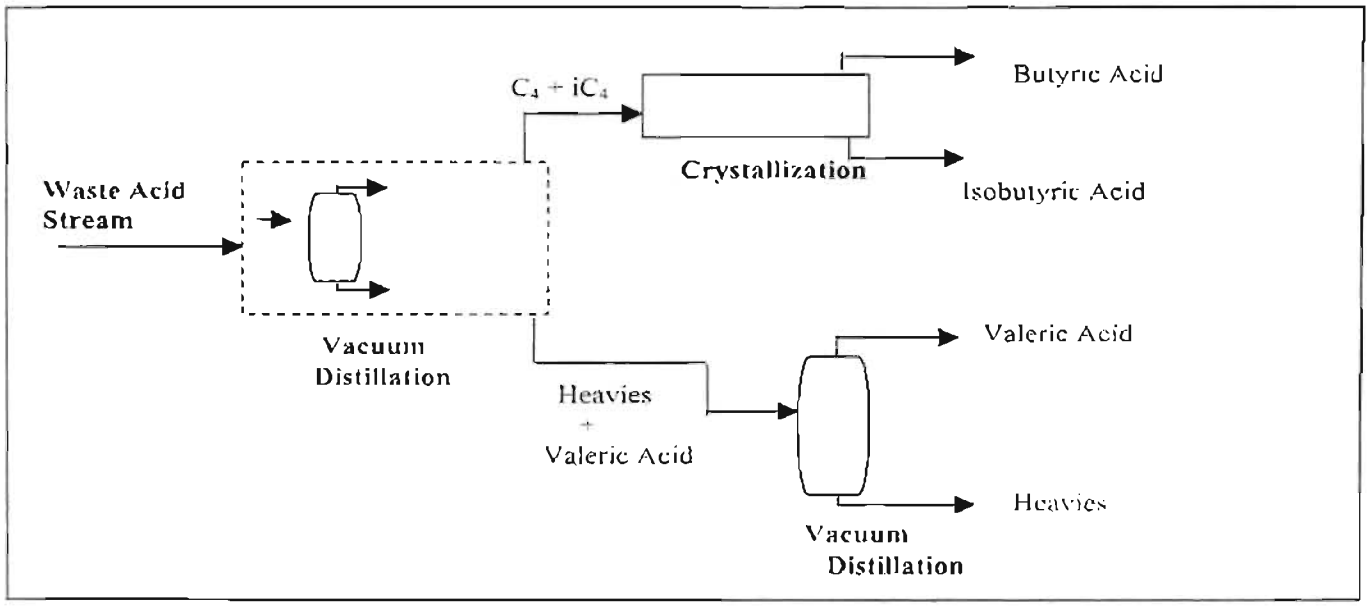

Figure 2-4: Flowsheet 1

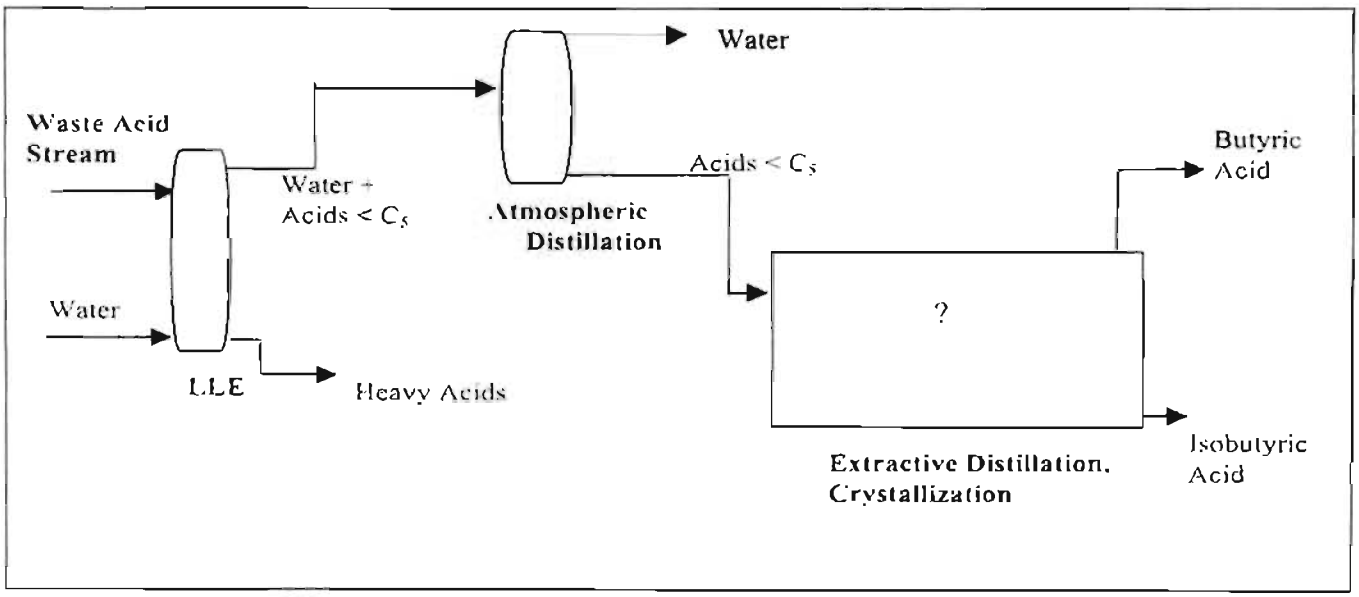

Figure 2-5: Flowsheet 2

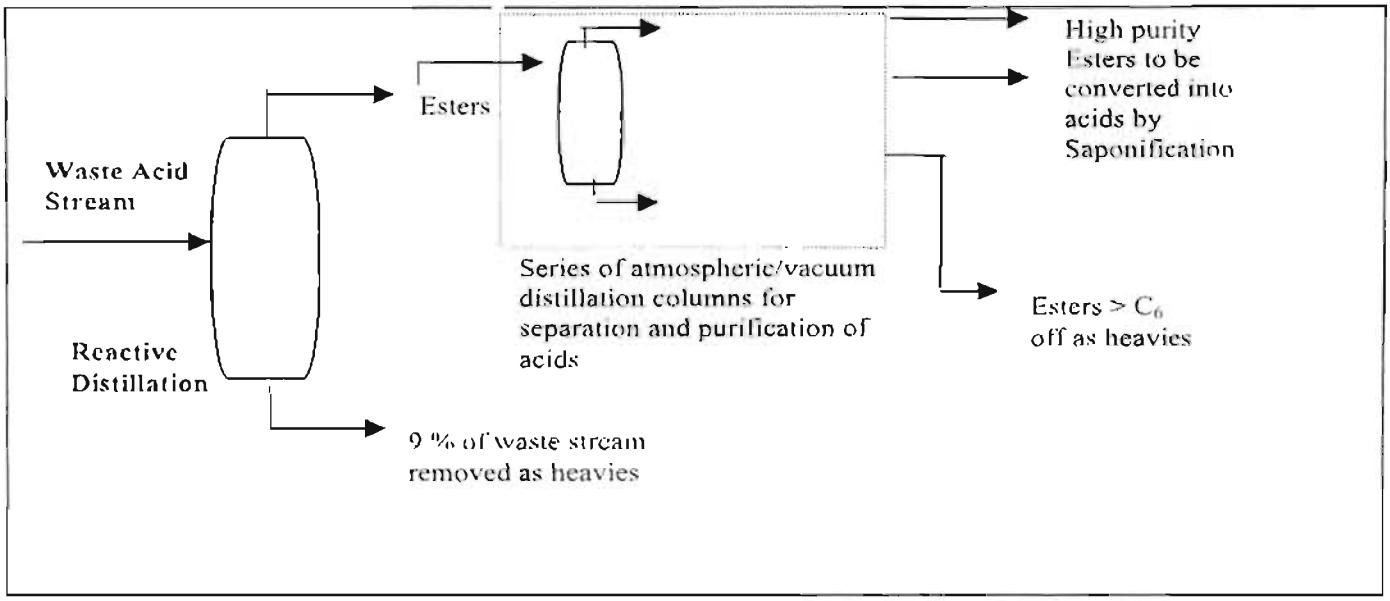

Figure 2-6: Flowsheet 3

Flowsheet 1 (Figure 2-4) is considered as the simplest and uses distillation as the main unit operation for fractionation of the acids and purification of the valeric acid. Because simulation showed that separation of butyric acid from its isomer would require many stages for a feasible route, crystallization was selected to separate the isomers due to their large difference in freezing points. The results obtained for the simulation sequence via distillation are shown in Figure 2-7. The first distillation column separates the butyric and isobutyric acids into the distillate and operates with a pressure of 58 kPa and 20 theoretical trays. Valeric acid with a purity greater than 95% and 80% recovery is produced by the combination of the second two columns, both of which operate under the same pressure of 58 kPa and have less than 15 theoretical trays.

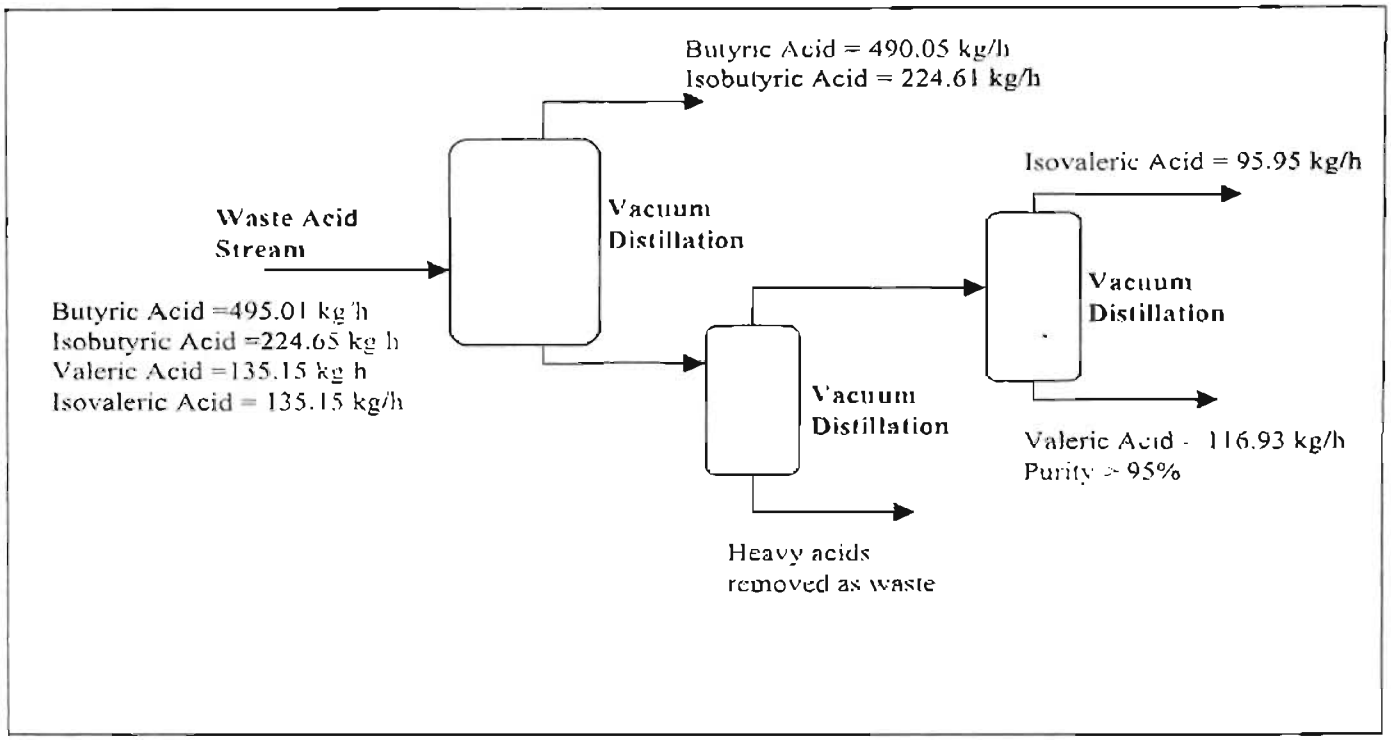

Figure 2-7: Flowsheet obtained from *Hysys* simulation

Flowsheet 2 (Figure 2-5) involves liquid-liquid extraction as the unit operation for extraction of the butyric and isobutyric acid for subsequent purification. The properties of the acids show that the acids with less than five carbon atoms are soluble in water whilst the remaining components are not. Water can thereafter be easily removed by atmospheric distillation as water has a high volatility in organic media and is thus easily stripped. Research by Kertes at al [1990] also showed that amides could be used to separate the acids from the rest of the waste stream, however there was no procedure available for separating the acids from the amides.

The third alternative was to use reactive distillation as a separation and purification route (Figure 2-6). The process utilizes chemical reaction of acids in the presence of an alcohol to form an ester. This is called Fischer Esterification. This process eliminates using vacuum distillation as esters have much higher volatility than their corresponding acids (Hart [1991]). It also has the advantage of eliminating working with the acids, which have a very undesirable smell as compared to esters and reduces the possibility of corrosion that may be caused by the acids.

Due to the time constraints of the project, only one of the process flowsheets discussed above had to be selected for further investigation. This was decided upon at a meeting held with key members from SASOL, who were closely involved in the project. At this meeting a decision was taken to further investigate process flowsheet 1 (Figure 2-4). The main reason for this choice is that the separation and purification route of distillation and crystallization could be used to separate and purify other valuable products from similar types of waste streams. Distillation is an extensively applied separation operation that separates most mixtures due to the differences in the boiling points of the components present in the various feed mixtures. Waste streams containing isomers that are generally more difficult to separate by distillation (due to small differences in boiling points) can be separated by freeze crystallization because of large differences in freezing points between the isomers and also the difference in shape between the isomers. In general one isomer does not fit easily into the first isomers crystal structure in the solid phase. Therefore, ideally the solid phase formed by partial freezing contains one of the isomers in its pure form.

At the meeting it was also decided to slightly change the problem definition of the project. The emphasis shifted from concentrating only on separating and purifying butyric and isobutyric acids from the waste acid stream. The recovery and purification of valeric acid was to be considered in a subsequent project, once the butyric and isobutyric acids had been successfully separated and purified.

CHAPTER
THREE

VAPOUR-LIQUID EQUILIBRIUM

Separation of a liquid mixture containing many different components can be achieved by distillation. This is possible when the composition of the vapour coming from the liquid mixture is different from that of the liquid. Therefore, the relation between the vapour and liquid compositions must be known in order to compute fractional distillation relationships and thus determine if separation is possible. This presents the need for vapour-liquid equilibrium (VLE) data.

In Chapter 2, distillation was selected as a base case for fractionation of the waste acid stream. One of the major advantages of modern day computers is that they avoid many assumptions made by engineers in calculating the height or number of trays required for distillation. This is due to the many rigorous calculation procedures developed for distillation calculations that only modern day computers can solve. Therefore, nowadays, most uncertainties in distillation design arise from uncertainties in VLE information.

A study by Peridis et al [1993] showed that a 3% decrease in relative volatility (See section below for definition of relative volatility) resulted in 70% increase in the number of stages required for a relatively difficult separation and an increase of 105% in reflux ratio. To avoid uncertainties in VLE it is therefore recommended that vapour-liquid equilibria be experimentally determined. However, for systems of more than two components, the experimental work required for a reasonably complete description rapidly mushrooms to impractical proportions (Raal & Mühlbauer [1998]).

Multicomponent VLE is generally predicted using experimental data between binary interactions of all the components in the multicomponent mixture. As an example, for this project 18 components are present in the waste acid stream. This would require measuring 153 binary systems over 306

days. Considering the time frame of this project measurements of all the binary systems would be impossible. To avoid this time consuming and expensive process, Null & Robert [1980] suggests measuring data for key component pairs present in a multicomponent system. These are generally between the main component and the remainder of the components making up the bulk of the mixture. Therefore, for this project measurements were made for the binary systems butyric acid + isobutyric acid, butyric acid + isovaleric acid, butyric acid + propionic acid and butyric acid + hexanoic acid. The binary system butyric acid + valeric acid was previously measured (DECHEMA Data Base [1999]) and was therefore not measured in this project.

For the remainder of the binaries not experimentally determined predictive techniques such as UNIFAC (Fredunsland et al [1977]) and ASOG (Kojima & Tochigi [1979]) have been recommended. Studies by Peridis et al [1993] show that the VLE of the nonkey components do not have any significant effects on the design of distillation processes.

To evaluate the performance of distillation in separation, the flowsheeting program (*Hysys*) was used. Figure 3-1 outlines the initial steps in setting up the distillation simulation. For the proper use of the simulation program an appropriate thermodynamic model must be selected. The choice of the thermodynamic model for a simulation can be one of the most important decisions for an engineer as this is the first step in simulation and affects all subsequent tasks in developing accurate physical properties, especially VLE data.

The importance of VLE in distillation cannot be overemphasized and much time in this project was spent on this particular topic, however it is perhaps impossible to do justice to the wide topic of VLE in a single chapter. This is evident from the numerous published texts and reviews on the subject. The reader is referred to the excellent texts of Walas [1985], Prausnitz et al [1986] and Raal & Mühlbauer [1998] for an in-depth coverage of VLE.

In this chapter low-pressure VLE is discussed with reference to:

- The theoretical aspects of VLE
- The equipment and procedure for measuring VLE
- Analysis of experimental results for subsequent calculation of interaction parameters

However, prior to this the concept of relative volatility is introduced and its relation to distillation is discussed as the concept of relative volatility is used extensively in the proceeding chapters.

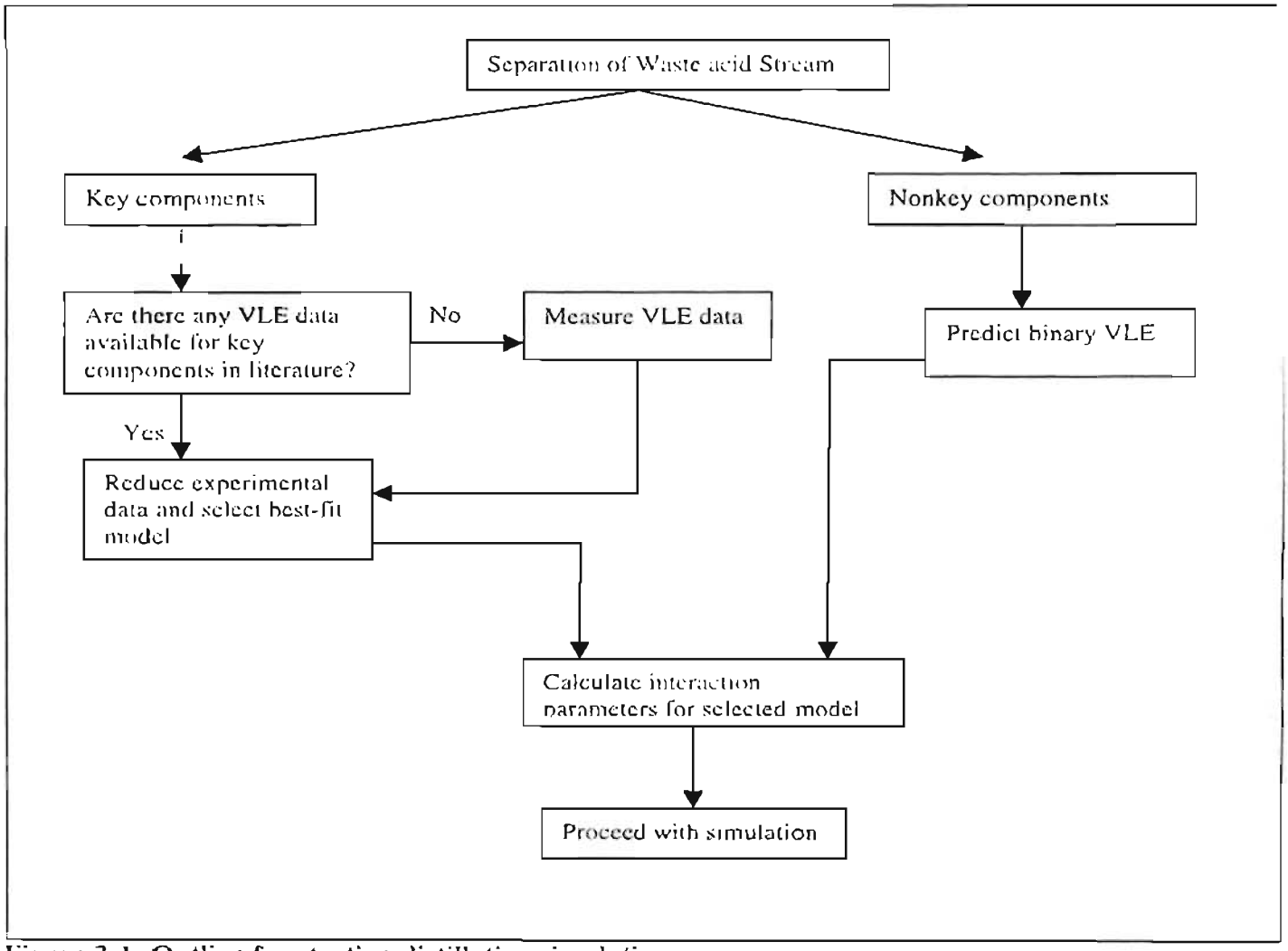

Figure 3-1: Outline for starting distillation simulations

3.1 Relative volatility

Distillation is a technique of separating components according to their relative volatility (α). Therefore, the relative volatility is a measure of the ease of separation. For a binary mixture (component 1 & 2) relative volatility can be defined as:

$$\alpha_{1,2} = \frac{y_1(1-x_1)}{x_1(1-y_1)} \tag{3-1}$$

In the above equation above x_1 and y_1 are the equilibrium mole fractions of component 1 in the liquid and vapour phase respectively. Component 1 is the more volatile component.

VLE data is generally presented as vapour-liquid (x-y) diagrams and temperature-composition (T-x-y) diagrams. These are shown in Figures 3-2 and 3-3 respectively. In Figure 3-2a the x and y axes show the concentration of the more volatile component in the liquid and vapour phase respectively. The 45^0 diagonal represents points at which vapour and liquid compositions are the same. The curve in Figure 3-2a is the equilibrium curve and shows how the more volatile component concentrates in the vapour. Tracing the dashed lines in Figure 3-2a shows how a liquid mixture containing 0.4 mole fraction of the more volatile component in the liquid is in equilibrium with vapour containing 0.6 mole fraction of the same component. Therefore if this vapour is collected and condensed one will end up with a mixture in which the more volatile component mole fraction has been enriched from 0.4 to 0.6.

Figure 3-2b illustrates the effect of relative volatility on the tendency of the more volatile component to concentrate in the vapour. The higher the relative volatility the greater the separation. For example, when the relative volatility is 5, a liquid mixture containing 0.2 mole fraction of the more volatile component is in equilibrium with vapour containing 0.56 mole fraction of the more volatile component. For this mixture it will take only a few steps to obtain a pure liquid of the more volatile component. Conversely, when the relative volatility is lower (e.g. $\alpha = 2$), a liquid mixture containing 0.2 mole fraction of the more volatile component is in equilibrium with vapor containing 0.38 mole fraction of the more volatile component. Under these conditions many more steps will be required to obtain a pure liquid of the more volatile component. x-y diagrams (also known as unit diagrams) and its use in screening distillation for separation is discussed in more detail in Chapter 4.

Figures 3-2a and 3-2b are x-y diagrams of "normal" mixtures. For certain systems there exists a composition (the point of intersection of the equilibrium curve and the 45^0 line) for which the vapour and liquid compositions are identical. Such systems are known as azeotropic. The x-y diagram for such a system is shown in Figure 3-4. At point A, once this vapour and liquid composition is reached the components can no longer be separated by simple distillation and other alternatives (e.g. extractive distillation and liquid-liquid extraction) need to be considered.

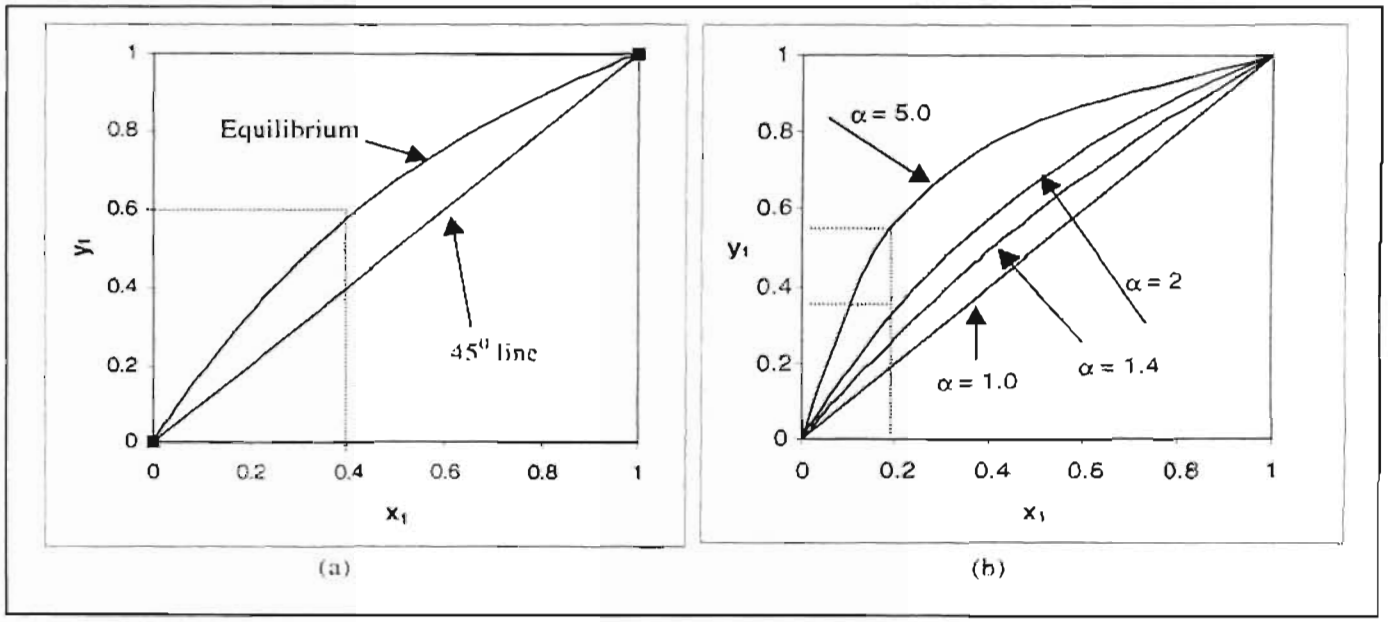

Figure 3-2: x-y diagrams. (a) Concentration of more volatile component in liquid (x) vs. vapour concentration (y). (b) Effect of relative volatility on the concentration of the more volatile component in the vapour.

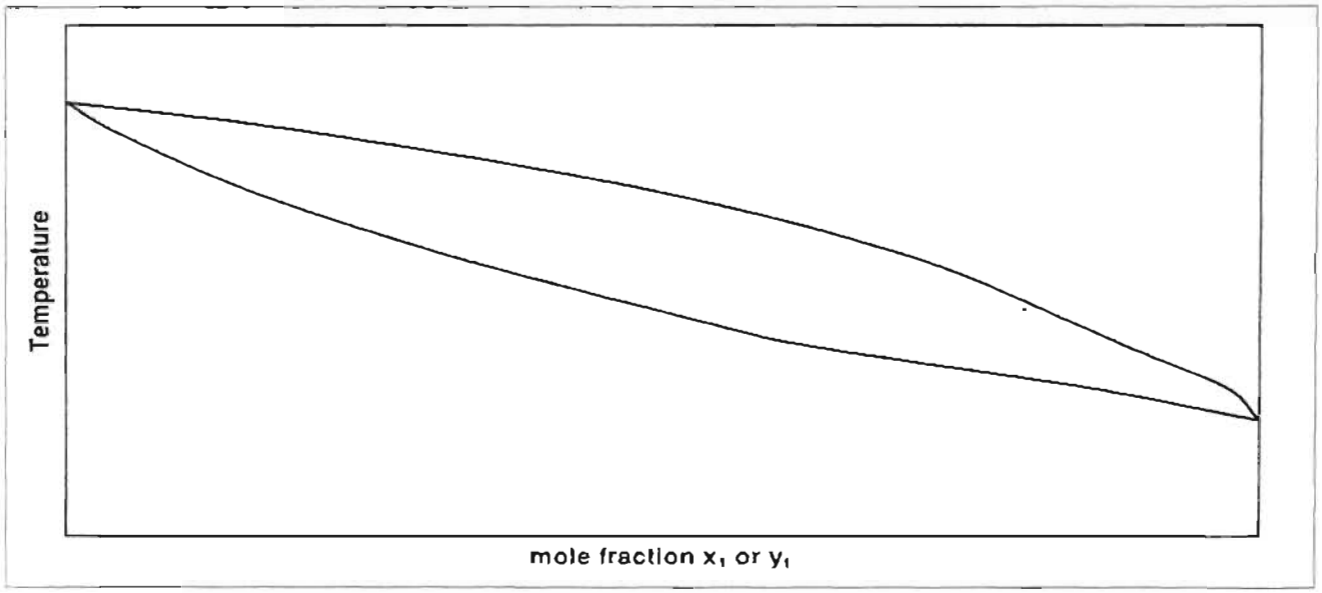

Figure 3-3: T-x-y diagram

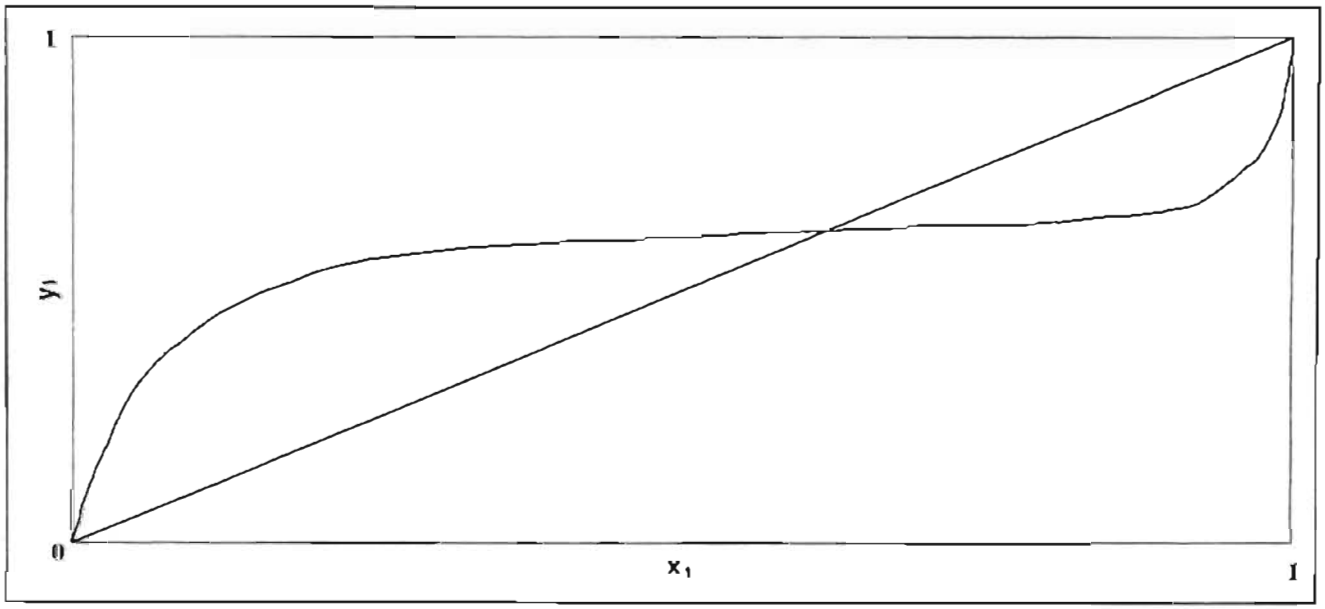

Figure 3-4: x-y curve for an azeotropic system

3.2 Theoretical Aspects of VLE

As discussed earlier, measurement of VLE is expensive and time consuming. It is therefore important that the data be correctly theoretically interpreted as this allows for interpolation, extrapolation and prediction of data to new conditions which subsequently provides a designer to explore a wide range of design alternatives in process simulation.

The development of the criterion for thermodynamic equilibrium between two phases is covered in Appendix B-1. For the case of VLE, a vapour phase (V) and liquid phase (L) are in equilibrium at the same temperature and pressure when their respective fugacities (f_i) are equal:

$$\hat{f}_i^V = \hat{f}_i^L \tag{3-2}$$

In the above equation " ^ " denotes the mixture property.

To use Equation 3-2, it is useful to define the mixture fugacities in terms of measurable quantities such as temperature, pressure and phase compositions. This is achieved by introducing dimensionless auxiliary functions. These are known as the fugacity coefficient and activity coefficient for the vapour and liquid phases respectively. The fugacity coefficient is related to the vapour phase as follows:

$$\hat{\phi}_i = \frac{\hat{f}_i^V}{y_i P} \tag{3-3}$$

In the above equation $\hat{\phi}_i$ is the fugacity coefficient of the vapour phase, y_i the vapour mole fraction and P is the system pressure.

Similarly, the activity coefficient (γ_i) is related to the liquid phase fugacity as follows:

$$\gamma_i = \frac{\hat{f}_i^L}{x_i f_i} \tag{3-4}$$

In Equation 3-4, x_i is the liquid mole fraction and f_i is the pure component fugacity.

The pure component fugacity is given by (Prausnitz et al [1980]):

$$f_i = \phi_i^{sat} P_i^{sat} \exp\left[\frac{V_i\left(P - P_i^{sat}\right)}{RT}\right] \tag{3-5}$$

In Equation 3-5, the exponential term is known as the Poynting correction factor, ϕ_i^{sat} and P_i^{sat} are the saturated vapour fugacity coefficient and saturated pressure of the pure component respectively. According to Prausnitz et al [1980], the Poynting correction factor and the saturated vapour fugacity coefficient can be treated as unity at low pressures. Therefore, Equations 3-3, 3-4 and 3-5 combined result in the following equation for low-pressure VLE:

$$y_i \hat{\phi}_i P = x_i \gamma_i P_i^{sat} \tag{3-6}$$

To use Equation 3-6, various thermodynamic models have been developed. Equations of state are generally used to predict vapour phase non-idealities and activity coefficient models calculate liquid phase non-idealities. The reader is referred to the excellent text of Walas [1985] for a comprehensive review of the many available thermodynamic models and their applications. The models used in this project for calculation of the fugacity and activity coefficients are discussed in the following sections.

3.2.1 Evaluation of fugacity Coefficients

In most cases, for low pressure VLE $\hat{\phi}_i$ is set equal to one. This represents ideal vapour phase behavior. However, for systems containing associating components (especially carboxylic acids), many authors including Prausnitz et al [1980] have reported large variations from ideal phase behavior even at very low pressures. This is due to the formation of dimers or trimers in the vapour phase. The mechanism and effect of dimerization is more clearly explained in Chapter 2.

There are very few cases in the literature where the problem of vapour phase associations is discussed in VLE. Tamir & Wisniak [1975, 1976, and 1982], Null & Robert [1980], and Girano et al [1981] discuss dimerization in VLE. For this project vapour phase fugacity coefficients were calculated using the virial equations of state for vapour phase chemical associations as described by Prausnitz et al [1980]. This was because this model was the only available one in the *Hysys* process simulator that accounted for vapour phase associations.

Carboxylic acids tend to dimerize through strong hydrogen bonding. The hydrogen bonding process can be observed as a chemical reaction:

$$i + j \leftrightarrow ij \tag{3-7}$$

where i and j are monomer molecules and ij is the complex (dimer) formed by hydrogen bonding. In order to describe the chemical reaction the following may be written:

$$k_{ij} = \frac{f_{ij}}{f_i f_j} = \frac{z_{ij}\phi_{ij}^{\#}}{P z_i z_j \phi_i^{\#} \phi_j^{\#}} \tag{3-8}$$

where: z is the true mole fraction of the species in equilibrium

$\phi^{\#}$ is the fugacity coefficient of the true species

P is the system pressure

k_{ij} is the reaction equilibrium constant

To utilize Equation 3-8, it has been shown by Nothnagel et al [1973] that ϕ_i is given by:

$$\phi_i = \frac{z_i \phi_i^{\#}}{y_i} \tag{3-9}$$

where: y_i is defined as the apparent mole fraction of component i in the vapour phase (apparent meaning that dimerization has been neglected) .

If it is assumed that the vapour solution behaves like an ideal solution, $\phi_i^{\#}$ can be calculated by the Lewis fugacity rule:

$$\ln \phi_i^{\#} = \frac{P B_i^{'}}{RT} \tag{3-10}$$

where: $B_i^{'}$ is the "free" contribution to the second virial equation as calculated by the Hayden & O'Connell method [1975].

The chemical equilibrium constant can be found from the relation:

$$k_{ij} = \frac{-(2 - \delta_{ij}) B_{ij}^{D}}{RT} \tag{3-11}$$

where: B_{ij}^{D} is the contribution of dimerization to the second virial coefficient as calculated by the Hayden & O'Connell method [1975].

$\delta_{ij} = 0$ $(i \neq j)$, $\delta_{ij} = 1$ $(i = j)$

The calculation of the fugacity coefficient for components *i* and *j* is therefore accomplished by solving the above equations with the restriction that the sum of z_i, z_j and z_{ij} equal to 1.

The Hayden and O'Conell method is a procedure for calculating contributions to the second virial coefficients. The calculation procedure for this method is discussed in detail by Prausnitz et al [1980]. Although this procedure is programmed in the *Hysys* process simulator, a separate program was written in the Matlab programming language. This was required for regressing the experimental data to separately calculate interaction parameters for the activity coefficient model. Appendix B-2 contains the computer program that was used. The chemical theory was also incorporated in this program to simultaneously calculate the fugacity coefficients. All input parameters required for the Matlab program were available in the *Hysys* simulation package. These values were checked with values given by Weast & Grasselli [1989], Reid et al [1998] and Prausnitz et al [1980].

3.2.2 Evaluation of activity coefficients

For isobaric experimentation, x_i, y_i and T values are recorded and pressure (P) is set. The fugacity coefficient is calculated as detailed above and the T values are used to calculate P_i^{sat} values. Using these values in Equation 3-6, the activity coefficient can be calculated. However, it is useful to evaluate the activity coefficient independent of the vapour mole fraction. This is because it is impracticable to obtain data sets in evaluating many different alternatives in process design. It is therefore useful to have models that allow for the interpolation and extrapolation of VLE data. For these purposes, many equations have been proposed to correlate activity coefficients. These include the Margules, Van Laar, Wilson, T-K Wilson, NRTL (Non-random two liquid), UNIQUAC (Universal Quasi-chemical), the regular solution method of Scathchard-Hildebrand and the group contribution methods UNIFAC (UNIQUAC Functional-group Activity Coefficients) and ASOG (Analytical Solution of Groups). The reader is referred to the texts of Walas [1985], Prausnitz et al [1986] and Raal & Mühlbauer [1998] for a detailed review on each of these methods.

In this project the NRTL and UNIFAC models were used to correlate and predict the liquid phase activity coefficients.

3.2.2.1 The NRTL model

The activity coefficients calculated from the experimental data, with fugacity coefficients calculated as described above, were correlated by means of the NRTL model. This equation was convenient in that it is readily converted to multicomponent systems and requires the least amount of data for distillation simulations. Also, as demonstrated in Section 3-6, values calculated using the NRTL model compared well with the experimental data. For the NRTL model, the activity coefficients are obtained using Equations 3-12 to 3-15:

$$\ln \gamma_1 = x_2^2 \left[\tau_{21} \left(\frac{G_{21}}{x_1 + x_2 G_{21}} \right)^2 + \left(\frac{\tau_{12} G_{12}}{(x_2 + x_1 G_{12})^2} \right) \right] \tag{3-12}$$

$$\ln \gamma_2 = x_1^2 \left[\tau_{12} \left(\frac{G_{12}}{x_2 + x_1 G_{12}} \right)^2 + \left(\frac{\tau_{21} G_{21}}{(x_1 + x_2 G_{21})^2} \right) \right] \tag{3-13}$$

where

$$\tau_{ji} = \frac{g_{ji} - g_{ii}}{RT} \tag{3-14}$$

$$G_{ji} = \exp\left[-\alpha_{ji} \tau_{ji} \right] \tag{3-15}$$

From the above equations, it is evident that the NRTL equation has three adjustable parameters, i.e. (g_{12}-g_{22}), (g_{21}-g_{11}) and α_{12}, which is equal to α_{21}. The parameter g_{ii} is an energy parameter, which is characteristic of the interaction between component j and i. These are calculated from experimental data and used as inputs into the *Hysys* process simulator. The parameter α_{12} is related to the non-randomness of the mixture and was set equal to 0.2 for all calculations. Small variations around this value did not effect the quality of the calculations.

3.2.2.2 The UNIFAC method

As it is impracticable to measure all the binary systems present in the waste acid stream, UNIFAC was used to predict the vapour-liquid equilibria for the remaining nonkey systems. UNIFAC is useful in this case, as it doesn't require any experimental data and uses structural groups to estimate component interactions. From structural information about organic compounds available in the built-in databank of the *Hysys* simulation package, UNIFAC is able to predict activity coefficients. This method has been suggested by many researchers, including Carlson [1996] and is

especially recommended for components with a low priority (nonkey components). In principle the UNIFAC method is a functional group contribution method developed by Fredenslund [1977] based on the UNIQUAC model proposed by Abrams & Prausnitz [1975] and is claimed to be superior to most estimation techniques. This model is therefore available in most modern day process simulators, including *Hysys*. Fundamentally, the activity coefficient is assumed to be made up of two contributions known as configurational (C) and residual (R):

$$\ln \gamma_i = \ln \gamma_i^C + \ln \gamma_i^R \tag{3-16}$$

where $\ln \gamma_i^C$ (the combinatorial term) and $\ln \gamma_i^R$ (the residual term) are defined as functions of the following parameters:

$$\ln \gamma_i^C = f(q_i, x_i, \Phi_i, Z, \theta_i, l_i) \tag{3-17}$$

where $q_i, x_i, \Phi_i, Z, \theta_i, l_i$ are parameters, calculated as shown in Appendix B-3, and

$$\ln \gamma_i^R = f(\nu_k^{(i)}, \Gamma_k, \Gamma_k^{(i)}) \tag{3-18}$$

In Equation 3-18, $\nu_k^{(i)}, \Gamma_k, \Gamma_k^{(i)}$ are parameters, calculated as shown in Appendix B-3.

3.3 Equipment

Several techniques have been developed for the experimental determination of VLE. These include the following:

- Circulation (Dynamic) Method
- Bomb Method
- Dynamic Flow Method
- Dew and Bubble Point Method
- Distillation Method

Robinson & Gilliland [1950], Hala et al [1967] and most recently Raal & Mühlbauer [1998] discuss each of these methods together with their advantages and disadvantages.

Today, the most commonly used methods are the static and dynamic methods. Although distillation processes can be evaluated either by isobaric or isothermal data, isobaric data is preferred by the industrial sector as it gives a truer reflection of an actual distillation column. Therefore, for this particular project, isobaric data at sub-atmospheric pressures were measured. Since static methods

measures only isothermal data, the circulation method has been adopted. Circulation methods have been known to produce results of high accuracy in a rapid and simple manner (Joseph [2001]). This method operates by circulating vapour through a system and bringing it into repeated contact with the liquid until no further change in the composition of either phase takes place. Joseph [2001] provides an excellent review on the development of the circulation method and the various types of apparatus used in this method.

A block diagram of the experimental set-up is shown in Figure 3-5. The various components of the experimental set-up include a VLE still, Schott 10 *l* and Pyrex 5 *l* ballast flasks, a TECHNE cold finger, a Fischer VKH 100 pressure controller, a LABOTEC water bath with glycol - water mix and two pumps.

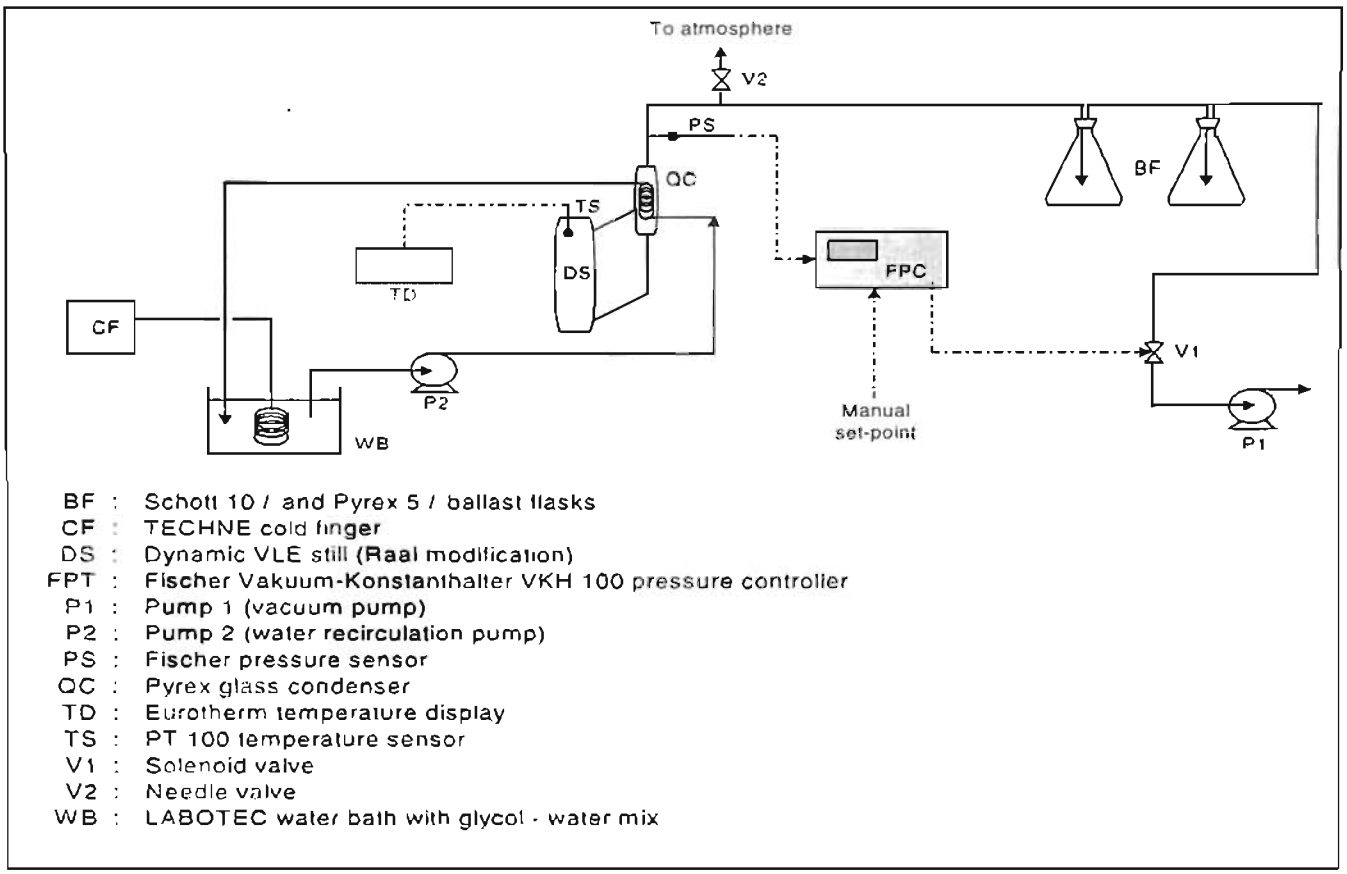

Figure 3-5: Schematic diagram of the VLE apparatus set-up

3.3.1 Vapour-Liquid Equilibrium Still

A highly refined dynamic VLE still (Figure 3-6), based on the Yerazunis et al [1964] still has been designed by Raal (Raal & Mühlbauer [1998]). The still is constructed from specially blown glass and is suitable for low-pressure measurements. Harris [2001] and Joseph et al [2001] have described the still in detail. It is worth noting the advantages of the design:

- Correct positioning of temperature sensors provide for accurate temperature measurement.
- The use of high-vacuum valves provide constant and stable pressure control.
- Both liquid and vapour samples are extracted easily and do not affect equilibrium operating conditions.
- The use of packing in the equilibrium chamber ensures rapid attainment of equilibrium due to intimate contact between the vapour and the liquid and the expansion of interfacial surface area.
- Several vacuum jackets and lagging streams prevent both heat losses and super heating from occurring.
- Stirring in the condensate receiver eliminates temperature and concentration gradients. This ensures high reproducibility of the vapour sample concentrations.
- Stirring in the boiling chamber which ensures thorough mixing of the returning condensate before evaporation. This prevents "flashing" and produces smooth boiling.
- A system of internal and external heaters in the boiling chambers. This feature ensures rapid boiling, permits precise control of the circulation rate and provides nucleation sites for smooth boiling.

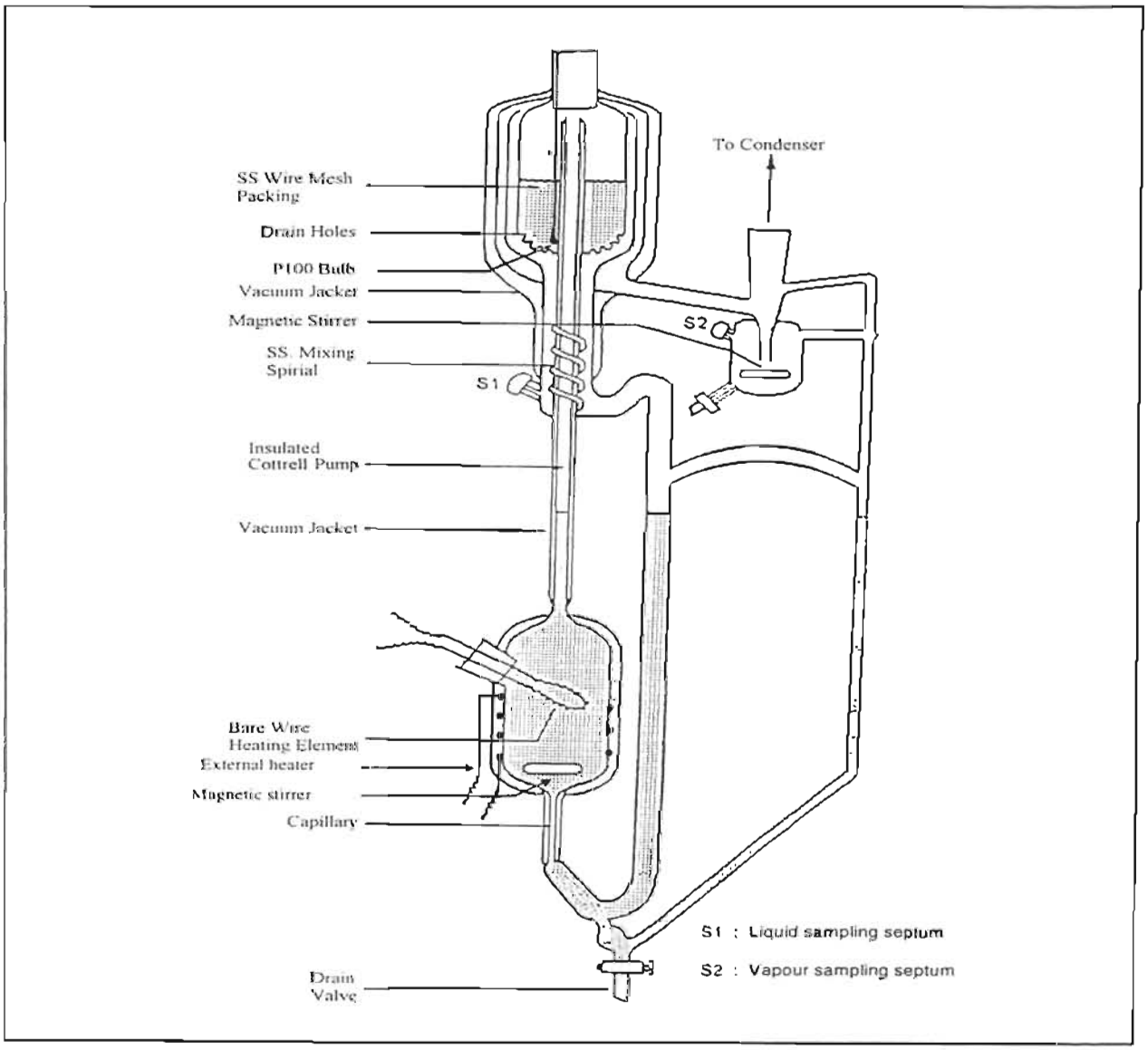

Figure 3-6: Dynamic VLE still of Raal (Raal & Mühlbauer [1998])

3.3.2 Temperature and pressure measurement

A Eurotherm temperature display was used to indicate the resistance of the PT-100 temperature sensor embedded in the equilibrium chamber. This accurately measured the equilibrium temperature. Before experimentation, however, the PT-100 temperature sensor has to be calibrated. This is discussed in the section below. The accuracy of temperature measurement is estimated to be within ±0.02 K.

The pressure was monitored with a Fisher pressure transducer. Accuracy of the pressure measurement is estimated to be within ±0.03 kPa.

3.3.3 Pressure control

For isobaric operation the pressure is maintained at a constant set-point that is controlled by a Fischer pressure controller which either vents to atmosphere through needle valve V_2 (Figure 5-1) or connects to the vacuum pump through solenoid valve V_1 (Figure 5-1). By actuation of the solenoid valve, leading to a vacuum pump and atmosphere, the pressure in the still can be controlled. Control of the still pressure is estimated to be within ± 0.1% of the set pressure. However, before the pressure controller can be used it is necessary to calibrate it to determine the actual pressures to which it is controlling. This is discussed in Section 3.4.2.

3.3.4 Composition analysis

The equilibrium compositions of the samples were determined using a gas chromatograph (GC). Gas chromatography is a method of separating and identifying certain substances. For this project two gas chromatographs was used. For the cyclohexane/ethanol system a Shimadzu, model GC 17A gas chromatograph was used. This GC could not be used for the carboxylic acids, as the column in the Shimadzu could not separate the carboxylic acids. Therefore, for the carboxylic acids a Varian, model 3300, GC was employed. The column used in the Varian was a 30-m megabore capillary column of 0.53-mm diameter with 007-FFAP on fused silica, whilst a 2.5 m long, 2.2 mm ID and 3.2 mm OD stainless steel column packed with 80 to 100 mesh Poropak Q was used in the Shimadzu. A flame ionisation detector was used in both gas chromatographs. The output from the Shimadzu GC were analysed and converted into a peak area signal by Shimadzu integrated software. The outputs from the Varian GC were analysed by a Varian 4270 Integrator.

3.4 Experimental Procedure

Experimental determination of vapour-liquid equilibria involves many steps. Before commencing with the actual measurement of VLE data, the VLE equipment must be tested for leaks and cleaned. The temperature sensor, pressure sensor and gas chromatograph must also be calibrated.

3.4.1 Detection of leaks

For sub-atmospheric conditions, to maintain stable operation and prevent contamination of the fluids under investigation it is necessary to eliminate any leakage into the VLE equipment. This involved drawing a vacuum in the equipment with a vacuum pump and then controlling the pressure to a specified value. Once the pressure stabilises, the vacuum pump is switched off and the pressure is monitored An increase in pressure indicates the presence of a leak into the system Generally, if a leak is present, it is difficult to detect. If there is a leak it must be eliminated before proceeding with experimentation.

3.4.2 Pressure Calibration

Prior to any calibration, the still must be thoroughly cleaned to clear the still of any impurities. This is accomplished by circulating acetone in the VLE still. Operation of the VLE still is discussed below. Once this procedure is complete the acetone is emptied with any remaining acetone removed by creating a vacuum in the VLE still.

For calibration of the pressure sensor, a mercury manometer is connected in parallel to the pressure sensor. A pressure is set on the controller and once operation is steady the pressure reading from the controller is recorded. The manometer reading and atmospheric pressure (obtained from a NIST traceable electronic barometer) are also recorded. The true pressure is calculated as follows:

$$P_{actual} = P_{atm} - |\Delta height(Hg)| \tag{3-19}$$

This procedure is repeated several times. The actual pressure is then plotted versus the pressure reading and a linear relationship is obtained. Calibration curves are shown in Appendix B-4 (Figure B-1).

3.4.3 Temperature Calibration

To calibrate the temperature sensor, the true temperature within the still is determined and plotted versus the reading displayed. The true temperature is determined by boiling a pure component in the still at several different pressures. Provided the chemical is of high purity (>99.5% pure) and the pressure calibration is correct, the Antoine equation can be used to determine the vapour pressure temperatures. In this project cyclohexane was used. A plot of these true temperatures versus the temperature reading yields a linear relationship and can be found in Appendix B-4 (Figure B-2).

3.4.4 Calibration of the gas chromatograph

The gas chromatographs used in the experimentation were discussed in an earlier section. The Shimadzu, model GC 17A was used for the test system (cyclohexane/ethanol) and the Varian, model 3000, gas chromatograph was used for the binary systems involving butyric acid. The operating procedures for both these gas chromatographs are given in Table 3-1.

It is important to calibrate the GC detector, as the percentage composition given by the integrator may not be a true representation. Calibration of the GC detector was based on the GC area ratio method, which is discussed by Raal and Mühlbauer [1998]. In general, for a binary system, it is possible to equate:

$$\frac{x_1}{x_2} = \frac{F_1}{F_2}\frac{A_1}{A_2} \tag{3-20}$$

In the above equation, x is the mole fraction in the sample, A is the area produced by the GC integrator and F is the response factor. From Equation (3-20) it is obvious that to calibrate the GC it is necessary to obtain the response factor. Response factors are unique to systems but are constant regardless of sample size (Raal and Mühlbauer [1998]). However, not all systems have constant response factors throughout the entire composition range.

Table 3-1: Gas chromatograph operating conditions

Gas chromatrograph condition	Shimadzu GC 17A	Varian 3000			
	Binary system being measured				
	cyclohexane (1) + ethanol (2)	isobutyric acid (1) + butyric acid (2)	propionic acid (1) + butyric acid (2)	butyric acid (1) + isovaleric acid (2)	butyric acid (1) + hexanoic acid (2)
Nitrogen carrier gas flow rate [ml/min]	35	10	10	10	10
Oven temperature Profile					
Initial temperature [^{0}C]	120	130	120	135	150
Temperature ramp [^{0}C/min]	None	None	None	None	None
Final temperature [^{0}C]	N/A	N/A	N/A	N/A	N/A
Hold Time [min]	N/A	N/A	N/A	N/A	N/A
FID detector					
Temperature [^{0}C]	200	220	220	220	220
Attenuation	8	8	8	8	8
Range	10	10	10	10	10
Hydrogen flowrate [ml/min]	30	30	30	30	30
Air flow rate [ml/min]	300	300	300	300	300
Injector tempetature	220	240	240	240	240

For a clearer understanding on the use of this method, an example of detector calibration is shown for the Isobutyric acid (1)+Butyric acid (2) system (Figures 3-7 and 3-8). The calibration graphs for the other systems measured are given in Appendix B-4 (Figures B-3 to B10). Nine samples were gravimetically prepared and analysed. A plot of A_1/A_2 vs. x_1/x_2 is shown in Figure 3-7. If the slope (F_2/F_1), of Figure 3-7 is equal to the inverse of the slope, (F_1/F_2), of Figure 3-8, it implies that the response factor ratios are exactly constant over the full composition range. For this example, the F ratios and their inverse are directly related and the response factor ratio is constant over the entire composition range. It is vital that the applicability of a constant response factor be validated.

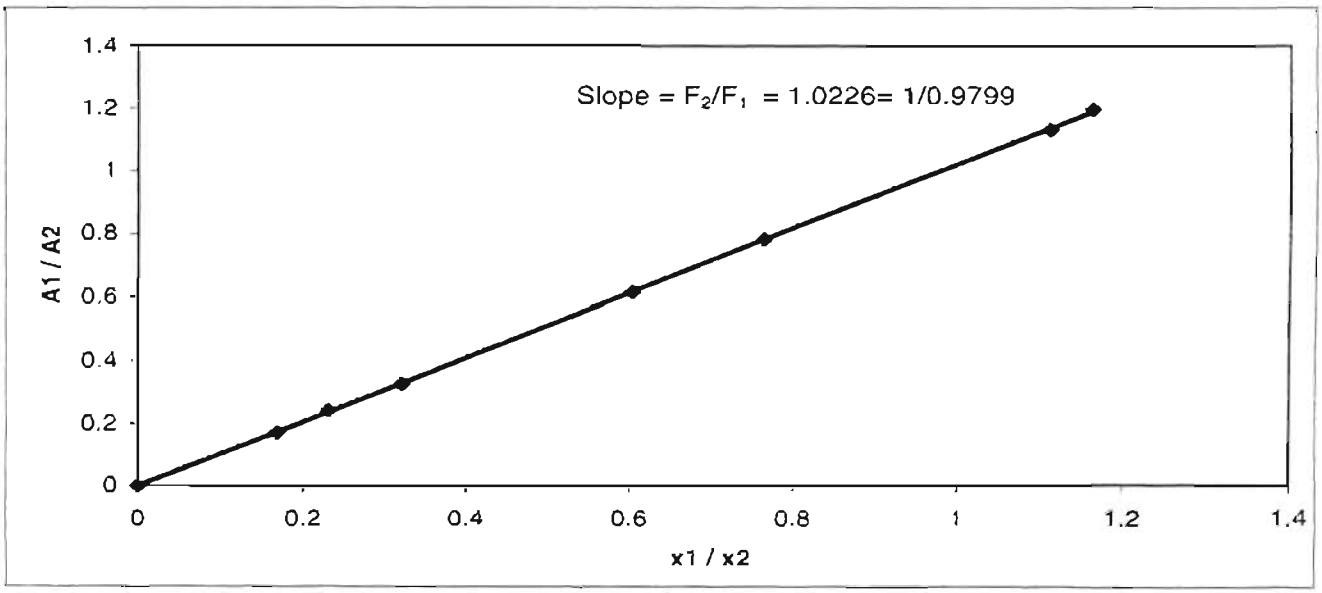

Figure 3-7: Gas chromatograph (Varian 3000) calibration for isobutyric acid (1) + butyric acid (2)

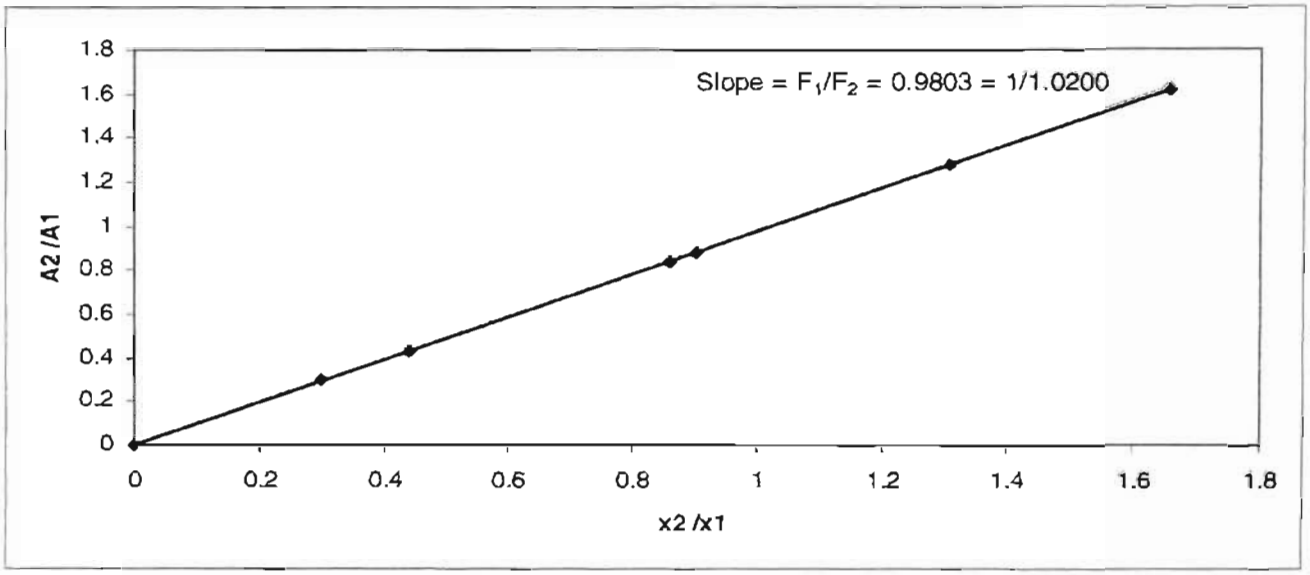

Figure 3-8: Gas chromatograph (Varian 3000) calibration for isobutyric acid (1) + butyric acid (2)

3.4.5 Procedure for measurement of isobaric VLE data

Once the equipment has been tested for leaks, cleaned and calibrated, the actual measurement of VLE data can begin.

After the Eurotherm temperature display, pressure transducer and cooling water supply is switched on, the VLE still is filled with the liquid of interest. It is suggested that starting with a pure component and then adding more and more of the second component until the entire composition range is covered. The pressure set point is then specified and the vacuum pump switched on. This starts to decrease the pressure towards the specified set point.

Once the system becomes stable at the specified pressure, the internal and external heaters are turned on. The power input to the boiling chamber should then be gradually increased until the 'plateau' region is reached. It is important to operate the still around this region, as operation outside this region would result in erroneous boiling point readings. The reader is referred to work done by Kneisl et al [1989] for further information in this regard. It is also important that sufficient heat is supplied so that a fairly fast pumping action and good circulation is achieved.

After a while (generally more than 30 minutes), and once the temperature has stabilised equilibrium is reached. Equilibrium time differs for many components and it is suggested that once the temperature has stabilised, the compositions of the vapour and liquid is analysed at short intervals. A constant composition and temperature will verify equilibrium conditions. For the systems measured equilibrium times ranged from 30 minutes to 90 minutes.

Once equilibrium has been reached temperature, liquid composition and vapour composition are noted. Samples for the vapour and liquid are removed through the sample septa and analysed by gas chromatograph. For analysis, approximately 0.3µl of sample is injected into the gas chromatograph over three times and an average of the results is used in calculations.

3.5 Experimental Results

The results for the cyclohexane + ethanol system are listed in Table 3-2 and shown in Figures 3-9 and 3-10. This system was measured at 40kPa. The GC detector calibration curves for this system are shown in Appendix B-4, Figures B-3 and B-4.

Table 3-2: Vapour-liquid equilibria for test system cyclohexane (1) + ethanol (2) at 40kPa.

x_1	y_1	T (K)
0.000	0.000	329.59
0.028	0.180	325.23
0.155	0.503	317.56
0.315	0.588	315.00
0.391	0.600	314.38
0.513	0.604	314.40
0.550	0.601	314.70
0.652	0.616	314.80
0.695	0.620	314.88
0.848	0.640	314.90
0.928	0.686	316.42
1.000	1.000	325.76

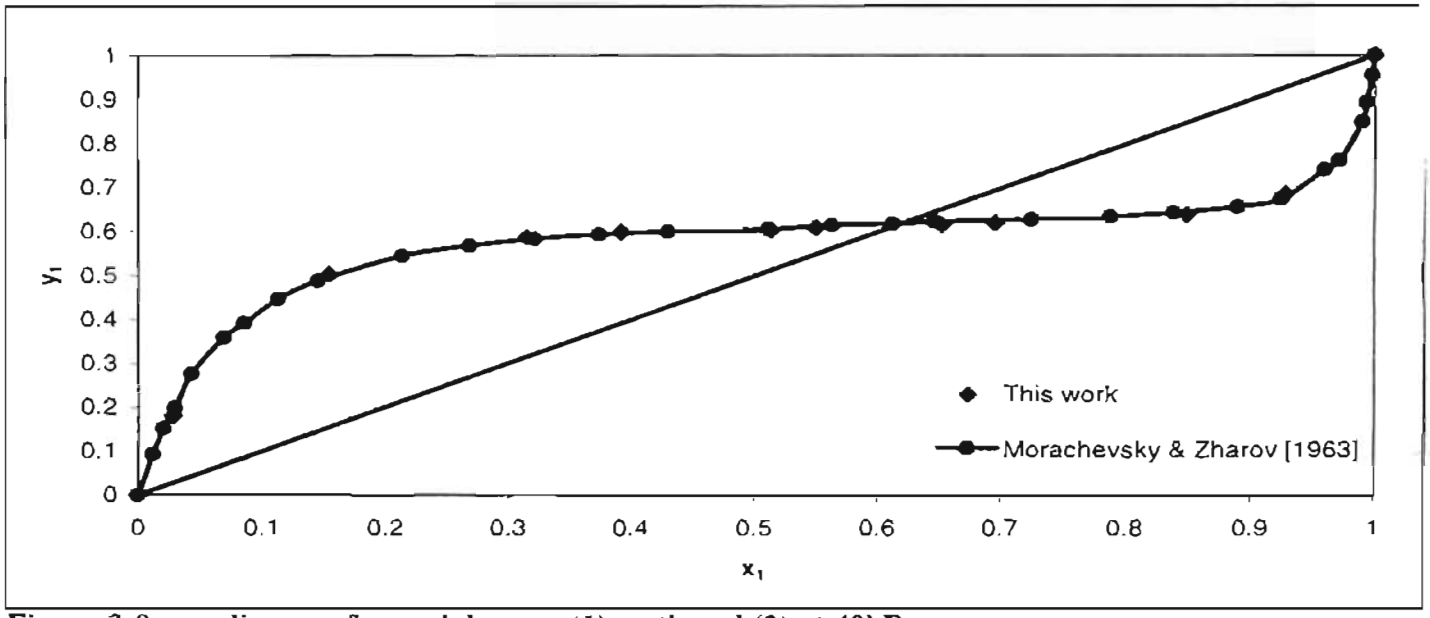

Figure 3-9: x-y diagram for cyclohexane (1) + ethanol (2) at 40kPa

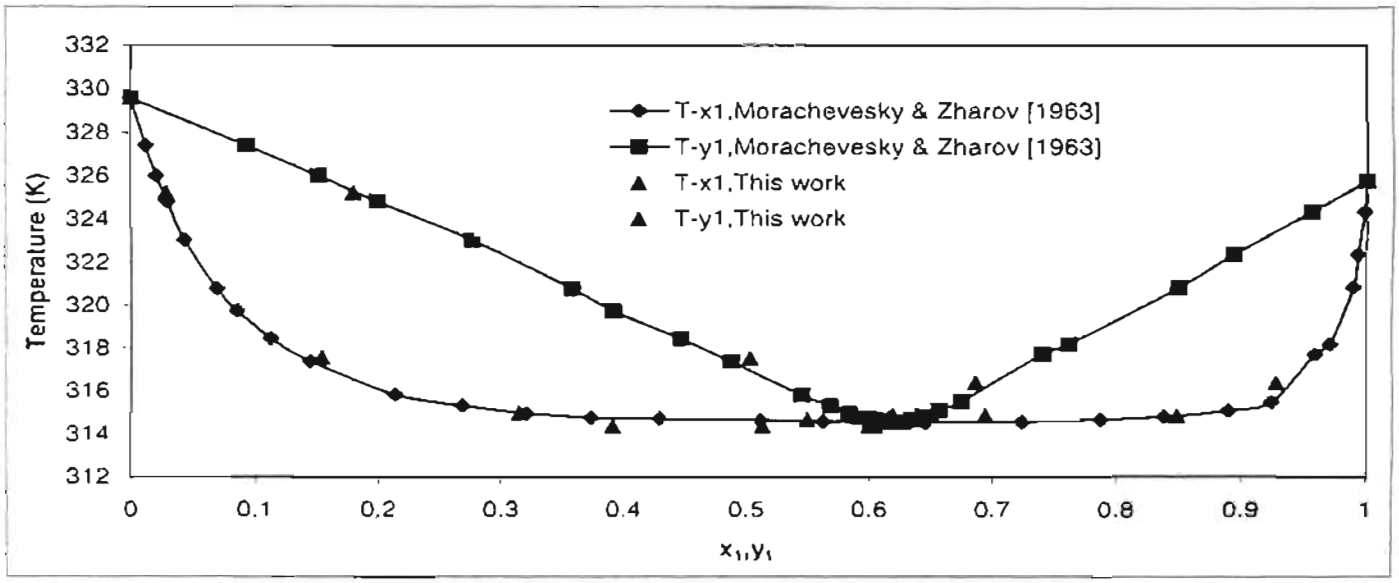

Figure 3-10: T-x-y diagram for cyclohexane (1) + ethanol (2) at 40kPa

The results for the binary vapour-liquid equilibria for the systems involving butyric acid are shown in Table 3-3 and Figures 3-10 to 3-17. All the systems were measured at 14kPa. Representative calibration curves for each of the systems under the operating conditions of Table 3-1 for the Varian 3000 gas chromatograph are shown in Appendix B-4, Figures B-5 to B-10.

Table 3-3: Experimental vapour-liquid equilibrium data for the acids

x_1	y_1	T (K)
Propionic Acid(1) + Butyric Acid(2)		
1.000	1.000	361.32
0.918	0.948	362.76
0.787	0.88	364.60
0.625	0.769	367.40
0.546	0.705	368.73
0.456	0.624	370.70
0.349	0.511	373.15
0.223	0.358	376.10
0.145	0.255	378.10
0.000	0.000	383.40
Isobutyric Acid (1) + Butyric Acid (2)		
1.000	1.000	327.16
0.975	0.987	373.10
0.877	0.927	374.33
0.792	0.865	375.43
0.663	0.731	377.09
0.521	0.584	378.90
0.361	0.407	380.80
0.260	0.299	381.89
0.212	0.251	382.38
0.000	0.000	383.40
Butyric Acid (1) + Isovaleric Acid (2)		
0.000	0.000	396.18
0.034	0.052	394.83
0.082	0.119	394.12
0.196	0.266	392.56
0.521	0.615	388.83
0.683	0.759	387.18
0.810	0.858	385.95
0.895	0.918	385.15
1.000	1.000	383.40
Butyric Acid (1) + Hexanoic Acid (2)		
0.000	0.000	411.41
0.042	0.192	410.47
0.154	0.511	401.95
0.323	0.732	395.86
0.545	0.835	391.62
0.625	0.853	390.39
0.856	0.970	386.82
1.000	1.000	383.40

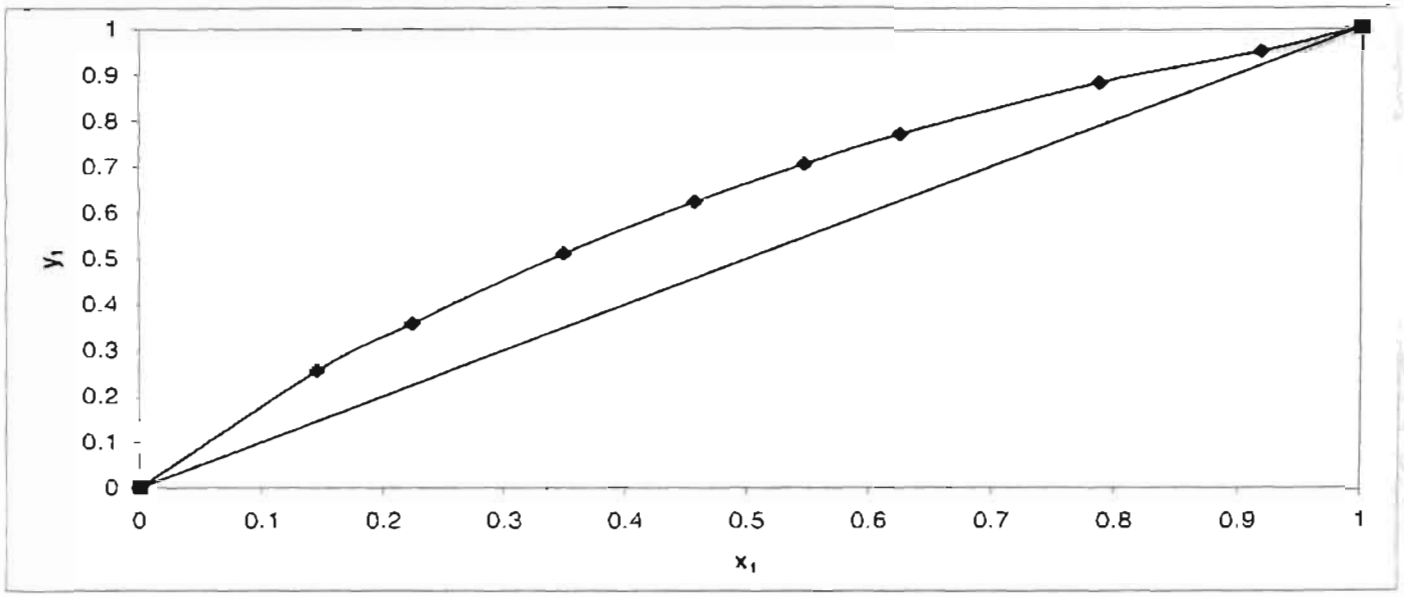

Figure 3-11: x-y diagram for propionic acid (1) + butyric acid (2) at 14kPa

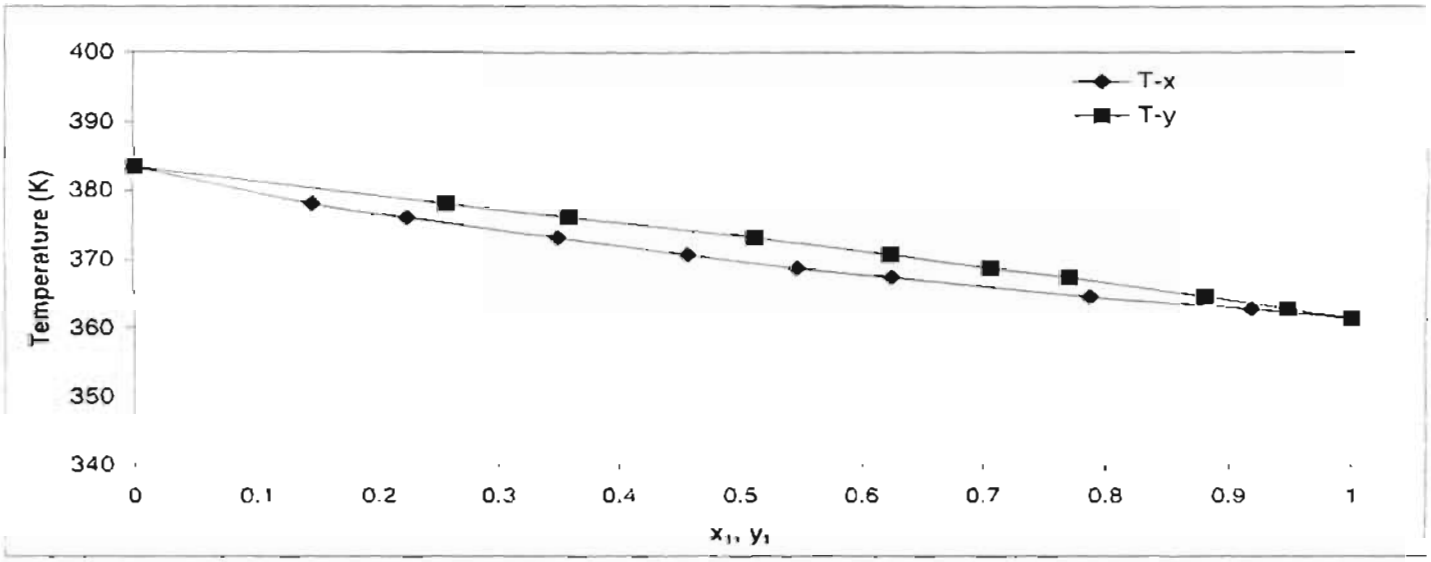

Figure 3-12: T- x-y diagram for propionic acid (1) + butyric acid (2) at 14kPa

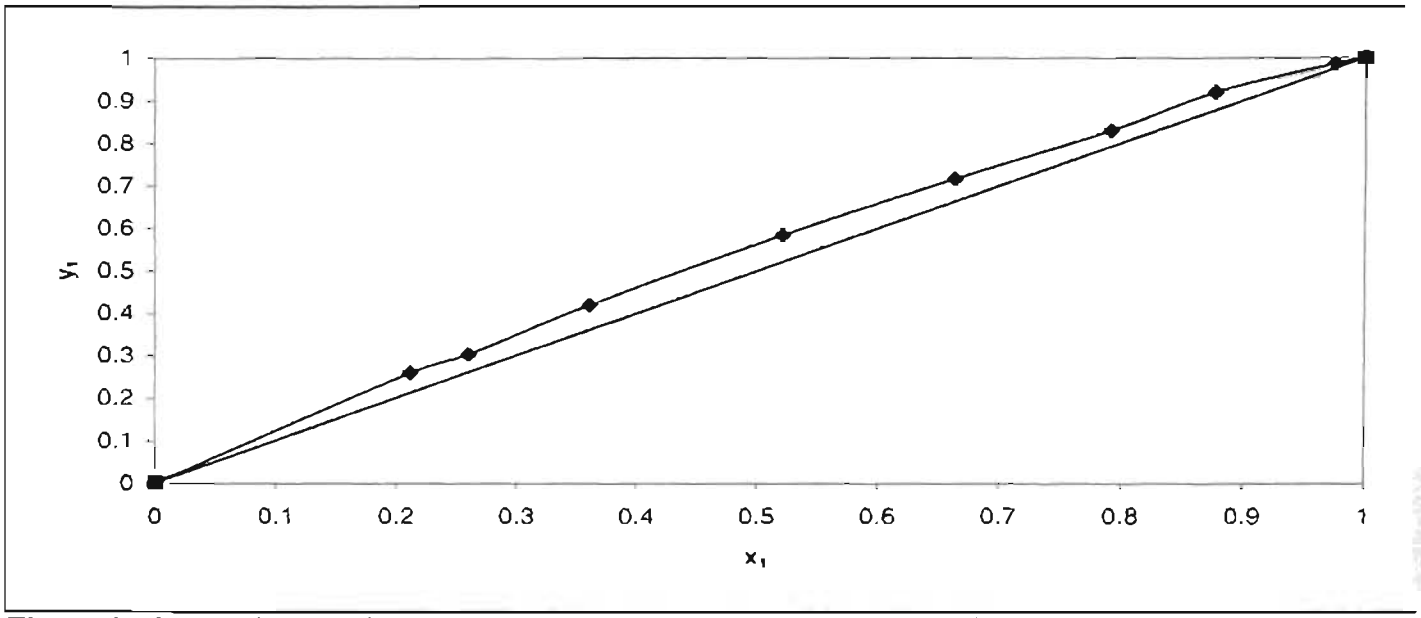

Figure 3-13: x-y diagram for isobutyric acid (1) + butyric acid (2) at 14kPa

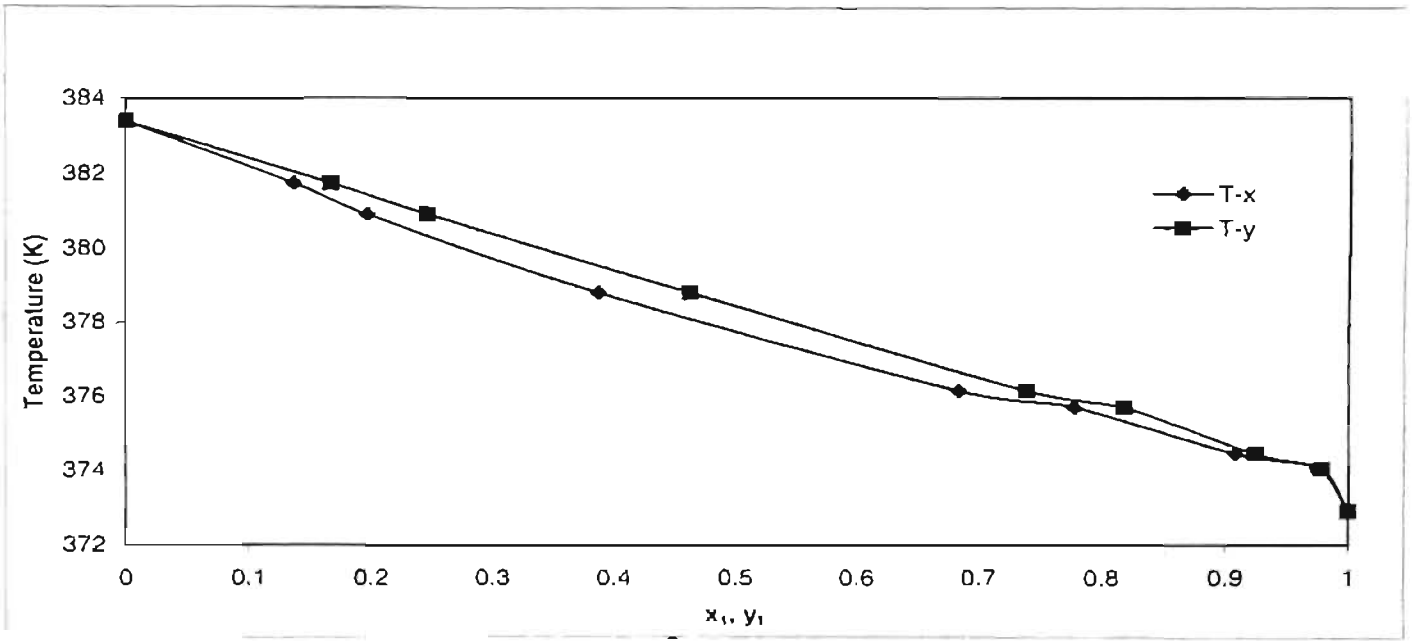

Figure 3-14: T-x-y diagram for isobutyric acid (1) + butyric acid (2) at 14kPa

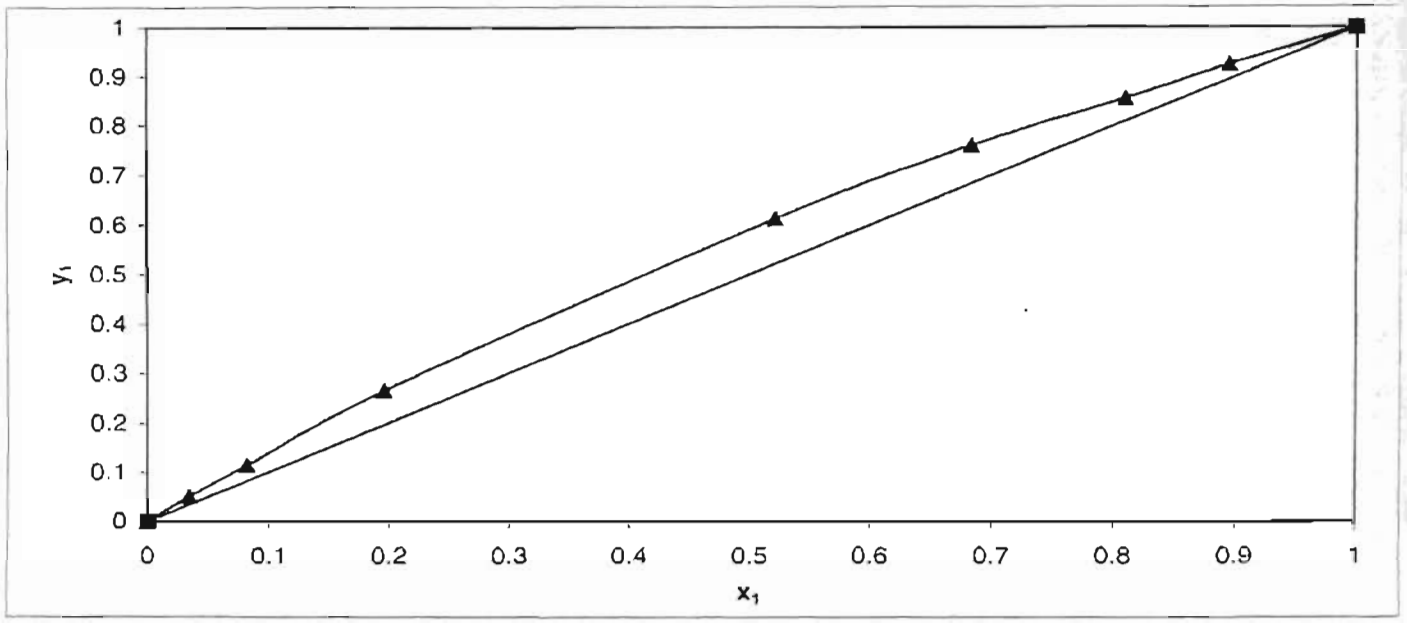

Figure 3-15: x-y diagram for butyric acid (1) + isovaleric acid (2) at 14kPa

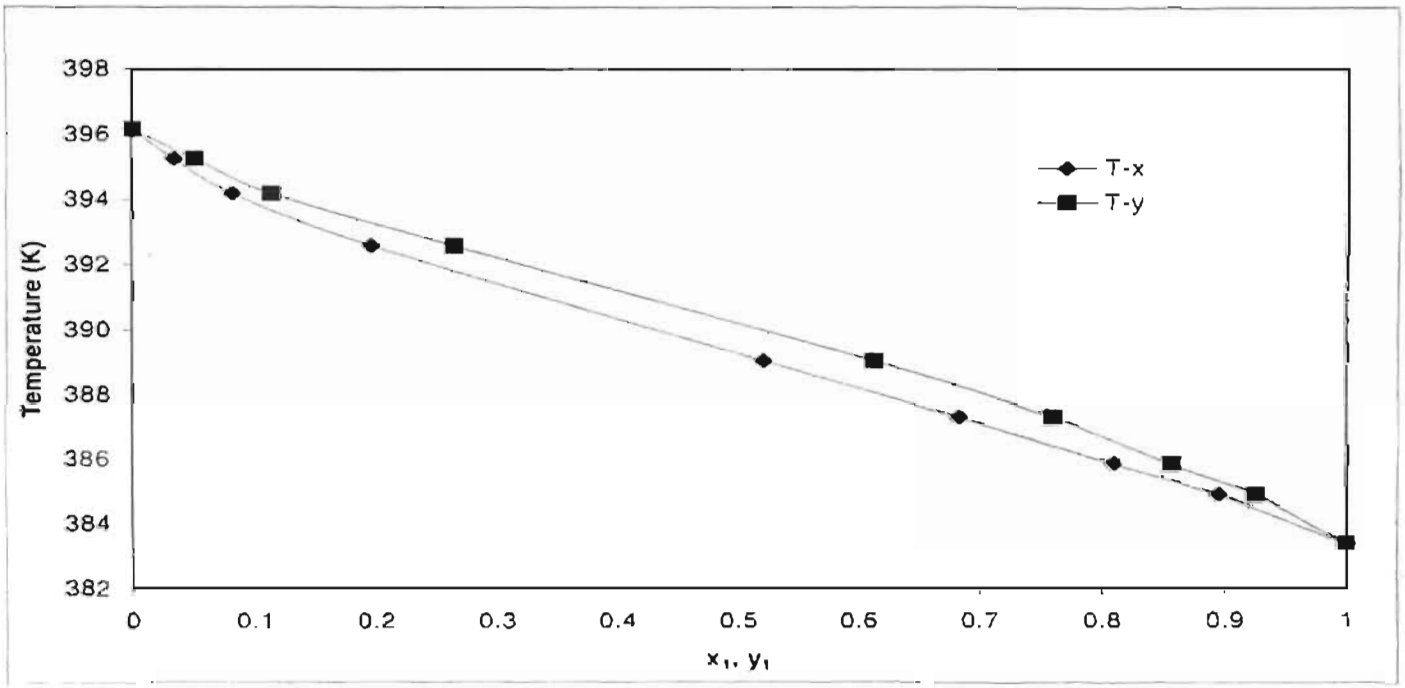

Figure 3-16: T-x-y diagram for butyric acid (1) + isovaleric acid (2) at 14kPa

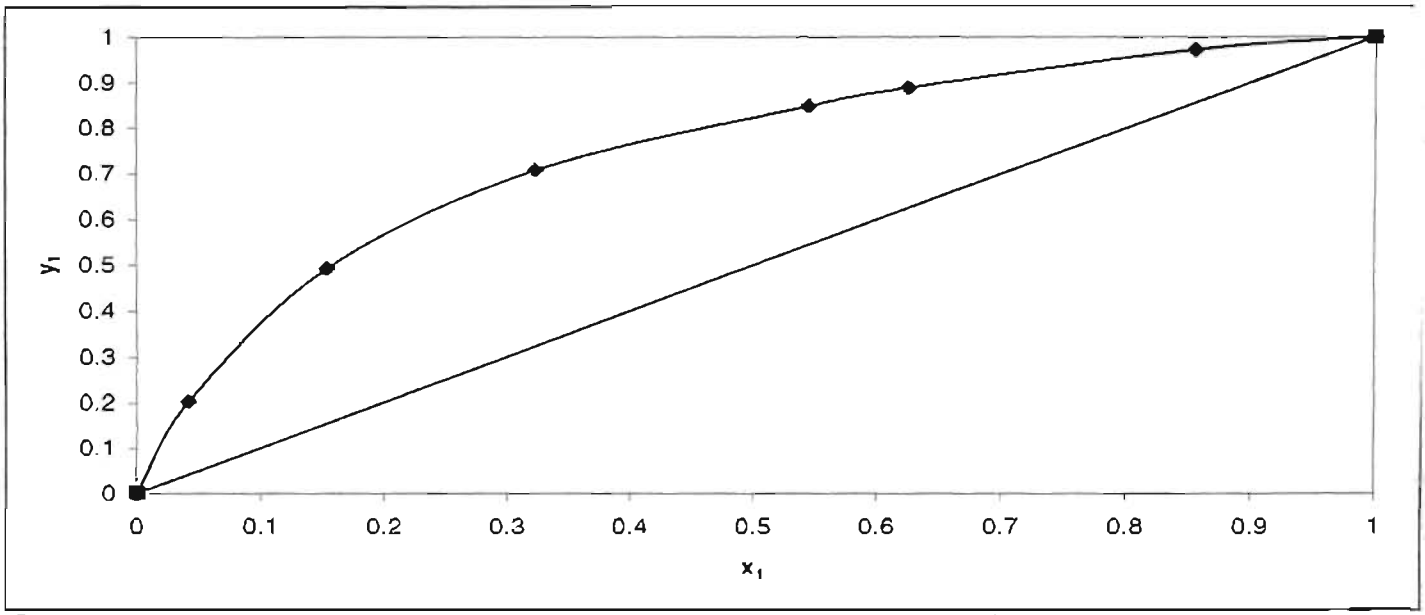

Figure 3-17: x-y diagram for butyric acid (1) + hexanoic acid (2) at 14kPa

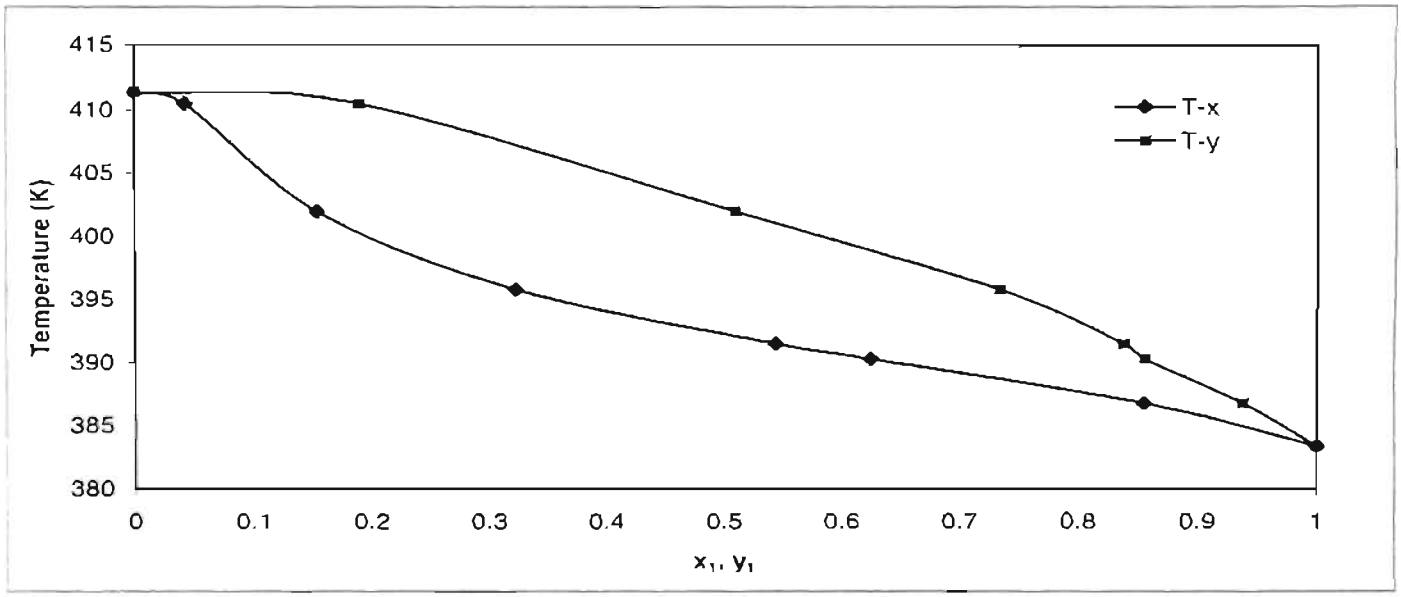

Figure 3-18: T-x-y diagram for butyric acid (1) + hexanoic acid (2) at 14kPa

3.6 Discussion

To obtain accurate VLE data it is crucial that high purity chemicals be used in experimentation. Cyclohexane, ethanol and butyric acid was purchased from Riedel-de Haën, whilst the remaining chemicals were purchased from Fluca Enterprises. The reagents were used without further purification after gas chromatographic analysis showed no significant impurities. The purities of the reagents were also checked by their refractive indexes and comparisons with literature values are shown in Table 3-4.

Table 3-4: Refractive Index and purity of chemicals

Reagent	Refractive index (293.15 K)		Minimum Purity (%)
	Experimental	Reference*	(as stated by supplier)
Cyclohexane	1.4266	1.4265	99.7
Ethanol	1.3611	1.3612	99.8
Butyric Acid	1.3978	1.3980	99.0
Isobutyric	1.3935	1.3930	99.0
Propionic Acid	1.3807	1.3809	99.0
Isovaleric	1.4025	1.4030	98.0
Hexanoic Acid	1.4169	1.4163	99.0

The results for the cyclohexane + ethanol system are listed in Table 3-2 and shown in Figures 3-9 and 3-10. This system was measured at 40kPa. This system was measured to test experimental equipment and procedure and was selected because it is highly non-ideal and has been used by various authors including Joseph [2001]. Figures 3-9 and 3-10 shows excellent agreement between the experimental data and those measured by Morachevsky & Zharov [1963] at 40 kPa. Gmehling and Onken [1977] assessed the quality of the data by Morachevsky & Zharov [1963] and found the data to be thermodynamically consistent.

Because the experimental data for the cyclohexane + ethanol compared well to the literature data (which was also found to be thermodynamically consistent), a high degree of confidence was placed in the performance of the still and the operating procedure. This gave confidence in measuring VLE data for unknown systems.

The results for the binary vapour-liquid equilibria for the systems involving butyric acid are shown in Table 3-3 and Figures 3-11 to 3-18. All the systems were measured at 14kPa, as this was the lowest pressure at which the equipment showed no pressure fluctuations. Once the data has been measured, it is important to access the quality of the measured data. This is usually done by means

of some thermodynamic consistency test. Over the years, many tests have been proposed to test the thermodynamic consistency of the VLE data. Thermodynamic consistency tests for binary low-pressure VLE data is extensively discussed in many thermodynamic textbooks (e.g. Raal & Mühlbauer [1998], Walas [1995] and Prausnitz et al [1986]. For this project the direct test proposed by Van Ness [1995] was used to test the experimental data for consistency. Basically the tests require minimizing the sum of the squares of the difference between the calculated and measured excess Gibbs Energy (which is a function of the activity coefficients) during the reduction of the experimental data. Subsequent calculation of the root mean square (RMS) value of $\delta \ln (\gamma_1/\gamma_2)$ then measures the consistency of the data. For clarity on this test refer to Appendix B-5. According to Van Ness [1995] values greater than 0.2 implies inconsistent data. The calculated root mean square values are listed in Table 3-5 and shows that all the systems measured were thermodynamically consistent except for the system butyric acid + hexanoic acid. The inconsistency for this system could possibly be attributed to the formation of trimers in the vapour phase, which were not considered in calculation of the vapour phase fugacity coefficients.

Table 3-5: Activity coefficient model parameters (g_{ij}-g_{ii}) for NRTL equation and calculated RMS $\delta \ln (\gamma_1/\gamma_2)$ values for consistency test.

System	$g_{12} - g_{11}$	$g_{12} - g_{22}$	RMS $\delta \ln(\gamma_1/\gamma_2)$
Propionic(1) + Butyric Acid(2)	1739.70	-1077.60	0.098
Isobutyric(1) + Butyric Acid(2)	-795.80	1032.50	0.0625
Butyric(1) + Isovaleric Acid(2)	-652.28	807.30	0.0281
Butyric(1) + Hexanoic Acid(2)	422.73	224.11	0.3735

As demonstrated in Figures 3-10 to 3-17 all the systems measured do not exhibit any azeotropes. This confirms that the acids can be separated by distillation. As explained earlier, azeotropes immediately disqualify simple distillation as a separation option. Another, noticeable feature of the x-y diagrams is that as the difference between the acid molecules increase, so does the relative volatilities. The closeness of the isobutyric acid + butyric acid equilibrium curve to the 45^0 line, however suggests that although separation between butyric and isobutyric acids is possible by distillation, it may not be feasible.

To determine whether separation would be feasible or not, the number of stages and reflux ratio need to be calculated. This was done using the process simulator *Hysys* and is discussed in Chapter 4. As explained earlier, for the proper use of *Hysys* an appropriate thermodynamic model must be selected to represent the liquid and vapour phases and ultimately the VLE of the mixture. For this project the NRTL model was used to describe the liquid phase and the virial equations of state for the vapour phase. These models are discussed in earlier sections. The process simulator requires interaction parameters for the NRTL model and these parameters were calculated by modeling the experimental data using the gamma-phi approach as discussed by Raal & Mühlbauer [1998]. VLE data reduction is discussed in many thermodynamic texts and has also been discussed by Joseph [2001] and Harris [2001]. The calculated interaction parameters are shown in Table 3-4. It is important to note that all the calculated curves in Figures 3-19 to 3-26, excluding Figure 3-20, using the NRTL activity coefficient model and the virial equation of state showed good representation of the experimental data. The calculated T-x-y curve for the system isobutyric acid + butyric acid (Figure 3-20) does not predict the experimental data too well. Although the experimental data points were verified in subsequent measurements, the irregularity in the T-x-y curve still existed. The reason for this irregularity therefore could not be explained. However, in spite of this the remaining curves (Figures 3-19 to 3-26) show good agreement between calculated and experimental values and provide confidence when using the NRTL and virial equation of state models in the *Hysys* process simulator to predict VLE for simulating distillation.

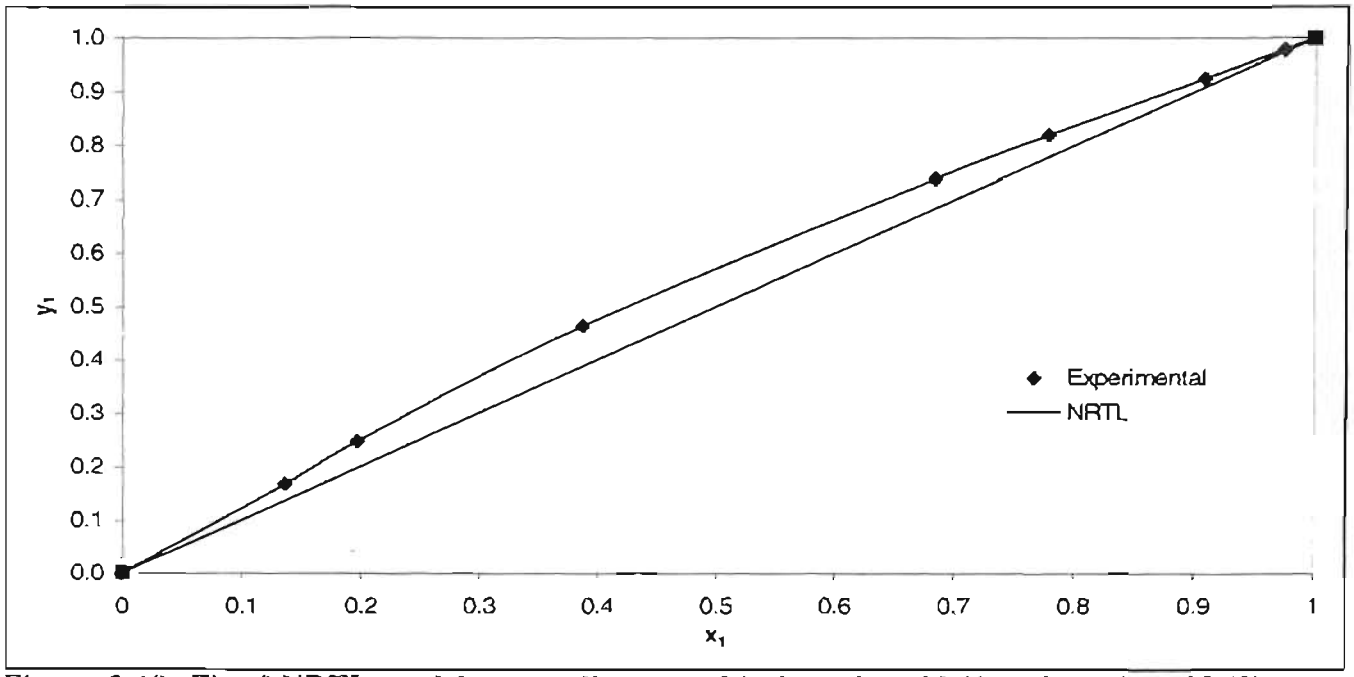

Figure 3-19: Fit of NRTL model to x-y diagram of isobutyric acid (1) + butyric acid (2) at 14kPa

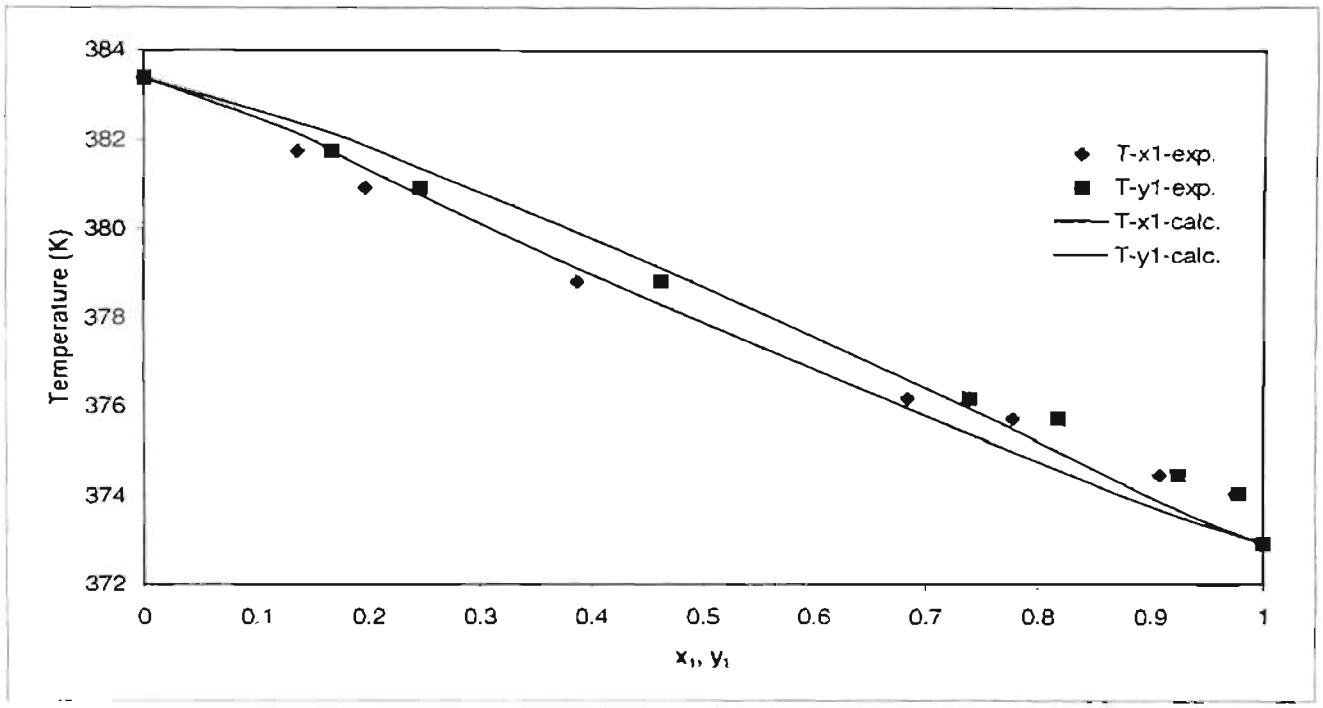

Figure 3-20: Fit of NRTL model to T-x-y diagram of isobutyric acid (1) + butyric acid (2) at 14kPa

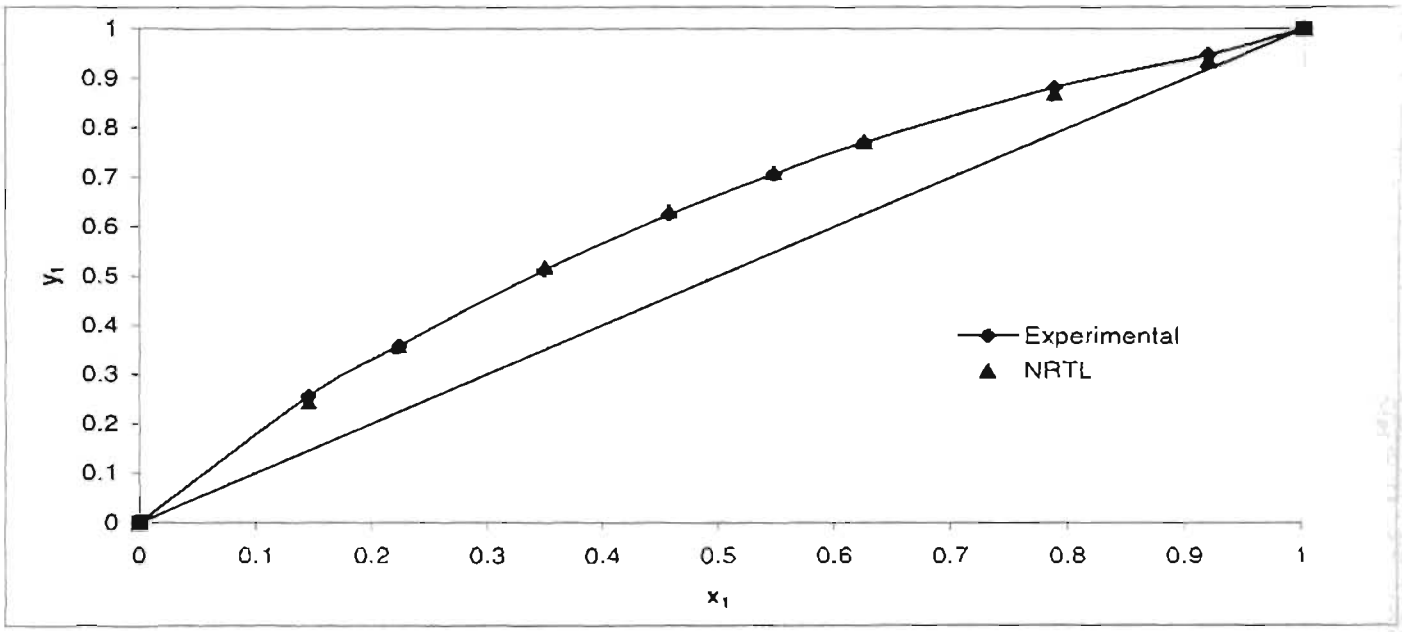

Figure 3-21: Fit of NRTL model to x-y diagram of propionic acid (1) + butyric acid (2) at 14kPa

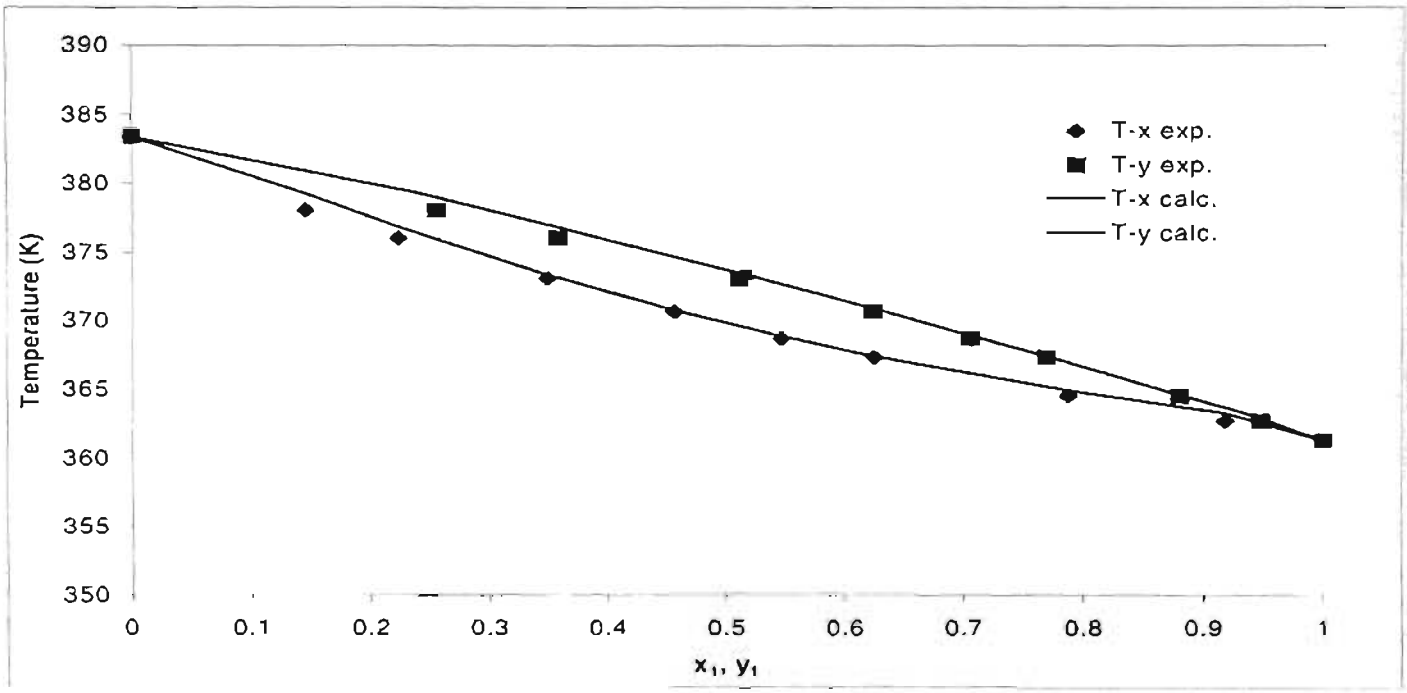

Figure 3-22: Fit of NRTL model to T-x-y diagram of propionic acid (1) + butyric acid (2) at 14kPa

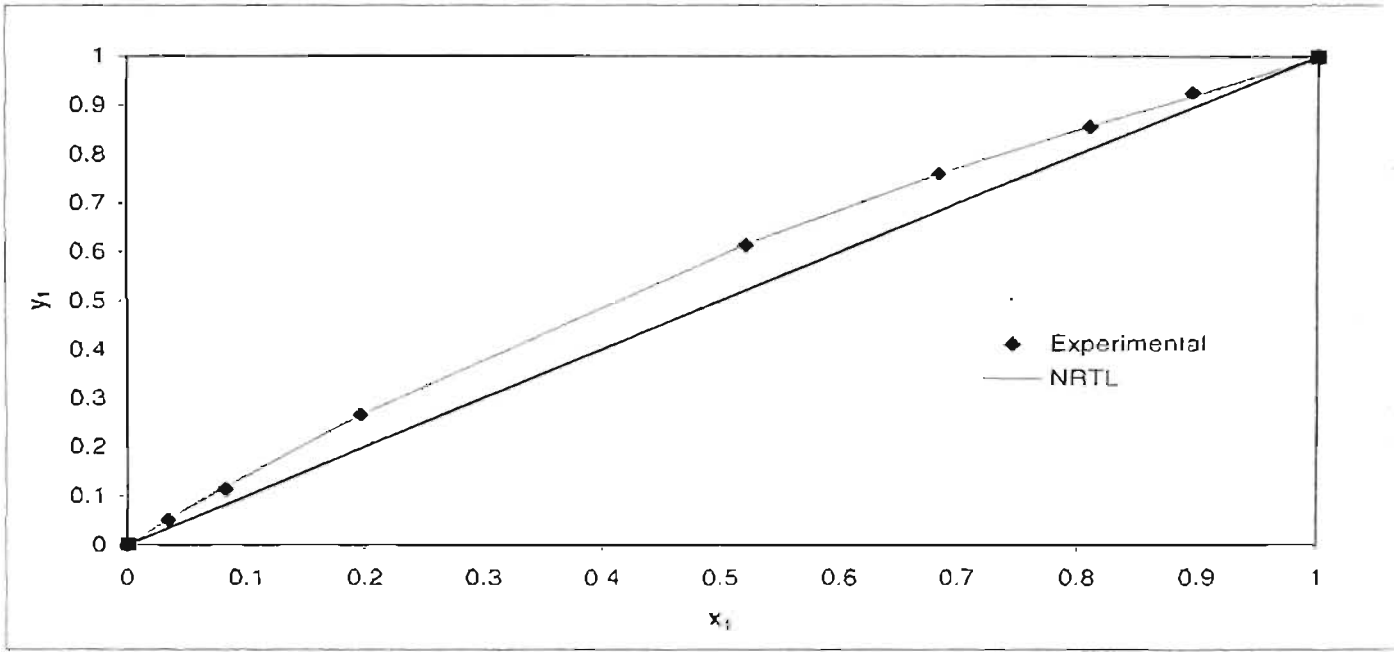

Figure 3-23: Fit of NRTL model to x-y diagram of butyric acid (1) + isovaleric acid (2) at 14kPa

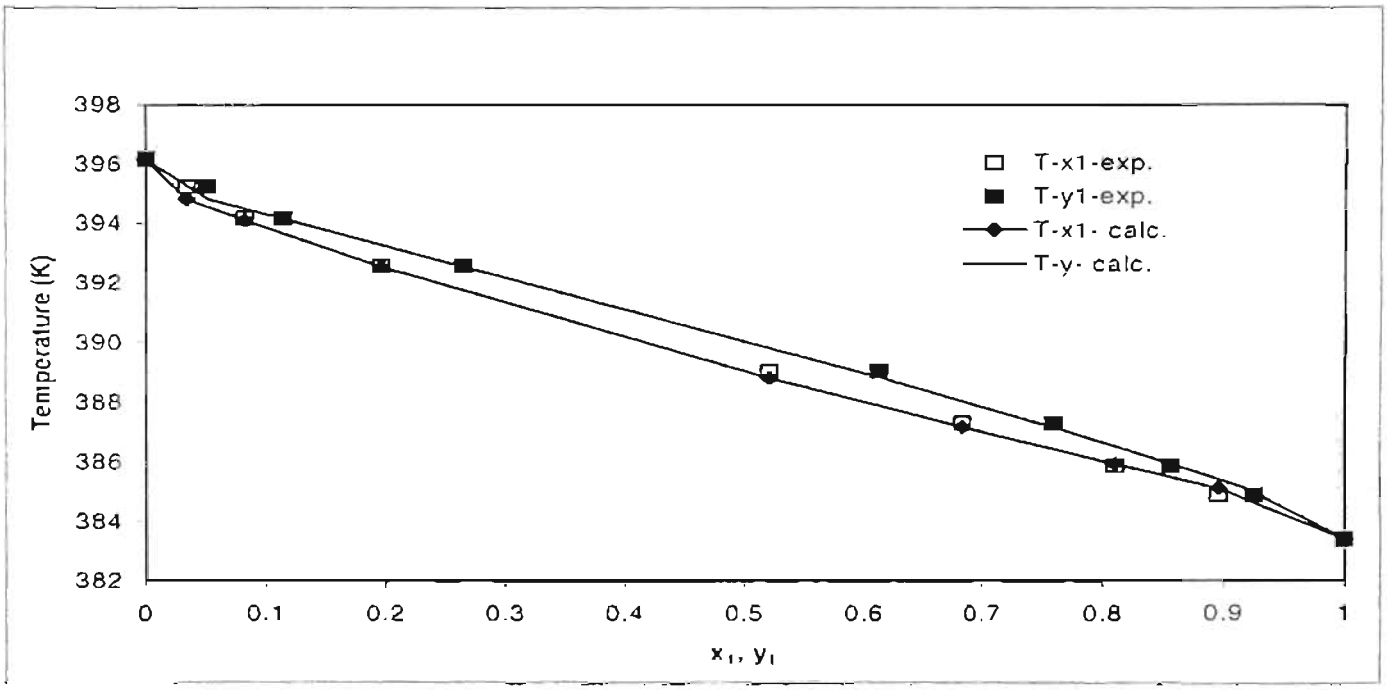

Figure 3-24: Fit of NRTL model to T-x-y diagram of butyric acid (1) + isovaleric acid (2) at 14kPa

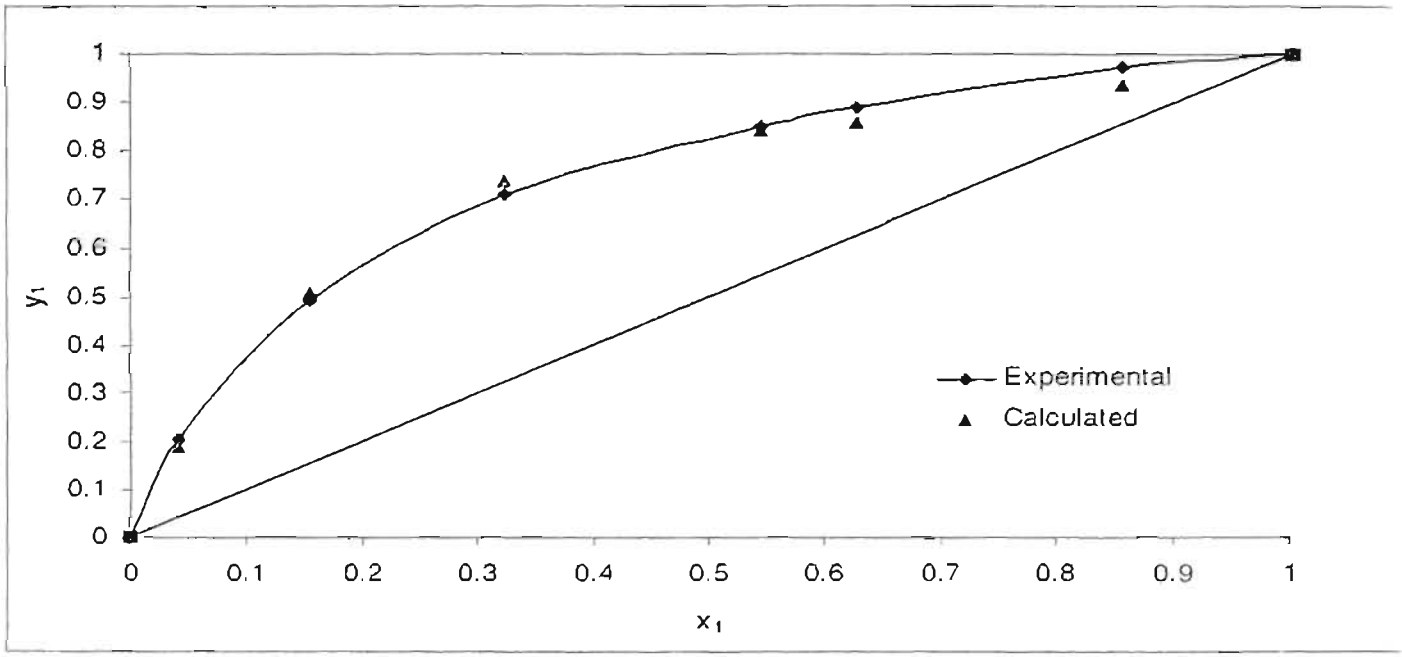

Figure 3-25: Fit of NRTL model to x-y diagram of butyric acid (1) + hexanoic acid (2) at 14kPa

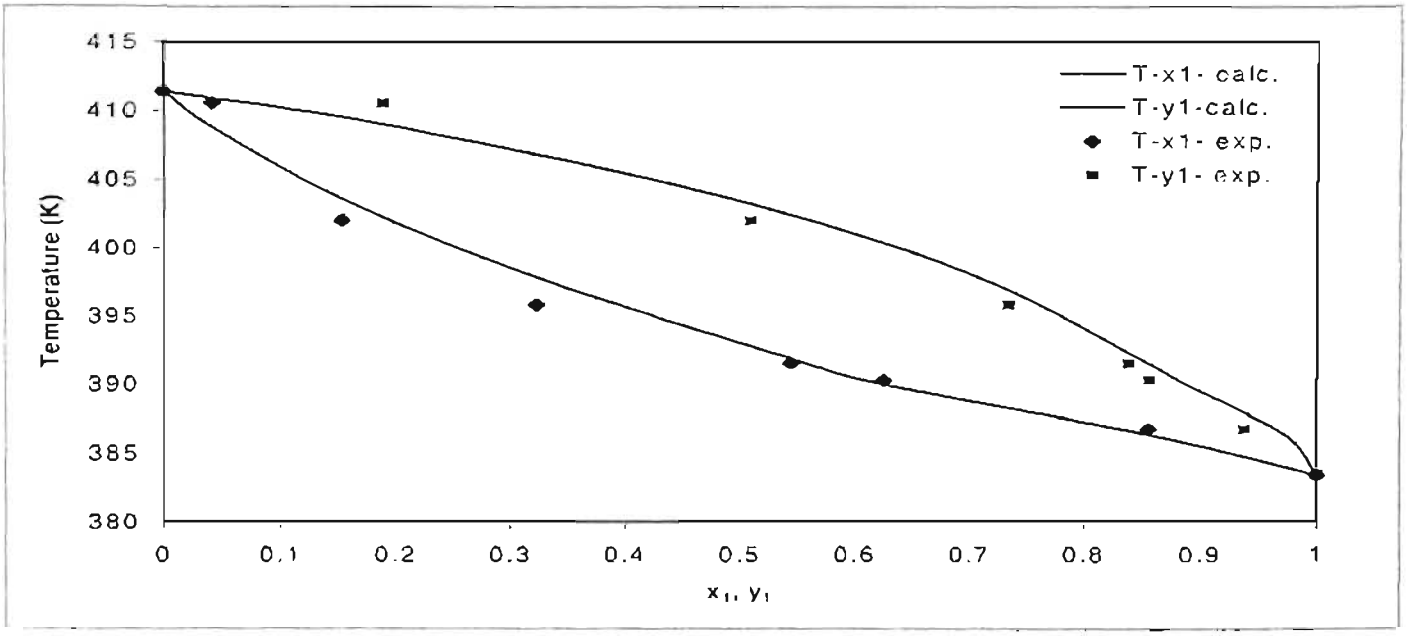

Figure 3-26: Fit of NRTL model to x-y diagram of butyric acid (1) + hexanoic acid (2) at 14kPa

CHAPTER
FOUR

DISTILLATION

In Chapter 2, distillation was chosen as a base case for separation of butyric acid and isobutyric acid from the rest of the stream, for subsequent purification by crystallization.

Distillation is a process in which a liquid or vapour mixture of two or more substances is separated into its component fractions of desired purity, by the application and removal of heat. The extent of separation depends on the difference in volatility between the components. This is directly related to the VLE data of the mixtures. Therefore, proper application of any distillation operation would require appropriate VLE data. Several types of distillation are reported in literature, each of which are designed to perform specific types of separation and each varying in complexity. One broad way of classifying the type of distillation is the mode of operation. This could either be represented by batch distillation or continuous distillation. Continuous distillation is discussed in this chapter.

A typical diagram of a simple continuous distillation column is shown in Figure 4-1. The feed (F) enters the column at a certain flowrate, temperature and pressure. These conditions define the condition of the feed (q). The product from the top of the column is removed as a liquid distillate (D) containing the more volatile components of the feed. The heavier components are removed as the bottoms (B) product. Some of the liquid from the top of the column is sent back to into the column as reflux (L) to increase the purity of the distillate. The reflux ratio (R), which is equal to the ratio of the reflux to the distillate therefore, controls the desired component purity in the distillate.

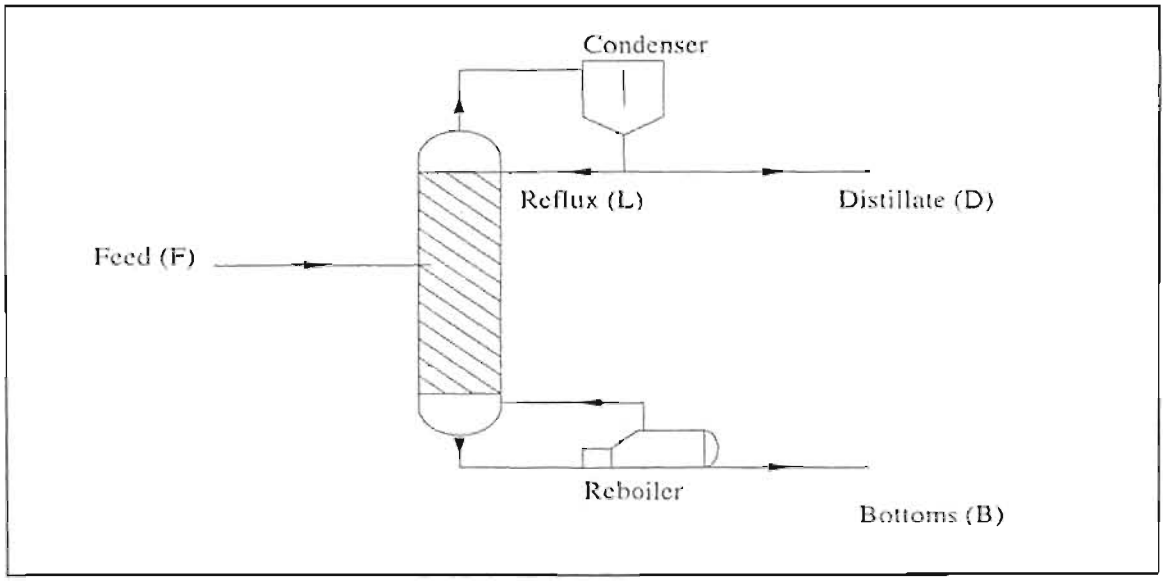

Figure 4-1: Sketch of a typical continuous distillation column.

A flowsheeting program, *Hysys*, was used to simulate the continuous distillation process employed for fractionation of the waste acid stream. However before simulation, VLE unit diagrams, approximate estimation methods and various rigorous methods are briefly reviewed. This is done to judge whether the simulation reflects the real world, understand how the simulator works and analyse the results obtained by a converged simulation.

4.1 VLE unit diagrams

Nowadays, computers are being widely used for distillation design. However, Kister [1992] states that graphical techniques are still widely used in modern distillation technology. He suggests using graphical techniques as an analytical tool to visualise and enable spotting pinched conditions, excessive reflux, incorrect feed points, and nonoptimal thermal conditions of the feed. For this project, VLE unit diagrams (also known as x-y diagrams) were employed mainly for screening distillation as a unit operation and visualizing the results obtained by computer simulation.

The McCabe-Thiele [1925] design method is the most widely used graphical technique in distillation design. By the simple application of this method to an available VLE x-y curve (obtained as discussed in previous chapter), the number of trays required to perform a binary separation is estimated. This method is extensively discussed in most books involving distillation,

viz. Kister [1992], Geankoplis [1993], Treybal [1980] and Perry & Green [1997]. The major assumption for this method is that it assumes constant molar overflow and this implies that:

- The molar heats of vaporization of the components are the same.
- Heat effects (heats of solution, heat losses to and from column, etc.) are negligible.
- For every mole of vapour condensed, 1 mole of liquid is vaporised.

The application of the McCabe-Thiele method in screening distillation for separating butyric acid from isobutyric acid is shown in Figure 4-2. The diagram was constructed with the following specifications:

- Mole fraction isobutyric acid in feed = 0.3
- Distillate composition (isobutyric acid) = 0.9
- Bottoms composition (isobutyric acid) = 0.1
- Feed available as saturated vapour

The above values were selected because they represent the existing feed conditions and the acids are to be produced in purities greater than 90% to be commercially attractive.

A minimum reflux ratio of 17 and 24 theoretical plates is obtained via the McCabe Thiele method. Two important conclusions that immediately eliminate distillation for purification of these two acids are drawn from these results. Firstly, for product purities greater than 90% exceptionally high reflux ratios will be required. This results in higher condenser and reboiler duties and therefore much higher operating costs. Secondly, the actual number of plates will be much greater than the theoretical value. This is because tray efficiencies are not considered in the method. Also, to run at an optimal reflux ratio more than 50 trays would be required to obtain desirable separation. This increases the capital and maintenance costs of the plant drastically. In such instances, Seader & Henley [1998] suggest that distillation not be considered as a base case and other alternatives be investigated.

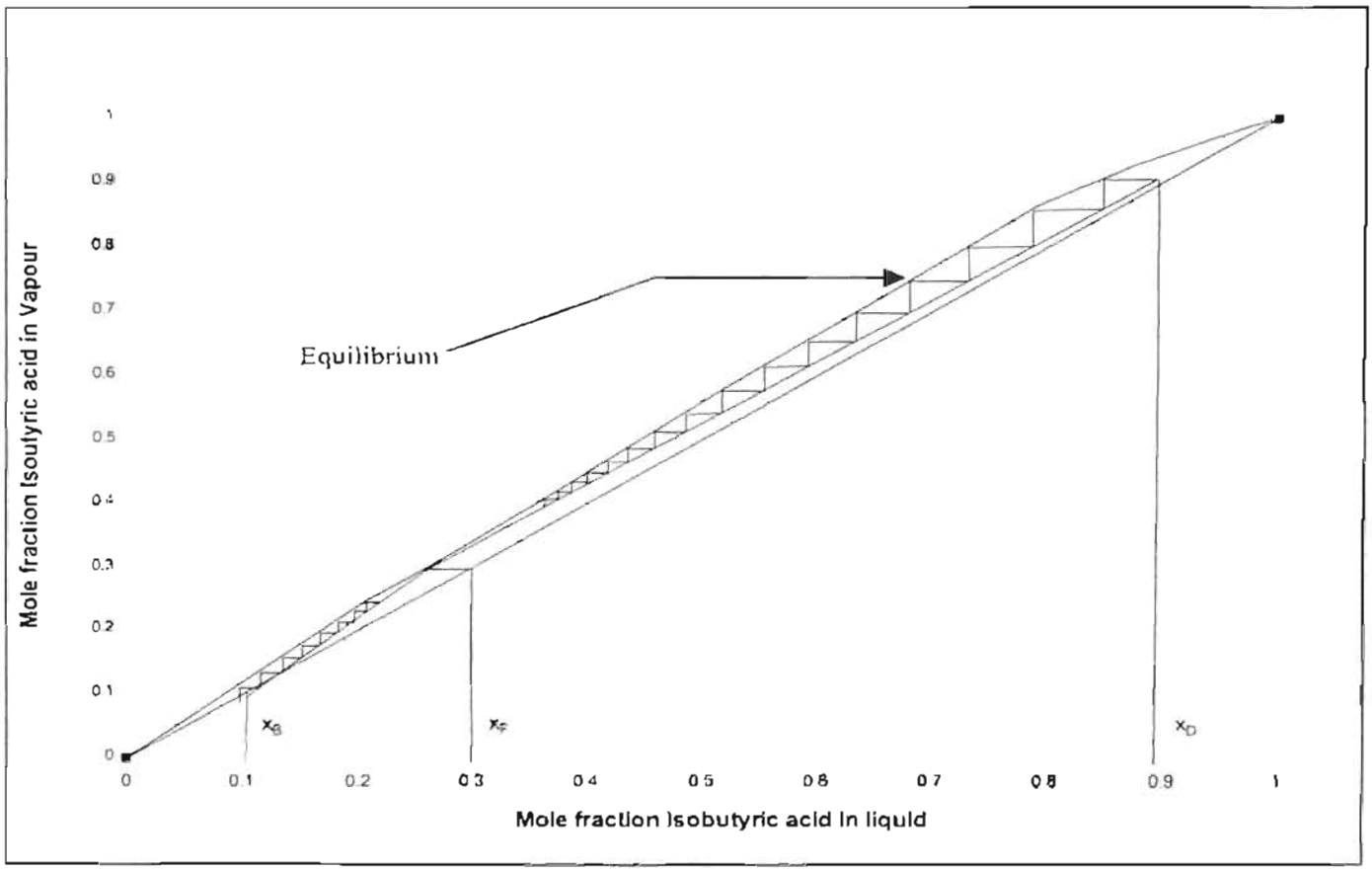

Figure 4-2: McCabe Thiele diagram for separation of Isobutyric acid and Butyric acid

Unfortunately, the McCabe Thiele method is only limited to binary distillation. Hengstebeck [1961] extended the use of x-y diagrams to multicomponent systems. However it is not as widely reviewed as the McCabe Thiele method. Hengstebeck's book [1961] should be consulted for a detailed discussion on his method. Briefly, Hengstebeck [1961] treats a multicomponent separation as a binary separation between the key components. This is based on the fact that in a typical distillation the flowrates of the nonkey components approaches constant, limiting rates in both the rectifying and stripping sections. Therefore, this method should not be used if the presence of non-key components has any significant effect on the volatility of the key components. Hengstebeck diagrams are applied in visualizing simulation results and is discussed in Section 4.5.

4.2 Numerical Short Cut Methods

Graphical techniques (x-y diagrams) are generally applied to visualize a separation problem. Shortcut numerical methods provide a starting point for various rigorous solution techniques. For most process simulators, it is recommended that a short cut distillation be performed prior to simulation by rigorous techniques. Therefore it is important to be familiar with the various shortcut numerical methods which could be used by process simulators. It must be emphasized, however, that shortcut methods are only accurate under the following two conditions:

- The components involved must form an ideal solution with constant relative volatilities.
- The nonkey components do not have volatility values between the two key components.

For this particular project the above conditions are not satisfied.

The two most frequently used empirical methods for estimating stage requirements for multicomponent distillations are correlations published by Gilliland [1940] and by Erbar and Maddox [1961]. These relate the number of ideal stages (N) required for a given separation, at a given reflux ratio (R), to the minimum number of stages (N_{min}) at total reflux and the minimum reflux ratio (R_{min}). For computer use the empirical curve of Gilliland has been replaced by an equation published by Eduljee [1975]. This is shown in Equation (4-1).

$$\frac{N - N_{min}}{N + 1} = 0.75 - 0.75\left(\frac{R - R_{min}}{R + 1}\right)^{0.5688} \qquad (4\text{-}1)$$

To use Equation (4-1) estimates of the number of stages at total reflux and the minimum reflux ratio are needed.

- Minimum number of stages

The two most common methods used to determine minimum number of stages are by Fenske [1932] and Winn [1958]. These methods are known as the Fenske equation and Winn's modification respectively. The mole fraction of the key components in the distillate (D), in the bottoms (B) and the average relative volatility of the key components are related to the minimum number of stages (N_{min}) by Equation (4-2).

This equation was proposed by Fenske [1932], and calculates N_{min} at conditions of total reflux.

$$N_{min} = \left[\frac{\ln\left(\left(\frac{x_{LK}}{x_{HK}} \right)_D \left(\frac{x_{HK}}{x_{LK}} \right)_B \right)}{\ln\left(\alpha_{LK/HK} \right)_{av}} \right] \qquad (4\text{-}2)$$

Winn's modification is similar to the Fenske equation, however it accounts for situations where an average relative volatility cannot be used due to large volatility variations with temperature.

- Minimum reflux ratio

Colburn [1941] and Underwood [1948] derived equations for estimating the minimum reflux ratio for multicomponent systems. Kister [1992] suggests the Underwood method as the most widely used. The equation can be stated in the form (4-3):

$$\sum \frac{\alpha_i x_{i,d}}{\alpha_i - \theta} = R_{min} + 1 \qquad (4\text{-}3)$$

where: α_i = the relative volatility of component i with respect to the heavy key component.

R_{min} = the minimum reflux ratio.

$x_{i,d}$ = mole fraction of component i in the distillate.

and θ is the root mean square of the Equation (4-4):

$$\sum \frac{\alpha_i x_{i,f}}{\alpha_i - \theta} = 1 - q \qquad (4\text{-}4)$$

where: $x_{i,f}$ = the mole fraction of component i in the feed, and q depends on the condition of the feed.

θ is calculated using Equation 4-4, by a trial and error procedure. The value of θ must lie between the values of the relative volatility of the light and heavy keys.

- Feed Stage Location

Estimates of the feed stage location are also required for specification in rigorous distillation methods. Kirkbridge [1944] developed an approximate method for determining feed locations:

$$\frac{N_R}{N_S} = \left[\frac{z_{HK}}{z_{LK}} \left(\frac{x_{B,LK}}{x_{D,HK}} \right)^2 \frac{B}{D} \right]^{0.206} \tag{4-5}$$

where: N_R = number of stages above the feed, including the condenser

N_S = number of stages below the feed, including the reboiler

z_{HK}, z_{LK} = component mole fractions of the heavy key and light key in the feed

B, D = Bottoms and distillate flow respectively.

$x_{B,LK}$ = mole fraction of light key component in bottoms

$x_{D,HK}$ = mole fraction of heavy key component in distillate

The results produced by simulating a shortcut distillation in *Hysys* are shown in Table 4-1.

Table 4-1: Results obtained by shortcut distillation using *Hysys*

Operating pressure (kPa)*	50
Feed flow (kmol/h)*	12.81
Operating reflux Ratio	3.8
Mole fraction light key in bottoms *	0.13
Mole fraction heavy key in distillate*	0.015
Bottoms Flow (kmol/h)	4.60
Distillate Flow (kmol/h)	8.21
Minimum reflux ratio*	2.0
Minimum number of trays	12
Number of theoretical trays	18
Feed stage location (from top)	11

* Parameters used as input in *Hysys* simulation. These values were chosen to obtain an optimum separation between the two key components.

Data for composition and flow of the waste acid stream as supplied Sasol (Table 2-5) were used to define the feed stream for the shortcut distillation. Butyric acid was chosen as the light key component and isovaleric acid as the heavy key component. This is because distillation was selected for separating the lighter acids (Butyric acid and isobutyric acid) from the rest of the waste stream. Since isovaleric acid is closest to butyric acid in composition and volatility it is likely to expect all components less volatile than isovaleric acid (e.g. valeric acid and hexanoic acid) to end up in the bottoms of a distillation column. Similarly, any component more volatile than butyric acid will end up as the top product of a distillation column. The concept of key components is discussed more clearly in Section 4-5. Results obtained by this shortcut distillation procedure are then used to provide estimates for simulations using rigorous solution techniques.

4.3 Rigorous Distillation Calculations

As stated earlier, shortcut distillation calculations are limited to ideal solutions and mostly to binary distillation. Rigorous distillation calculations provide much higher accuracy and accounts for many limitations encountered by shortcut distillation calculations. Most authors, including Holland [1981] and Kister [1992] insist on using rigorous methods for all distillation designs.

A rigorous distillation calculation basically involves solving a group of equations (also known as MESH equations) which describe the steady state behavior of a distillation column. These equations are as follows:

- Material and flow rate balance equations, both component and total.
- Equilibrium equations including the bubble point and dew point equations.
- Summation or stoichiometric equations.
- Heat or enthalpy or energy balances.

Also, when a rigorous calculation is performed, the following is usually specified:

- Rate, composition and condition of the feed.
- Number of stages in the column.
- Feed stage location.
- Separation specifications.
- Column pressure profile.

Over the past years many methods have been developed to solve the MESH equations. Up until recently eight basic classes have been published. These are listed, together with their applications, in Table 4-2. The reader is referred to Kister's book [1992] for a more detailed review on these methods. The inside-out methods have become the most commonly used method in most process simulators because of its robustness and its ability to solve a wide variety of columns.

Table 4-2: The eight basic methods for rigorous distillation calculations

Method	Application
Boiling Point	Narrow boiling, ideal systems
Sum Rates	Widest boiling systems
2N Newton	Narrow boiling systems, few trays
Global Newton	All types of mixtures including nonideal.
Relaxation	Nonideal and reactive systems
Inside-out	Wide variety of boiling systems, including ideal and nonideal systems
Nonequilibrium	Highly nonideal and reactive systems
Homotopy	Difficult to solve columns

For the purposes of this project, the flowsheeting program *Hysys* was available for use and it was programmed using the inside-out method published by Russel [1983]. This method is suggested to work well for systems containing a wide variety of boiling point ranges and for both ideal and nonideal systems. It also allows for a wide variety of specifications including multiple purity. However, there must be a balance between the number of specifications and the variables. One apparent limitation in this method is the failure of the program to account for enthalpy effects of the acids due to associations in the vapour phase.

4.4 *Hysys* simulation

Using a process simulator can be time consuming and frustrating if used in a haphazard manner. More importantly, not understanding the correct procedure can provide incorrect results. The following discussion deals with the procedure used to simulate distillation of the waste acid stream.

a) The most important consideration when starting the simulation is to select the correct thermodynamic package. All future results depend primarily on the thermodynamic package (Carlson [1996]). Since the NRTL equation worked well for modeling the VLE data of carboxylic acids (Chapter 3), it was decided to use the NRTL model for the thermodynamic package.
b) The components present in the waste stream were selected from the *Hysys* database. Most of the components were available on the database. Components heptanoic acid, 2-cyclohexen-1-one, 3 heptene-2-one trans, phenyl butyrate, cyclopentyl acetate, cyclohexyl acetate were treated as hypothetical components, the properties of which were predicted using the UNIFAC method.
c) Experimental binary interaction coefficients for key component pairs were then entered. These interaction coefficients were obtained using experimental VLE data and are discussed in Chapter 3. For distillation it is vital to have interaction coefficients which accurately estimate vapor-liquid equilibrium. Interaction coefficients for the nonkey components were estimated using the UNIFAC estimation technique. Although, this could lead to design uncertainties, the justification for this approach is the assumption that the nonkey components do not affect the volatility of the key components. This is verified in the next chapter concerning batch distillation.
d) The feed stream was then defined using conditions supplied by Sasol (Table 2-5).
e) A shortcut distillation was then run to provide estimates for the number of equilibrium stages reflux ratio and feed tray location. Shortcut distillation methods have been discussed in Section 4-2
f) Finally, the rigorous distillation was simulated with estimates obtained by the shortcut distillation.

4.5 Simulation Results

Results obtained by the converged *Hysys* simulation are shown in Table 4-3. The feed enters the column as subcooled liquid. The product compositions are given in Table 4-4. Figure 4-3 shows changes of vapour composition from stage to stage for the main components in the feed. Figure 4-4 shows the composition profile in the liquid phase.

Table 4-3: *Hysys* simulation results

Average operating pressure (kPa)	45
Maximum operating temperature (^{0}C)	146
Number of theoretical stages	18
Optimum reflux ratio	3.8
Stage efficiency	60%
Recovery of Butyric Acid	89%
Recovery of Isobutyric Acid	98%
Feed Flow-Waste acid stream (m^3/h)	1.33
Distillate Flow - Recovered stream (m^3/h)	0.82
Bottoms Flow- Heavy acids (m^3/h)	0.51

Table 4-4: Feed and product flow rate for main components

	Volume Flows (m^3/h)		
	Feed	Distillate	Bottoms
Propionic acid (n-C_3)	0.02	0.02	0.00
Isobutyric acid (i-C_4)	0.28	0.27	0.01
Butyric acid (n-C_4)	0.51	0.45	0.06
Isovaleric acid (i-C_5)	0.14	0.02	0.13
Valeric acid (n-C_5)	0.14	0.00	0.14
Hexanoic acid (n-C_6)	0.07	0.00	0.07
Heptanoic acid (n-C_7)	0.07	0.00	0.07

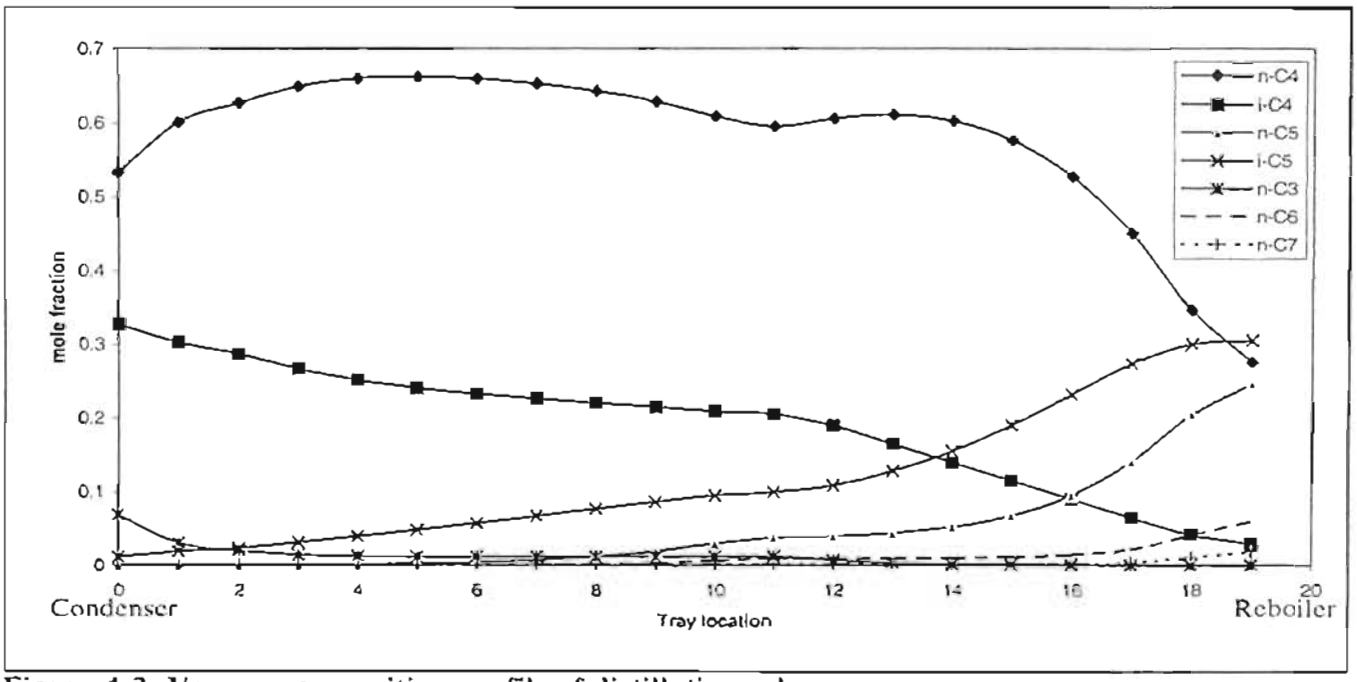

Figure 4-3: Vapour composition profile of distillation column

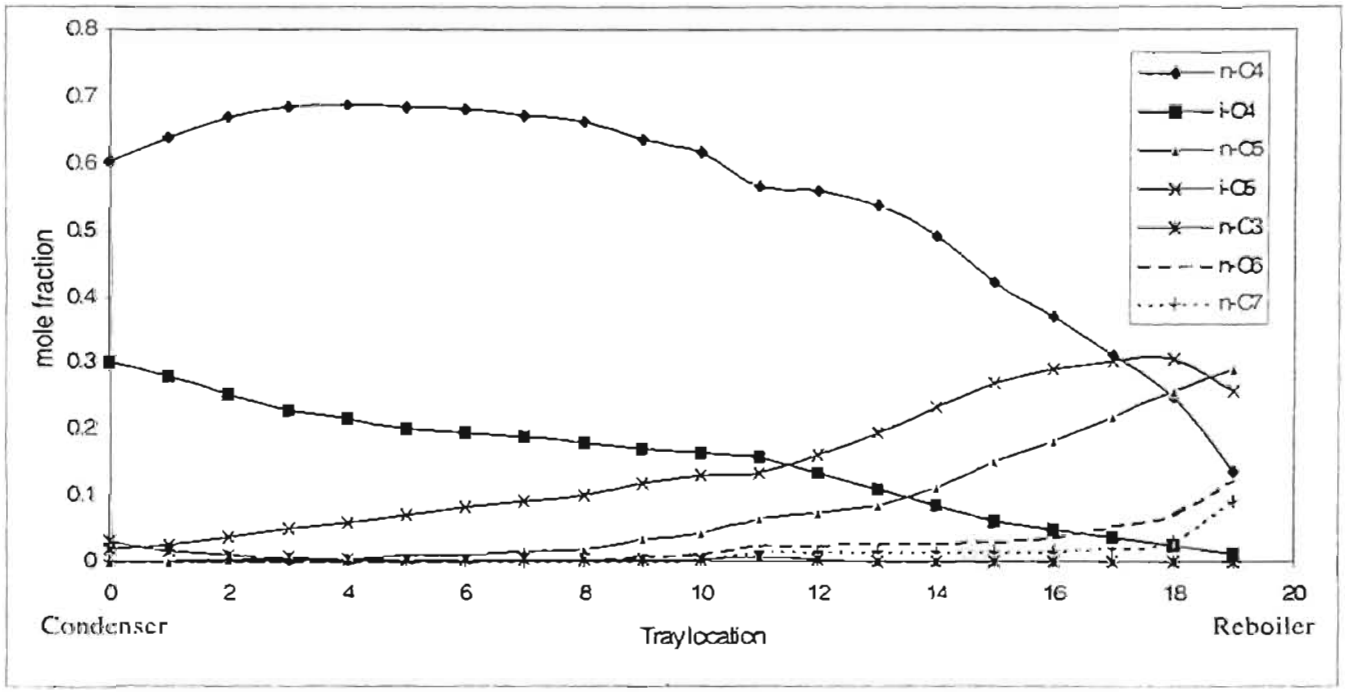

Figure 4-4: Liquid composition profile of distillation column

4.6 Analysis of Simulation Results

The profiles obtained in Figures 4-3 and 4-4 are best interpreted by the volatilities of the various species. Average relative volatilities are as follows:

Table 4-5: Volatility of main components

Component	Volatility (relative to n-C_4)
n-C_3	1.9
i-C_4	1.3
n-C_4	1.0
i-C_5	0.7
n-C_5	0.5
n-C_6	0.3
n-C_7	0.2

The separation is being achieved primarily between butyric acid and isovaleric acid, since, as shown in Table 4-4, most of the butyric acid and almost all of the more volatile components appear in the distillate, while most of the isovaleric acid and almost all of the less volatile components appear in the bottoms. Butyric acid and isovaleric acid are therefore called the key components, the more volatile (butyric acid) being the light key and isovaleric being the heavy key. These components appear in both the distillate and bottoms, while the other components (called nonkeys) are present almost exclusively in either the bottoms or distillate. Propionic acid and isobutyric acid are called light nonkeys since they are more volatile than the light key, while valeric acid, hexanoic acid and heptanoic acid are considered heavy nonkeys as they are less volatile than the heavy key component

Considering Figures 4-3 and 4-4, it is apparent that all components are present in their significant amounts at the feed stage. This is logical since all components are present in the feed which is introduced at that point. Above the feed the heavy nonkeys (n-C_5, n-C_6 and n-C_7) in both the liquid and vapour die out rapidly. Because of their low relative volatility with respect to all the other components present, these components do not enter the upflowing vapour on the stages above the feed to a large extent, and thus are not able to pass upward in the column far above the feed. A few stages suffice to reduce the mole fraction to a very low value. Valeric acid is more volatile than hexanoic acid and heptanoic acid and hence persists for a greater number of stages. Similarly the

light nonkeys, propionic acid and isobutyric acid, are so volatile that they do not enter the liquid to any great extent and thus are unable to flow down the column to any substantial extent. Therefore, these components drop to very low concentrations a few stages below the feed.

Next, it should be noted that the light nonkeys, propionic acid and isobutyric acid, have relatively constant mole fractions in the liquid and vapour above the feed until a point some two to three stages from the top of the column. These two components appear more significantly in the distillate product. The same applies for the heavy nonkeys, with valeric acid, hexanoic acid and heptanoic acid being present in the bottom product at more significant amounts. King [1971] derived a simple equation for estimating the limiting mole fraction of the nonkey components in a zone where it has a constant mole fraction below the feed. For the heavy nonkeys he proposed Equations 4-6 and 4-7 for limiting vapour and liquid compositions respectively.

$$y_{HNK,lim} = \frac{x_{HNK,B}\left(\frac{B}{V'}\right)}{\alpha_{LK/HNK} - 1} \tag{4-6}$$

where: $y_{HNK,lim}$ = limiting vapor mole fraction of heavy nonkey

$x_{HNK,B}$ = bottoms liquid mole fraction of heavy nonkey

$\alpha_{LK/HNK}$ = relative volatility of light key with respect to heavy nonkey

B, V' = bottoms liquid and vapor flow respectively

$$x_{HNK,lim} = \frac{y_{HNK,lim}}{K_{HNK}} \tag{4-7}$$

where $x_{HNK,lim}$ is the limiting liquid mole fraction of the heavy nonkey and K_{HNK} is an equilibrium value (= y_{HNK}/x_{HNK}).

For the light nonkeys King [1971] proposes Equations 4-8 and 4-9 for limiting liquid and vapor compositions respectively.

$$x_{LNK,lim} = \frac{y_{LNK,D}\left(\frac{D}{L}\right)}{\alpha_{LNK/HK} - 1} \tag{4-8}$$

where: $x_{LNK,lim}$ = limiting liquid mole fraction of heavy nonkey

$y_{LNK,D}$ = distillate vapor mole fraction of heavy nonkey

$\alpha_{LNK/HK}$ = relative volatility of light nonkey key with respect to heavy key

D, L = Distillate and reflux flow respectively

$$y_{LNK,lim} = x_{LNK,lim} \times K_{LK} \tag{4-9}$$

where $y_{LNK,lim}$ is the limiting vapor mole fraction of the light nonkey and K_{LK} is an equilibrium value (= y_{LK}/x_{LK}). Table 4-6 below shows values obtained using equations proposed by King [1971] and those from the Hysys simulation. Calculated values compare reasonably with those from profiles in Figures 4-3 and 4-4.

Table 4-6: Limiting compositions for nonkey components.

	Limiting liquid composition		Limiting vapour composition	
Light Keys	a	b	a	b
Propionic acid (n-C_3)	0.012	0.090	0.027	0.02
Isobutyric acid (i-C_4)	0.243	0.194	0.263	0.23
Heavy Keys				
Valeric acid (n-C_5)	0.056	0.050	0.048	0.04
Hexanoic acid (n-C_6)	0.032	0.025	0.022	0.02
Heptanoic acid (n-C_7)	0.029	0.022	0.009	0.001

Notes

a denotes values calculated by King's [1971] equations.

b denotes values estimated from profiles in Figures 4-3 and 4-4.

The mole fraction curves for the two keys, butyric acid and valeric acid, in Figures 4-3 and 4-4 may be understood in light of the above discussion of the nonkey profiles. The keys adjust in mole fraction so as to accommodate fractionation against the nonkeys as well as against one another. Therefore, the mole fraction of butyric acid tends to increase upward, and the mole fraction of isovaleric acid tends to increase downward in the column as a reflection of the fractionation between the two keys. At the very bottom of the column the composition of both the keys tend to start decreasing downward. This is the result of fractionation of the keys with the heavy nonkeys. Similarly, at the very top of the column, there is fractionation of the light nonkeys against the keys.

The temperature profile for the simulation is shown in Figure 4-5. As can be seen the temperature changes most rapidly at the top of the column and in the vicinity of the feed stage location. These are the regions where the compositions of the components are changing the fastest.

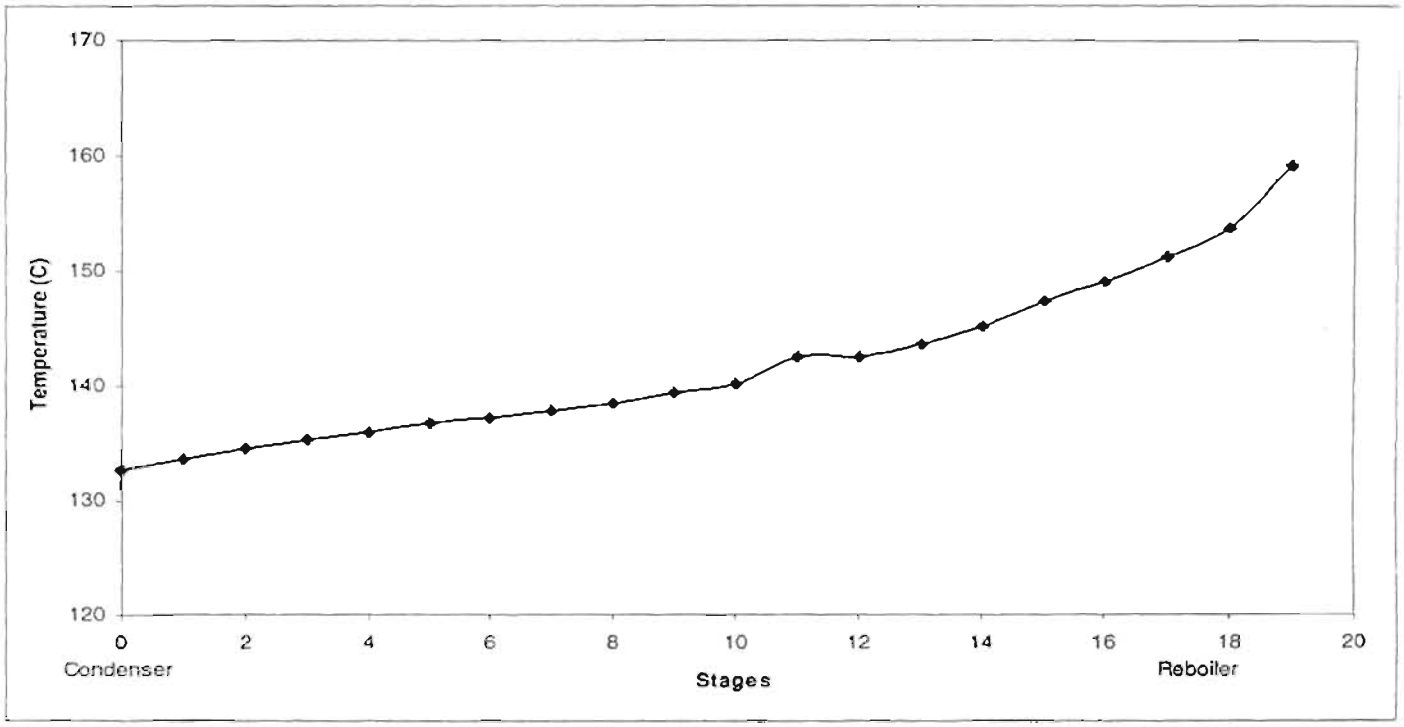

Figure 4-5: Temperature profile for distillation column

Composition profile plots often show the buildup of components in the column, forced there by the heavier or lighter components. These profiles do not show the relative separation between the key components and therefore x-y diagrams are better suited. Hengstebeck [1961] suggested analyzing the performance of a multicomponent distillation in terms of an equivalent binary distillation based upon the keys alone. This procedure has the feature of providing a familiar graphical representation of the distillation process which assists in understanding through visualization.

Hengstebeck's method suggests treating a multicomponent distillation as a binary involving the keys if the flows and compositions are based on the two keys alone. Therefore the composition of the light key ($y'_{n\text{-}C4}$, $x'_{n\text{-}C4}$) is related to the actual composition and are calculated using Equations 4-9 and 4-10 respectively.

$$y'_{n-C4} = \frac{y_{n-C4}}{y_{n-C4} + y_{i-C5}} \tag{4-9}$$

$$x'_{n-C4} = \frac{x_{n-C4}}{x_{n-C4} + x_{i-C5}} \tag{4-10}$$

Figure 4-6 shows the vapour liquid equilibrium curve for the equivalent binary system obtained using Hengstebeck's method. If the nonkeys do not affect the volatility of the key components, it is important that the curve obtained by this method compares favorably with the equilibrium curve obtained experimentally in Chapter 3.

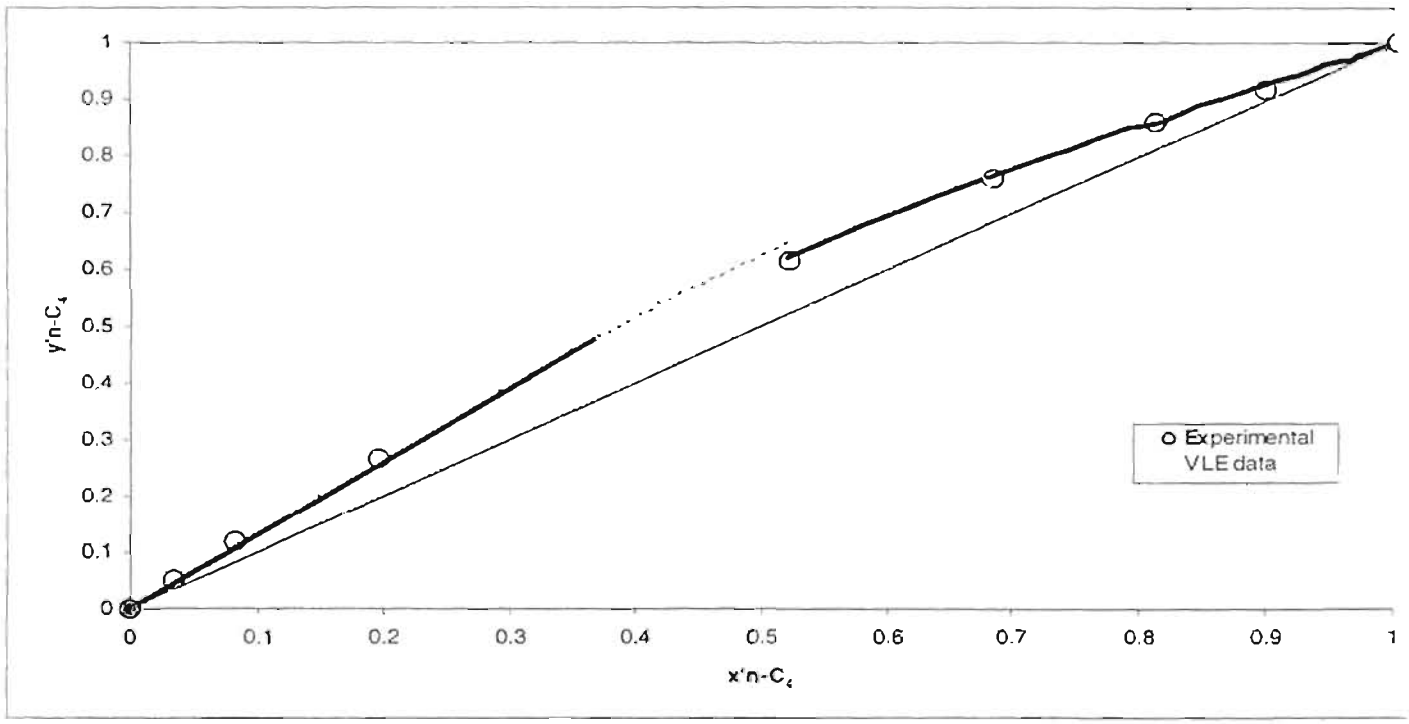

Figure 4-6: VLE curve obtained by Hengstebeck's method

As can be seen in Figure 4-6, there is good agreement between the curve produced by the simulator (shown by the bold line) and the experimental curve (denoted by circles). It must be noted, however, that the simulation in this instance was run at an operating pressure of 14kPa for comparison with experimentally measured VLE data. If the relative volatility of the key components were constant, there would not be a sudden shift in the curve as shown in Figure 4-6. However, in this particular case the relative volatility is a function of temperature. This portion of the curve relates to the position of the feed and as noticed in Figure 4-5 there is a sudden change in temperature at this location.

Rose [1985] suggests checking simulation programs by testing the program sensitivity to parameters. In this way a decision can be made as to which properties need to be determined experimentally. Generally, the most uncertainties in distillation simulations arise from uncertainties

in the VLE data (Nelson et al [1983]). For this project, simulations with an incorrect representation of the VLE data of the key components drastically changed the simulation results. Therefore, the VLE data of the key components were experimentally determined.

Ultimately, the simulation results show that butyric acid and isobutyric acid can be economically separated from the rest of the waste acid stream in a single distillation column. Since distillation is widely practiced and well documented, no experimental work was done to verify the simulation results and continuous distillation experiments should be considered at a pilot plant stage. However, batch work was undertaken to verify the relative separation between the key components. This is discussed in Chapter 5.

CHAPTER FIVE

BATCH DISTILLATION

The result of simulating a continuous distillation column in Chapter 4 showed that separation of butyric and isobutyric acids from the rest of the waste acid stream is theoretically possible. Due to the huge expenses and time required to build a continuous distillation column a simple batch distillation experiment was recommended and undertaken. The main objective of this experiment was to verify separation of the acids using a sample of the waste acid stream obtained from Sasol. Batch distillation also provides invaluable insight into the actual process of distilling the waste acid stream and identifies possible problems that can not be identified by simulations.

Batch distillation as a specific industrial unit operation, has received renewed interest during the last few years (Furlonge et al [1999]). This is especially so since there has been an increase in the market for small volume, high value, specialty chemicals. Also batch distillation is more flexible than other unit operations because the same equipment can be used for several products and operating conditions. Batch distillation is discussed in many texts involving distillation viz. Perry [1998], Seader & Henley [1998] and Kister [1992]. The reader is referred to these texts for in-depth coverage of this topic. In this Chapter, batch distillation equipment and experimental procedures are discussed. Experimental results are also presented and discussed.

5.1 Experimental Setup

The batch distillation equipment set-up is shown in Figure 5- 1. The various components of the experimental set-up include a Batch Distillation still, Schott 10 *l* and Pyrex 5 *l* ballast flasks, a TECHNE cold finger, a Fischer VKH 100 pressure controller, a LABOTEC water bath with glycol - water mix and two pumps (a vacuum pump and a water recirculation pump).

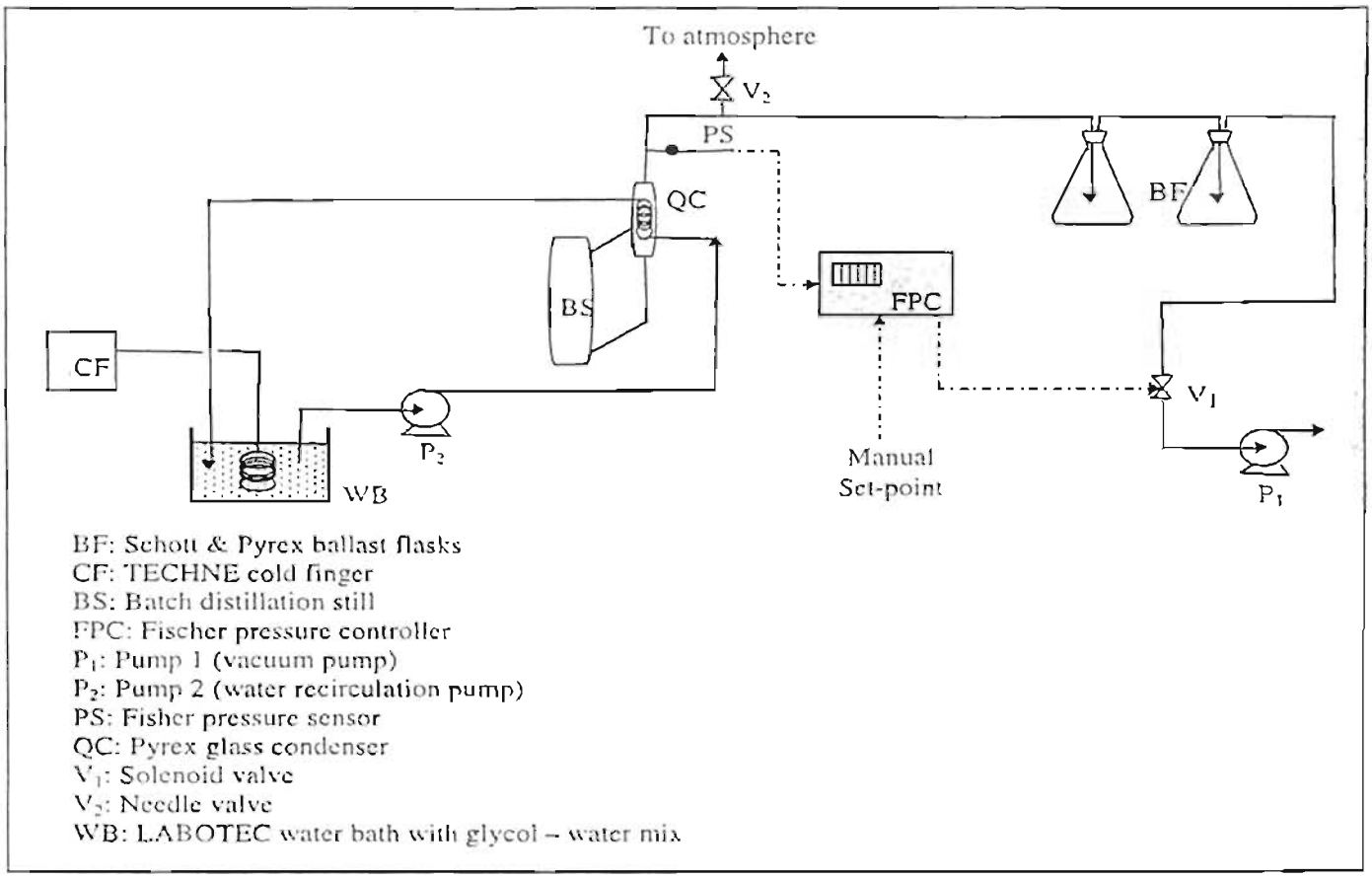

Figure 5-1: Experimental set-up for batch distillation.

5.1.1 Batch Distillation Apparatus

There are various types of batch distillation column configurations. Figure 5-2 shows the various types of column configurations that are most commonly used.

The simplest form of a batch still (Figure 5-2a) consists of a heated vessel (pot or reboiler) and a condenser. No trays or packing are used; therefore these stills do not provide separation to any great extent. For a more detailed discussion on these types of columns the reader is referred to the text of Seader & Henley [1998].

By analogy with continuous distillation columns, the conventional batch distillation column is known as a "batch rectifier" (Figure 5-2b). This column consists of a heated vessel (pot or reboiler), a condenser and a tray or packed column (rectifying column). The rectifying column concentrates the more volatile components in the vapor. The feed mixture is introduced at the bottom and the desired product is removed through the top of the column (distillate).

In contrast to a "batch rectifier", an inverted batch distillation column (Figure 5-2c) concentrates the less volatile components in the liquid. This column is also known as "batch stripper", where the feed mixture is introduced at the top of the column and the desired product is removed from the reboiler (bottoms). The reader is referred to work by Bernot et al [1991] for a comprehensive review on this type of column.

The most recent development in the configuration of batch distillation columns is the middle vessel batch distillation column (Figure 5-3d). This type of column was first proposed by Devyalith et al [1981] and is extensively reviewed by Safrit [1996] and most recently by Barlo & Bottean [1997]. In this type of column the feed is split between the condenser and the reboiler with the more volatile products being removed as distillate and the less volatile products being removed as bottoms simultaneously.

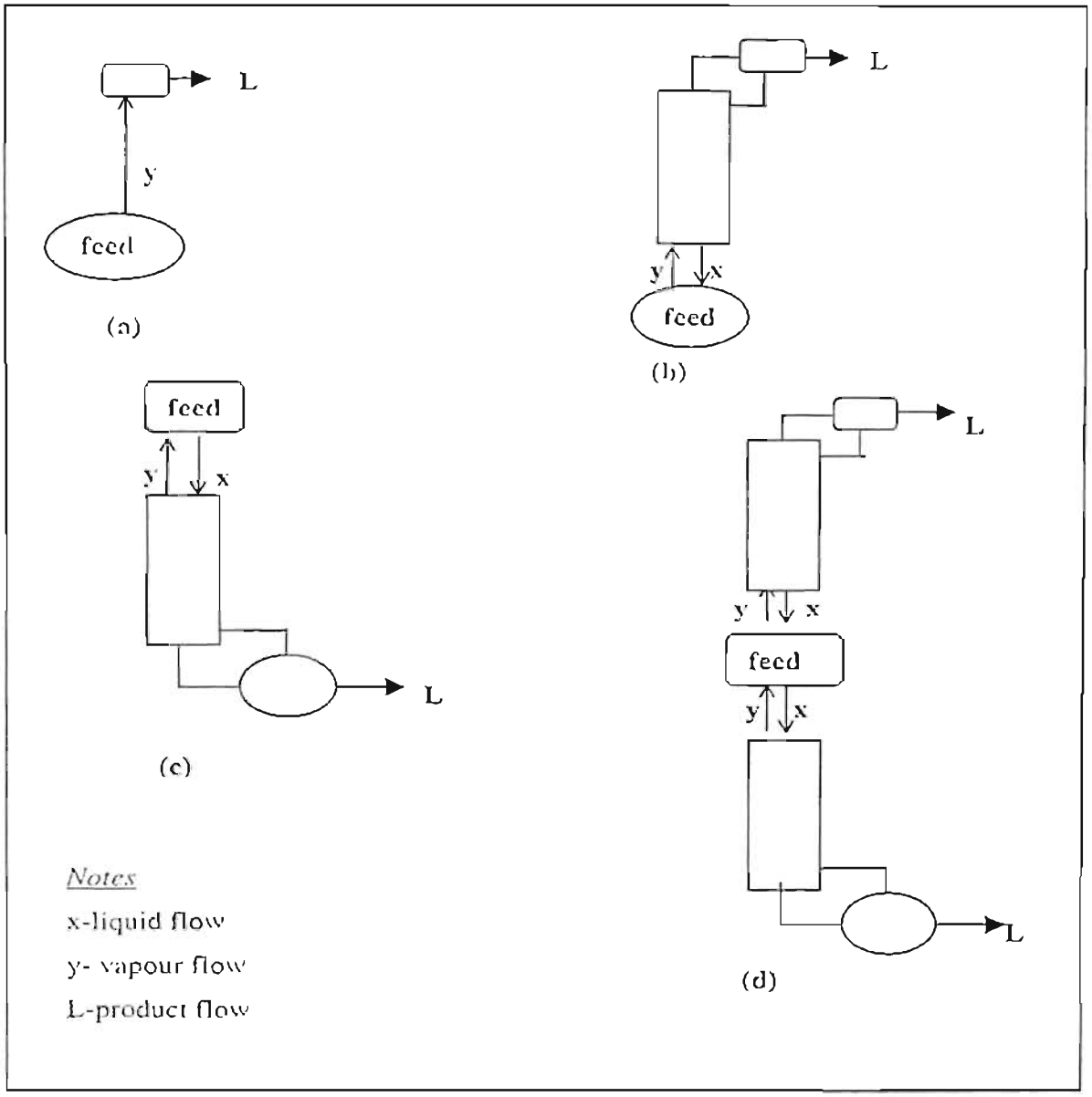

Figure 5-2: Batch distillation – (a) simple distillation, (b) batch rectifier, (c) batch stripper, (d) middle vessel column.

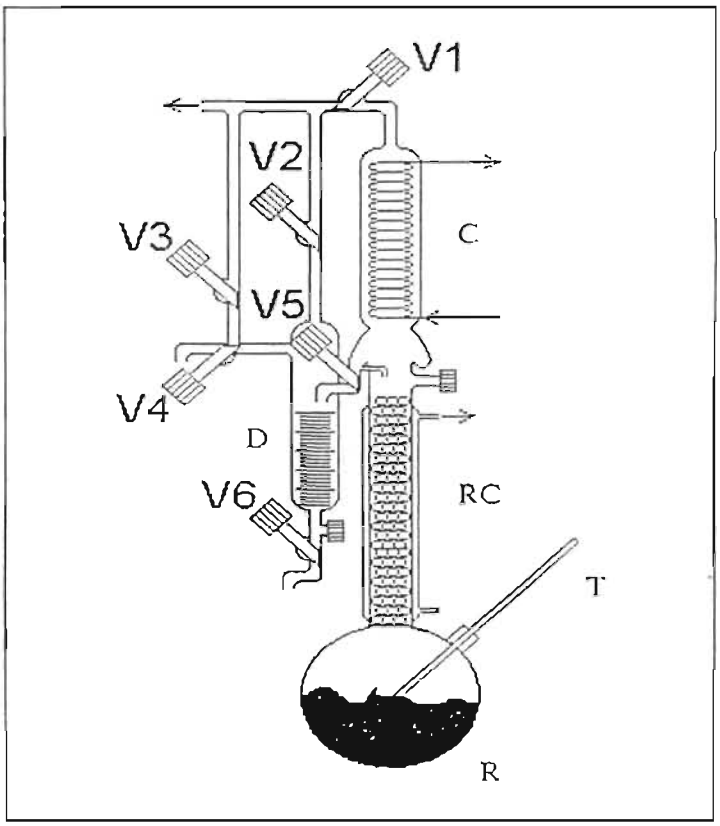

Figure 5-3: Batch Distillation apparatus.

For the purposes of this project, a batch rectification still was used (Figure 5-3). This still was used in experimentation since the aim of batch distillation in this project was to recover butyric and isobutyric acids, which are the more volatile components. The still consists of a rectifying column (RC) with a condenser (C), reboiler (R) and distillate collecting equipment (D). The rectifying column is a vacuum jacketed glass apparatus equipped with stainless steel packing providing an equivalent of four theoretical trays. The reboiler is electrically heated and a glycol-water mixture cools the condenser. A thermometer (T) is also located in the reboiler. The flow of liquid from the condenser can be split into (a) reflux to the column and (b) overhead distillate product, which fills into the distillate collecting equipment. This is achieved by opening or closing valve V_5.

5.1.2. Temperature and pressure measurement

A thermometer present in the reboiler measured the temperature. The pressure was monitored with a Fischer pressure transducer. The accuracy in temperature and pressure measurements was not investigated in the batch distillation experiments, as the main aim of the experiments was to determine if separation of the acids is possible.

5.1.3. Pressure control

For isobaric operation the pressure was maintained at a constant set-point that was controlled by a Fischer pressure controller which either vents to atmosphere through needle valve V_2 or connects to the vacuum pump through solenoid valve V_1 (These valves are shown in Figure 5-1). By actuation of the solenoid valve, leading to a vacuum pump or atmosphere, the pressure in the still was controlled. Control of the still pressure was estimated to be within ± 0.1% of the set-point pressure.

5.1.4. Composition analysis

The compositions of the distillate samples were determined using a Varian, model 3300, gas chromatograph (GC). The column used was a 30-m megabore capillary column of 0.53-mm diameter with 007-FFAP on fused silica. The flame ionisation detector was used.

5.2 Experimental Procedure

The apparatus was first cleaned and tested for leaks in a similar procedure described in Chapter 3. Once this was successfully completed the actual batch distillation experiment was conducted.

5.2.1 Start-up

A sample of the waste stream as obtained from SASOL was first analysed by the gas chromatograph to determine the composition of the waste acid stream. The reboiler was then filled with 450ml of this sample. The pressure controller was then switched on and a pressure of 250kPa was then set. At this point the vacuum pump was switched on, after which the solenoid valve (V_1 in Figure 5-1) was open. This decreased the pressure towards the set-point pressure. The cold finger (Figure 5-1) was then turned on to maintain a temperature of 15^{0}C in the water bath. The cooling liquid pump (P_2 in Figure 5-1) was also switched on.

5.2.2 Heating of the fluid in the Reboiler

Once the system had reached the set-point pressure, the power input to the reboiler was switched on. The power input was then gradually increased to prevent the liquid in the reboiler from boiling too fast and therefore flooding the column. The liquid was brought to boil with the system under total reflux. This meant that the reflux valve V_5 (Figure 5-3) had to be closed. A cycling procedure was then used to set the pattern for column operation. Operating procedures have been developed by Bogart [1937], Smoker & Rose [1940] and Scrodth et al [1967]. For this project the method developed by Scrodth et al [1967] was adopted as it is recommended for difficult industrial separations. The unit was then operated at total reflux until equilibrium was established.

5.2.3 Sampling and analysis

Samples were withdrawn according to the following established procedure (developed by Scrodth et al [1967]:

- Once equilibrium was established at total reflux, reflux valve V_5 (Figure 5-3) was fully open. A 50ml distillate sample was then removed as total draw-off for a short period of time, after which the column was again returned to total-reflux operation until equilibrium was established.

The distillate samples were then analysed using a gas chromatograph. The procedure for operating the gas chromatograph is discussed in Chapter 3 and the operating conditions are shown in Table 5-1. This cycle was repeated until the desired recovery and separation was obtained.

Table 5-1: Gas chromatograph operating conditions

Gas chromatograph condition	
Nitrogen carrier gas flow rate [ml/min]	30
Oven temperature Profile	
Initial temperature [^{0}C]	130
Hold Time [min]	30
Temperature ramp [^{0}C/min]	5
Final temperature [^{0}C]	180
Hold Time [min]	15
FID detector	
Temperature [^{0}C]	200
Attenuation	8
Range	10
Hydrogen flowrate [ml/min]	30
Air flow rate [ml/min]	300
Injector temperature	220

5.3 Results and Discussion

Two separate batch distillation experiments were conducted, each with different objectives.

The first batch distillation (batch 1) was an attempt to recover more than 80% of the butyric and isobutyric acids from the waste acid stream. The operating conditions for distillation of this batch are shown in Table 5-2. The lowest pressure at which the system showed no fluctuations was 25kPa and was therefore set as the operating pressure.

Table 5-2: Operating conditions for distillation of first batch

Pressure	25 kPa
Average reboiler temperature	130°C
Reboiler size	500 ml
Temperature - cooling liquid	15°C

The sample from SASOL'S waste acid stream is a dark, viscous liquid. The experiment was run over six hours during which time a colorless, less viscous liquid was produced from the initial sample of Sasol's waste stream. However, at the end of the run some form of black tar had formed in the reboiler. Systems containing materials that form tars plug or foul continuous distillation columns thus rendering them inoperable. The Hysys simulations discussed in Chapter 4 could not have predicted this important factor. However, it is believed that these tars could have been formed by the decomposition of certain materials present in the waste acid stream in smaller compositions and can be eliminated by running a continuous distillation column at a lower pressure.

Due to the many components present in the waste stream, it was not possible to calibrate the gas chromatograph as discussed in Chapter 3. Therefore, relative concentrations were used to determine compositions. Results at the end of the first run (batch 1) are shown in Table 5-3.

Table 5-3: Material balance for distillation of first batch*

Component	Reboiler		Distillate (ml)	% Recovery
	Start (ml)	End (ml)		
Propionic acid	15.0	4.4	10.6	71
Isobutyric acid	63.0	6.6	56.4	90
Butyric acid	178.0	16.5	161.5	91
Isovaleric acid	69.0	11.0	58.0	84
Valeric acid	45.0	22.0	23.0	51

* Crude estimates have been used as results have been rounded off to accommodate for material being held up in the column.

The results in Table 5-3 are best explained by considering the material balance for one of the components as an example. At the start of the experiment there was 178 ml butyric acid in the reboiler. At the end of the first run (after six hours), only 6.5 ml remained in the residual left in the reboiler. The remaining butyric acid (161.5 ml) is seen in the accumulated distillate cuts. This means that 91% of the butyric acid was recovered from the waste acid stream by batch distillation.

Figure 5-4 shows distillate composition profiles for this run. The profiles are analogous to the profiles obtained by the *Hysys* simulations discussed in Chapter 4. In continuous distillation the profiles are discussed in terms of tray location with the concentration of the more volatile components increasing from feed to condenser and the less volatile components increasing from the feed location to the reboiler. For batch distillation, the profiles can be interpreted in terms of time with the more volatile components (i.e. propionic acid, butyric acid and isobutyric acid) increasing in concentration during the first three hours and the less volatile components increasing in the next three hours. Therefore, this confirms the assumptions that the nonkey components do not affect the volatility of the key components.

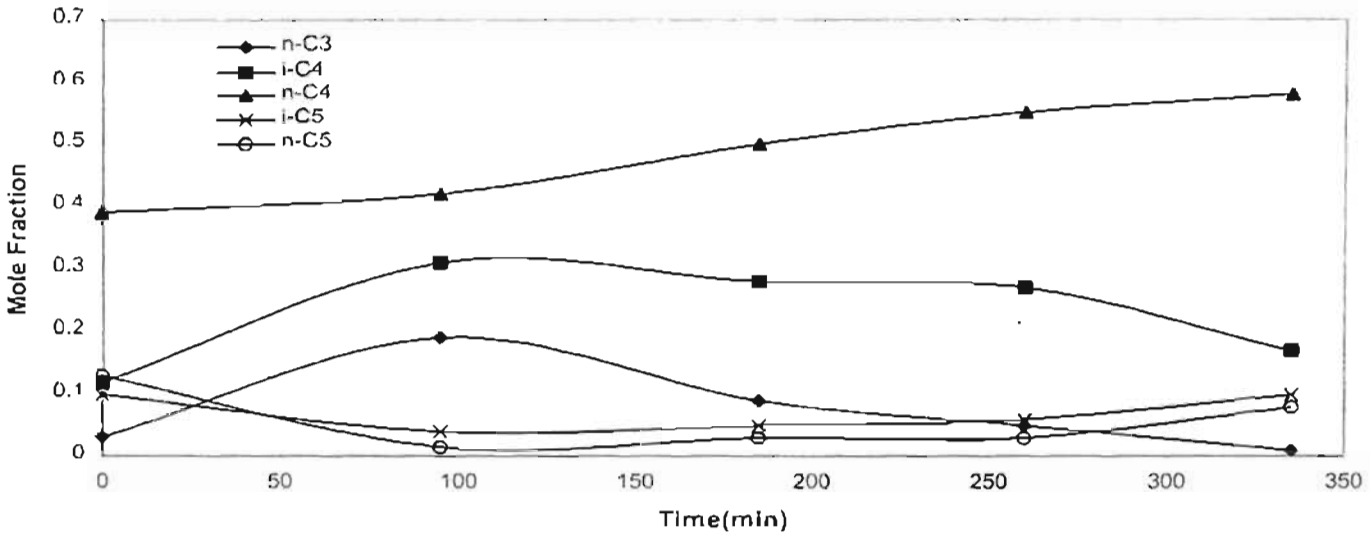

Figure 5-4: Distillate composition profile for batch distillation of waste acid stream –Batch 1

The recovered distillate from the first batch was then used as starting material for the second batch distillation (Batch 2). This experiment was run with the same operating conditions as the previous batch. The objective of this experiment was to explore the possibility of producing a distillate containing more than 90% of the butyric and isobutyric acids combined. This was necessary for subsequent purification by crystallization.

The results of the second batch distillation are shown in Table 5-4, where it is seen that the light key component (butyric acid) and light nonkey components (propionic acid and isobutyric acid) end up almost exclusively in the accumulated distillate cuts. The residual left in the reboiler after approximately five hours contain mostly the heavy key component (isovaleric acid) and the heavy nonkey component (valeric acid). Approximately 95% of the total recovered distillate composition consisted only of butyric and isobutyric acids. Distillate composition profiles for the second batch are shown in Figure 5-5. These profiles follow the same pattern as those discussed for the first batch.

Ultimately, batch distillation results show that separation of butyric acid and isobutyric acid from the rest of the waste acid stream by distillation is possible.

Table 5-4: Material balance for distillation of second batch*

Component	Still		Distillate (ml)
	Start (ml)	End (ml)	
Propionic acid	2.1	0.1	2.0
Isobutyric acid	24.0	0.3	23.7
Butyric acid	69.0	1 1	67.9
Isovaleric acid	14.6	11.5	3.1
Valeric acid	18.0	17 4	0.6

* Crude estimates have been used as results have been rounded off to accommodate for material being held up in the column.

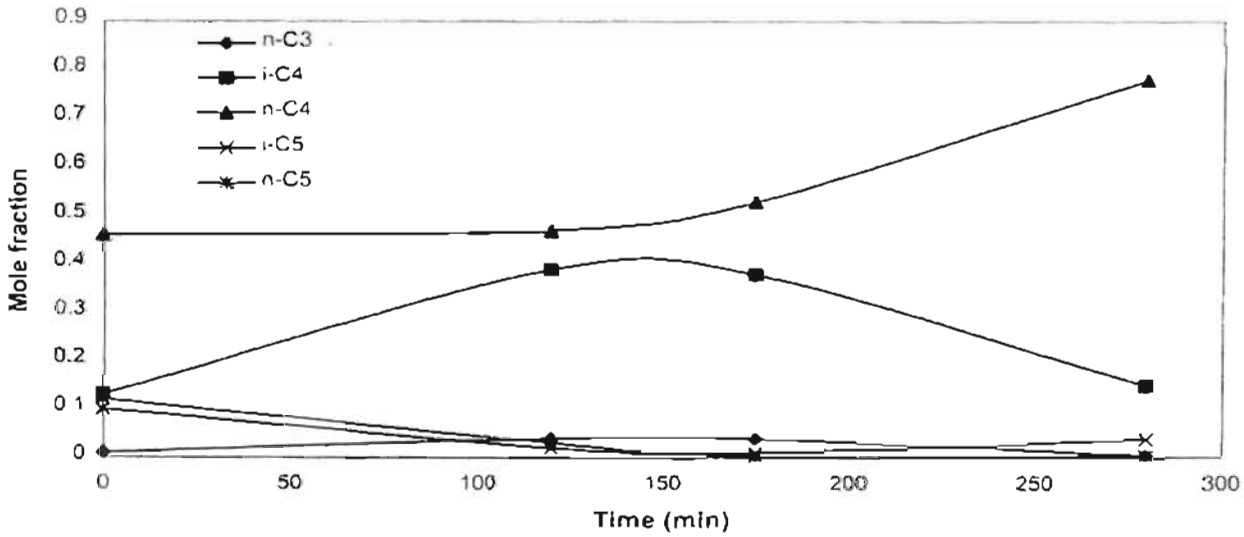

Figure 5-5: Distillate composition profile for batch distillation of waste acid stream –Batch 2

CHAPTER
SIX

FREEZE CRYSTALLIZATION

The process of forming a solid phase from a liquid phase is known as crystallization. Crystallization is in itself a broad topic and has many applications ranging from separation of isomers to precipitation of salts. An excellent text that extensively covers crystallization is by Mullin [1961]. As discussed in Chapter 2, freeze crystallization was selected for purification of butyric and isobutyric acids. In freeze crystallisation, two or more soluble species, in the absence of a solvent, are separated by partial freezing.

The understanding of crystallization as a separation process (more specifically, freeze crystallization) is known to a lesser extent than distillation. This is demonstrated by the voluminous literature on distillation compared to the literature on freeze crystallization. Solid-liquid phase equilibria forms the basis for all crystallization processes and is vital in screening the feasibility of crystallization as a separation process. Therefore, the basis of freeze crystallization and a theoretical framework for determining solid-liquid equilibria is presented in this chapter.

A simple experiment was also conducted to prove that solidification of butyric acid from a liquid mixture of butyric and isobutyric acids is indeed possible. The results of this experiment are also presented and discussed in this Chapter.

6.1 The basis of Freeze Separation

In essence, freeze crystallization is a very simple concept. If an impure liquid material is cooled to its freezing point and further heat is removed, then some of the material will solidify. In most systems this solid will be a pure component (Wynn [1992]). Impurities will concentrate in the remaining liquid, which is known as the residue. Purified product is recovered by separating the solid from the residue and remelting it.

All freeze separation processes are based on the difference in component concentrations between solid and liquid phases that are in equilibrium. This is most easily understood by referring to Figure 6-1. A eutectic system is shown in Figure 6-1, as a study by Mutsuoka & Fukushima [1986] found that over 85% of systems of binary mixtures were eutectic ones.

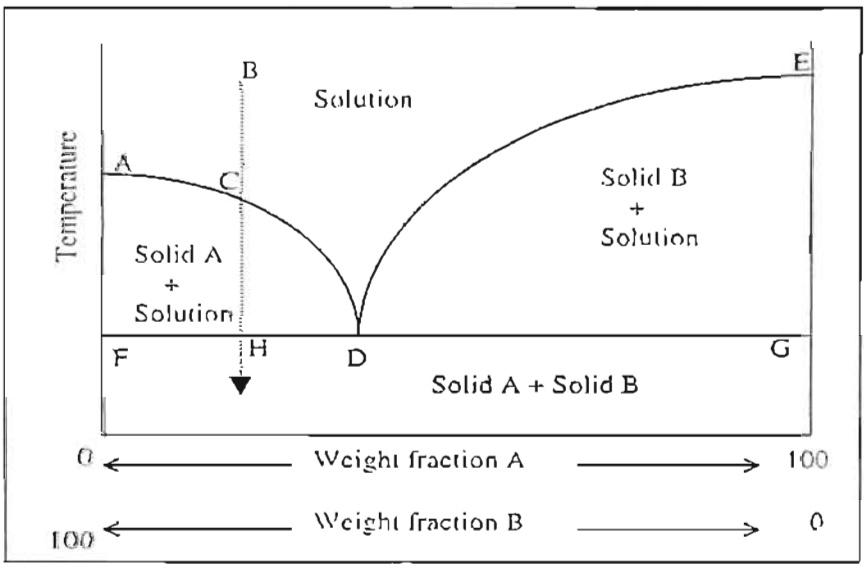

Figure 6-1: Binary solid-liquid equilibrium diagram

Points E and A are the freezing points of component A and B respectively. At these temperatures the pure components are present in a solid phase. Temperature-composition points located above the curve ADE correspond to a homogenous liquid phase. In a binary mixture, a point is eventually reached where both components crystallize simultaneously. This is known as the eutectic point and is shown by point D.

If a liquid solution of composition and temperature represented by point B is cooled along the vertical dashed line, it will remain a liquid until the line intersects curve AD at point C. At this point, usually only one component in the solution crystallizes (in this case component A) and that crystal is pure. This is because most solids are immiscible with other solids due to the geometry of the crystal lattice of different substances. Therefore, impurities cannot fit into the growing solid phase.

If the temperature is cooled further, more crystals of component A will form and the remaining liquid will become richer in component B. As the temperature is lowered, a point is reached (Point H) corresponding to the eutectic temperature. At this point the two-phase system consists of solid A and a liquid of the eutectic composition given by point D. Any further cooling causes the eutectic solution to solidify. Therefore, the two components solidify simultaneously, however two distinct solid phases will be formed.

The above discussion means that most compounds exhibiting eutectic behavior can be theoretically completely purified in a single stage of freeze crystallization. The only restriction is that enough of crystallizing component must remain in the solution to prevent the liquid phase from reaching the eutectic point.

6.2 Evaluating freeze crystallization as a separation operation

Many points need to be considered when selecting freeze crystallization as a separation operation. Wynn [1992] lists and discusses these points as the following questions:

1. Can the mixture be purified by distillation?
   If the components in a mixture can be separated in their desired specifications by distillation then freeze crystallization should not be considered. This is because it is cheaper to install and operate a distillation column as compared to crystallization equipment. Distillation is generally not recommended for mixtures containing components with low relative volatilities and those mixtures that are thermally unstable.

2. Will the material crystallize?

   Because rate processes are critical in freeze crystallization, it is difficult to predict how a mixture will separate without pilot plant results. If a chemical has not been pilot tested, then a simple freeze test in the laboratory will give some indication of its behavior. Such a test was conducted in this project and is discussed in a later section. Generally, if the freeze-test analyses show a promising degree of purification, then an industrial separation may be feasible.

3. Is melting point important?

   The lower the melting point of a component, the more expensive the process. This is because refrigeration is required to crystallize low-melting-point components and these costs increase with a decrease in melting point temperatures. Insulation costs also increase at lower temperatures and at very low temperatures the ductility of materials of construction becomes an issue.

4. How important is product purity?

   In most cases the solid phase contains a pure component. Impurities generally arise during separation of the solid and liquid phase, however implementing a subsequent washing operation can prevent this.

5. How important is product recovery?

   Recovery in most systems is limited by the existence of a eutectic. In some cases, freeze crystallization produces higher purities and lower product recovery than distillation. In such a case both techniques can be combined to form a process known as fractional crystallization. Lipowicz [1981], Dye & Ng [1995] and most recently Berry and Ng [1997] discusses these types of hybrid processes together with their applications and tradeoffs. The reader is therefore referred to these reviews for further information on combining distillation and freeze crystallization processes.

6.3 Solid-liquid equilibria

The method of predicting or experimentally determining solid-liquid equilibrium is not important so long as it provides the accuracy for the intended use. Preliminary analysis requires much less precise data than would a final design. Experimental methods are cumbersome, time consuming and expensive. Heist [1980] recommends using them only when a decision to use a freeze-separation process has already been made and accurate design data are required. For preliminary evaluations, predictive techniques have been developed.

As in the case of vapor-liquid equilibrium (Chapter 3), the calculation of solid-liquid phase equilibrium can start from the criterion for equilibrium, which has been developed by Smith & Van Ness [1987] and is illustrated in Appendix B-1. Therefore, at equilibrium, the respective fugacities (f_i) of the components in both the solid phase (S) and liquid phase (L) are equal:

$$\hat{f}_i^{\,L} = \hat{f}_i^{\,S} \tag{6-1}$$

In Equation (6-1), " ^ " denotes the mixture property.

The fugacity of the mixture ($\hat{f}_i$) is related to the product of the mole fraction (x_i), activity coefficient (γ_i) and the fugacity of the pure species ($f_{i,pure}$). Therefore, the following expressions for the solid and liquid phases are obtained:

$$\hat{f}_i^{\,S} = x_i^S \gamma_i^S f_{i,pure}^S \tag{6-2}$$

$$\hat{f}_i^{\,L} = x_i^L \gamma_i^L f_{i,pure}^L \tag{6-3}$$

Substituting equations (6-2) and (6-3) into (6-1) and rearranging gives:

$$\frac{f_{i,pure}^S}{f_{i,pure}^L} = \frac{x_i^L \gamma_i^L}{x_i^S \gamma_i^S} \tag{6-4}$$

In most systems the pure solid crystallises out, so that the fugacity of the solid phase at equilibrium can be replaced by the fugacity of the pure solid ($x_i^S \gamma_i^S = 1$):

$$\frac{f_{i,pure}^S}{f_{i,pure}^L} = x_i^L \gamma_i^L \tag{6-5}$$

The ratio of the pure component fugacities ($f^{S}_{i,pure} / f^{L}_{i,pure}$) can be calculated via a thermodynamic cycle discussed by Prausnitz et al [1986]. If the temperature-dependence of the heat capacity difference is neglected, the following equation is obtained:

$$\ln \frac{f^{S}_{i,pure}}{f^{L}_{i,pure}} = \frac{\Delta h_{m,T_{tr},i}}{RT}\left(1 - \frac{T}{T_{tr}}\right) - \frac{\Delta c_{P,i}\left(T_{tr} - T\right)}{RT} + \frac{\Delta c_{P,i}}{R} \ln \frac{T_{tr}}{T} \qquad (6\text{-}6)$$

In the above equation, $\Delta h_{m,T_{tr},i}$ is the latent heat of fusion at the triple point, T is system temperature, T_{tr} the triple point temperature of component i, and $\Delta c_{P,i}$ is the difference in liquid and solid molar heat capacities for component i.

To simplify Equation (6-6) further, Jakob et al [1995] state that conditions at the triple point are usually close to the melting point. Therefore this allows the substitution of melting point conditions for triple point conditions (i.e. $T_{tr,i} \cong T_{m,i}$ and $\Delta h_{m,i} \cong \Delta h_{m,T_{tr},i}$). In addition, the last two terms in Equation (6-6) are of opposite sign and tend to cancel out in the vicinity of the melting point. Substitution of Equation (6-5) into (6-6) with these simplifications gives:

$$\ln x_i^{L} \gamma_i^{L} = \frac{\Delta h_{m,i}}{RT}\left(1 - \frac{T}{T_{m,i}}\right) \qquad (6\text{-}7)$$

Equation (6-7) is used to predict the solid-liquid phase behavior for preliminary process-design calculations. The data required are the latent heat of fusion at the melting point temperature, the melting temperature and the activity coefficient of the solution. Melting temperatures and latent heats for organic compounds may be found in books by Weast [1983] or Weast & Grasselli [1989]. Activity coefficients in solid-liquid systems are sparse but they do exist for many binary vapour-liquid equilibrium systems. Therefore, Rousseau & Moyers [1987] suggest estimating solid-liquid activity coefficients directly from vapor-liquid equilibrium data obtained at higher temperatures. With this information, the freezing -point temperature of a solution may be calculated as a function of liquid composition.

If a solution is assumed to be ideal, Equation (6-7) further simplifies to the following equation:

$$\ln x_i^L = \frac{\Delta h_{m,i}}{RT}\left(1 - \frac{T}{T_{m,i}}\right) \tag{6-8}$$

Equation (6-8), also known as the Van Hoft equation, is recommended to predict solid-liquid equilibria of binary systems containing isomers (Muir & Howat [1982]). To demonstrate its use as a predictive tool for systems containing isomers, comparison between the predicted and experimental phase curves for the 1,3-xylene+1,2-xylene system is presented in Figure 6-2. The prediction is very good with a mean deviation of 0.3K over the temperature range and therefore ensures confidence in using the developed equations to determine solid-liquid equilibria of binary systems containing isomers. It must be made clear, however, that these techniques become less accurate as the difference in molecular size increase.

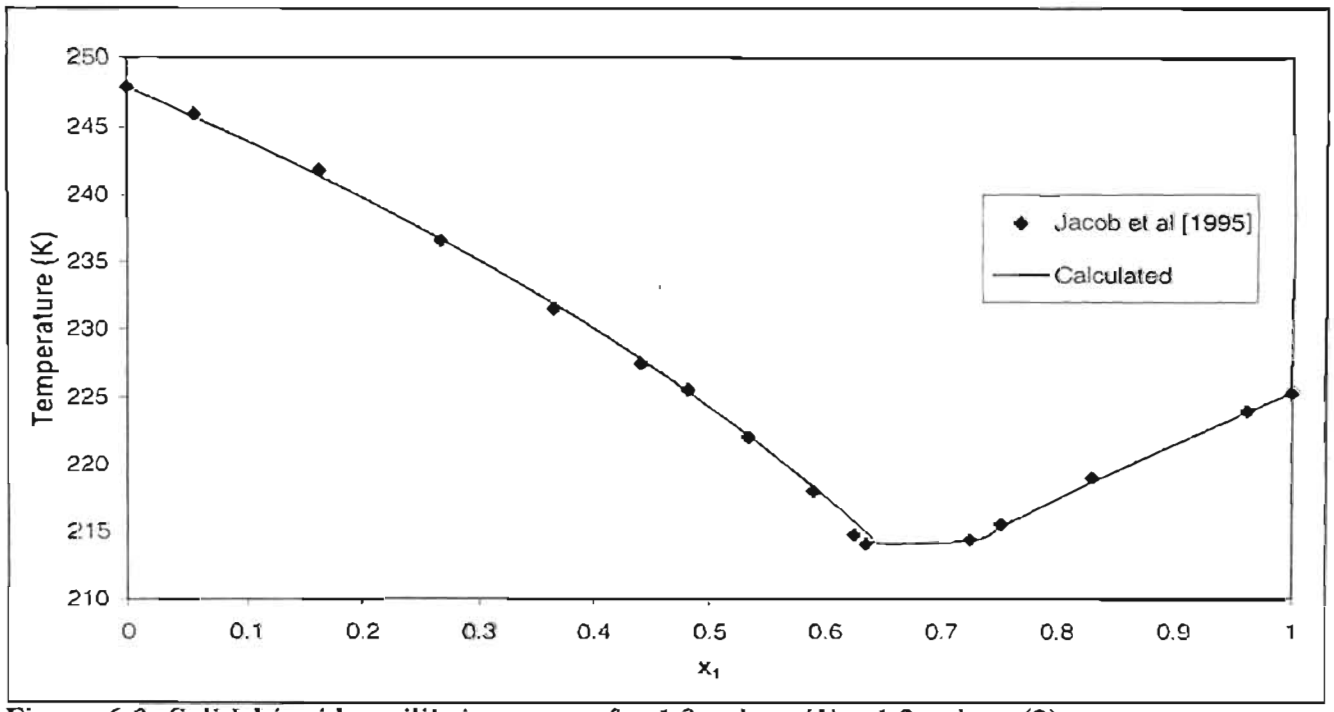

Figure 6-2: Solid-Liquid equilibrium curve for 1,3-xylene (1) + 1,2-xylene (2)

6.4 Experimental Set-up and procedure

A simple experiment was set-up (Figure 6-3) to demonstrate solidification of butyric acid out of a liquid mixture of butyric acid and isobutyric acid.

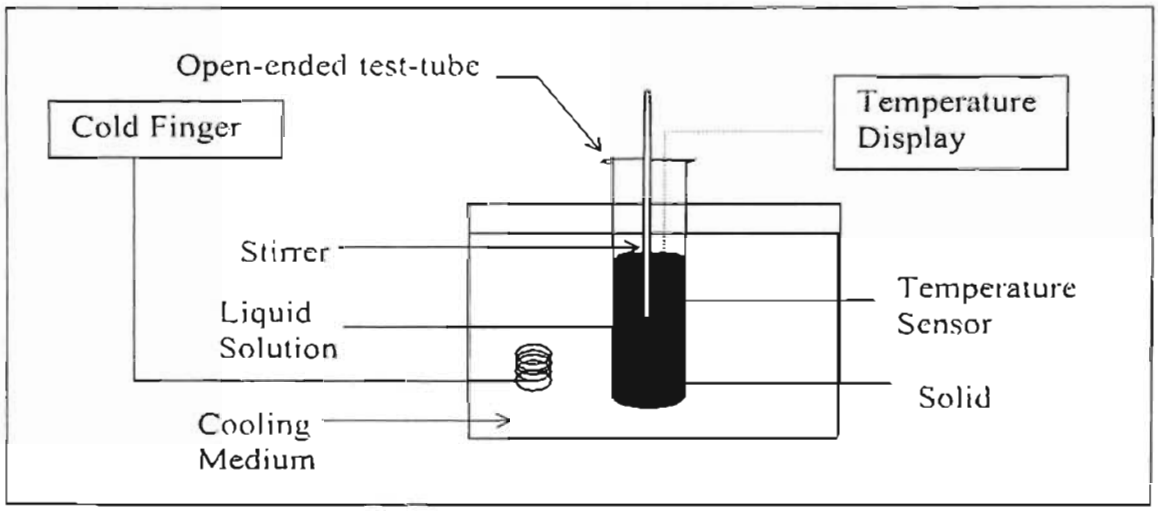

Figure 6-3: Experimental set-up for crystallization experiment

A solution consisting approximately 87% butyric acid and 13% isobutyric acid was made up to a volume of 10 ml in a Pyrex glass tube. The butyric acid was purchased from Riedel-de Haën, whilst the isobutyric acid was purchased from Fluca Enterprises. The reagents were used without further purification after gas chromatographic analysis showed no significant impurities. The purities of the reagents were also checked by their refractive indexes and comparisons with literature values are shown in Table 3-4, Chapter 3.

The glass tube containing the acids was then placed into a liquid bath (cooling medium) with polystyrene providing insulation against the atmosphere. A Eurotherm temperature indicator was used to display the resistance of the PT-100 temperature sensor placed in the liquid solution. A TECHNE cold finger, with a minimum operating temperature of -20^{0}C was used to maintain the temperature of the cooling medium. The cooling medium consisted of a mixture of water and ethylene glycol. Manipulation of the relative concentrations of ethylene glycol and water in the cooling medium prevents the cooling medium from solidifying. This relationship is determined from the solid-liquid equilibrium of the binary mixture and has been measured by Ott et al [1972] and is shown in Figure 6-4. Using this figure, a mixture of 80-vol% water and 20-vol% ethylene glycol was chosen to make up the cooling medium to prevent it from solidifying.

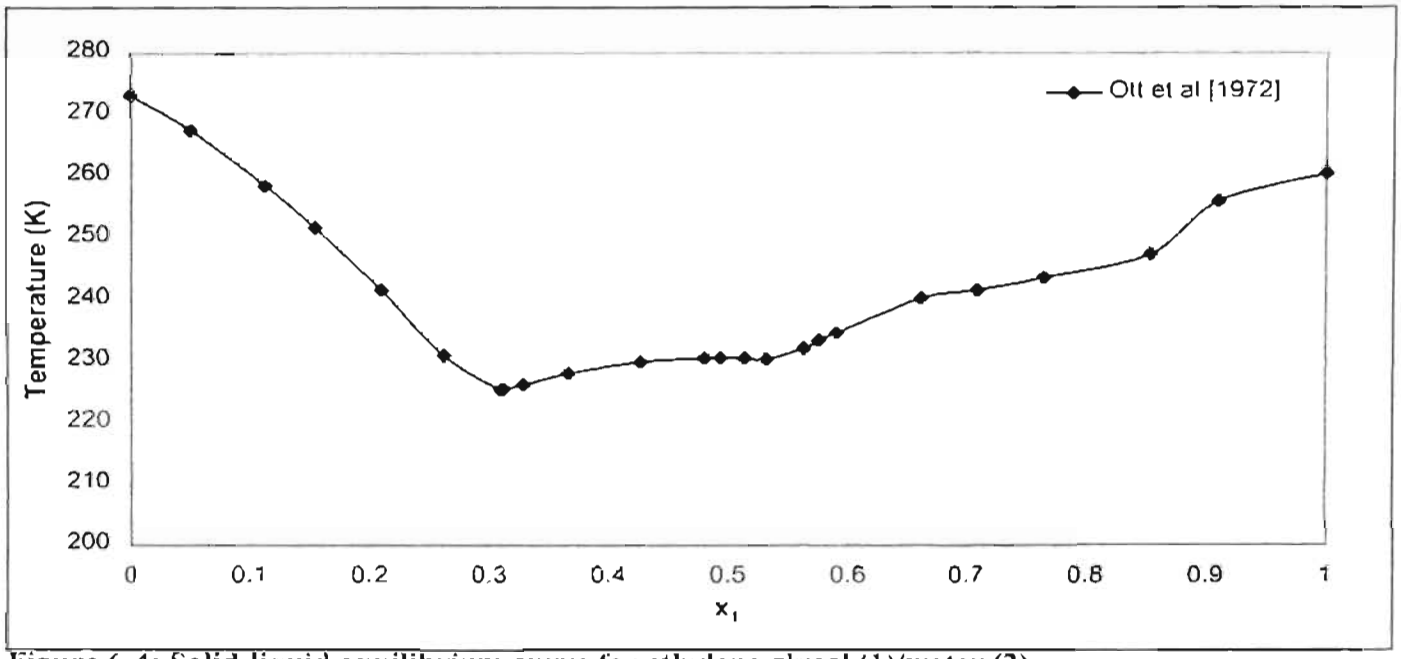

Figure 6-4: Solid-liquid equilibrium curve for ethylene glycol (1)/water (2)

6.5 Results and Discussion

The solid-liquid equilibrium curve for the isobutyric acid/butyric acid system as predicted by Equation (6-8) is shown in Figure 6-5.

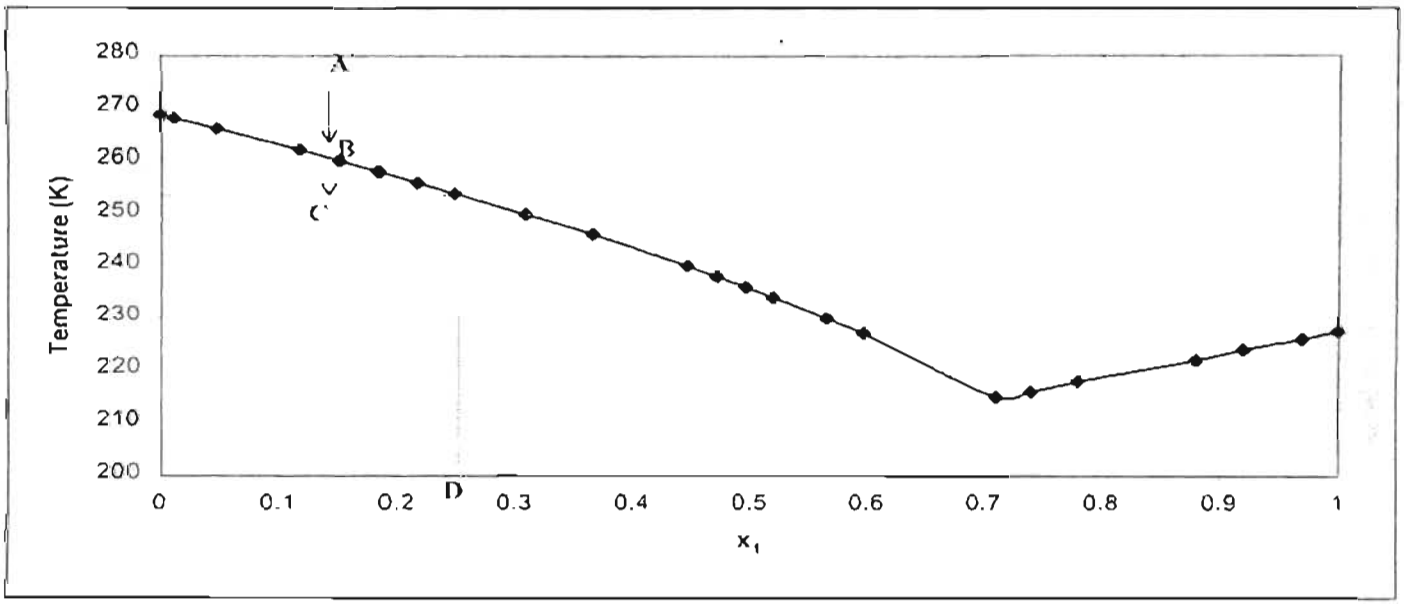

Figure 6-5: Predicated solid-liquid equilibrium curve for isobutyric acid (1)/butyric acid (2)

Many experiments were attempted to crystallize butyric acid from the mixture of butyric acid and isobutyric acid. However, initial attempts were unsuccessful because of the following reasons:

- The mixture of acids was initially placed in a closed container. This prevented the solution from being in contact with air particles. It has been suggested by Tammann [1898] that dust particles from air are, in many cases, responsible for initiation of crystallization. Therefore, an open ended tube was used (Figure 6-3).
- The surface of the container had to be scratched to provide a rough surface. The initial smooth surface was not appropriate as studies (Price [1997]) showed that scraped surfaces are more efficient than smooth surfaces.

With the above considerations and changes, a solution of pure butyric acid was crystallized. This encouraged experimentation with a mixture of both the acids. The results of the experiment are best explained by referring to the solid-liquid equilibrium curve in Figure 6-5. The experiment began with a crystal free undersaturated solution with a composition of 87-mole % butyric acid and 13-mole % isobutyric acid (Point A, Figure 6-5). This composition was used as it was suitable for use with the limitations in the equipment (A mixture with a composition freezing below -20^{0}C had to be selected). This was determined by the solid- liquid equilibrium curve (Figure 6-5).

At -12 C, after 1.5 hours, the first crystal started to form. This corresponds closely to point B in Figure 6-5. The temperature of the solution continued to drop, with the solid phase increasing in size, until a temperature of -19^{0}C (Point C, Figure 6-5). After this point, the temperature remained constant and no more solid appeared to form. This was the lowest temperature that could be achieved by the available equipment.

Analyses of the solid and liquid phases by gas chromatograph are shown in Table 6-1. The operating conditions for the gas chromatograph are the same as those used to determine vapor-liquid equilibrium (Table 3-1). The compositions compare well with those predicted (Point D, Figure 6-5).

Table 6-1: Results of crystallization experiment

	Butyric acid (mole fraction)	Isobutyric acid (mole fraction)
Start	0.87	0.13
Liquid	0.78	0.22
Solid	0.94	0.06

It is believed that a small amount of the isobutyric acid from the liquid phase was carried over with the solid when separating the two phases. This resulted in the small amount of the isobutyric acid in the analysis of the solid phase. This can be remedied by washing the solid with excess butyric acid.

It would have been appropriate to determine the eutectic compositions experimentally because this point determines if sufficient recovery is possible. However, this was not possible because of equipment limitations. Nevertheless, the experiment has shown that pure butyric acid can be produced by crystallization.

No mention of purifying isobutyric acid has yet been made. In order to effect a complete separation of both butyric and isobutyric acids, the separation process must recover butyric acid in its pure form and then isobutyric acid. This is achieved by using two crystallizers at two different operating temperatures. For the purification of isobutyric acid, the solid-liquid curve (Figure 6-5) shows that a starting mixture of 80% isobutyric acid and 20% butyric acid would produce pure isobutyric acid crystals by operating a crystallizer at -55^{0}C.

Although purification of butyric acid by freeze crystallization has been experimentally verified, it must be noted that this chapter has just briefly reviewed freeze crystallization as a separation operation and serves mostly to demonstrate that purification of butyric and isobutyric acids is possible by freeze crystallization.

CHAPTER
SEVEN

ECONOMIC FEASIBILITY

The goal of most engineering feasibility studies is to determine whether the project is economically viable. Although many aims of this project relate to reducing hazardous environmental emissions, the successful implementation of this project will ultimately depend on the profitability over the existing technology (incineration). Therefore an economic evaluation was undertaken to determine if separation and purification of the acids is profitable. Preliminary estimates (accurate to within ± 30%) were employed to obtain costs for the selected separation and purification route. These estimates included:

- Market evaluation and forecasting
- Capital cost estimation
- Operating cost estimation
- Profitability Evaluation

7.1 Market Evaluation and Forecasting

Market evaluation and forecasting is a key element in evaluating the economic feasibility of a new project. Factors affecting the product market are.

- Sales revenue – The product of sales volume and selling price. This affects the financial income of the project directly.
- Volume of product required – This factor has a direct bearing on the sizing decision of the plant.
- Specification of product quality – This influences process and equipment design. It also affects the environmental impact of the product over its entire life cycle.

Butyric and isobutyric acids may be classified as fine chemicals because they are currently made in lower volumes and are required to adhere to tighter specifications for their functions in food additives and pharmaceuticals. Therefore, these acids have to be produced in high purities (see table below for sales specifications as stipulated by Celanese Chemicals).

Table 7-1: Specifications for the production of butyric and isobutyric acids.

1. Butyric acid		
Butyric acid	wt. %	minimum 99.5
Isobutyric acid	wt. %	maximum 0.2
Water	wt. %	maximum 0.1
Heavy metals	ppm^2	maximum 0.1
2. Isobutyric acid		
Isobutyric acid	wt. %	minimum 99.5
Butyric acid	wt. %	maximum 0.15
Water	wt. %	maximum 0.1
Heavy metals	ppm^2	maximum 0.1

Butyric and isobutyric acids are currently being produced by five international companies viz.: BASF, Celanese, OXENO, Eastman and Daicel Chemical industries. Table 7-2 below lists approximate production figures for each company.

Table 7-2: Production figures for butyric and isobutyric acids (Bizzari et al [1999])

Company	Location	Annual Production (tpa)
-Butyric acid		
Eastman	United States	8500
Celanese	United States	4500
BASF	Germany	10 000
OXENO	Germany	10 000
Daicel Chemical Industries	Japan	300
- Isobutyric acid		
Eastman	United States	10 000

Butyric acid is widely known for its presence in butter. However, it is consumed mainly in the production of cellulose acetate butyrate (CAB). This is a plastic that is used in many applications such as pen barrels, eyeglass frames and screwdriver handles. Although recent reports have shown a decline in CAB usage due to competition from other plastics, there has been a growth in alternate uses for butyric acid. These include the production of various flavorings, fragrances and herbicides. Furthermore, butyric acid is gaining importance in the pharmaceutical industry, where recent studies (Gillet et al [1997]) have shown its need in the form of cancer treatment.

The main use of isobutyric acid is its conversion to plasticizer, which is used for plastics and lacquers. It is also used to extract mercaptans from petroleum and for conversion to esters, which are used in flavors and fragrances.

Figure 7-1 demonstrates the trends in the U.S consumption figures for butyric and isobutyric acid. It is estimated that the U.S constitutes roughly 40% of the international markets for these acids (Bizzari et al [1999]). The remainder includes exports to countries such as Canada, Mexico, Japan, Israel and the Netherlands.

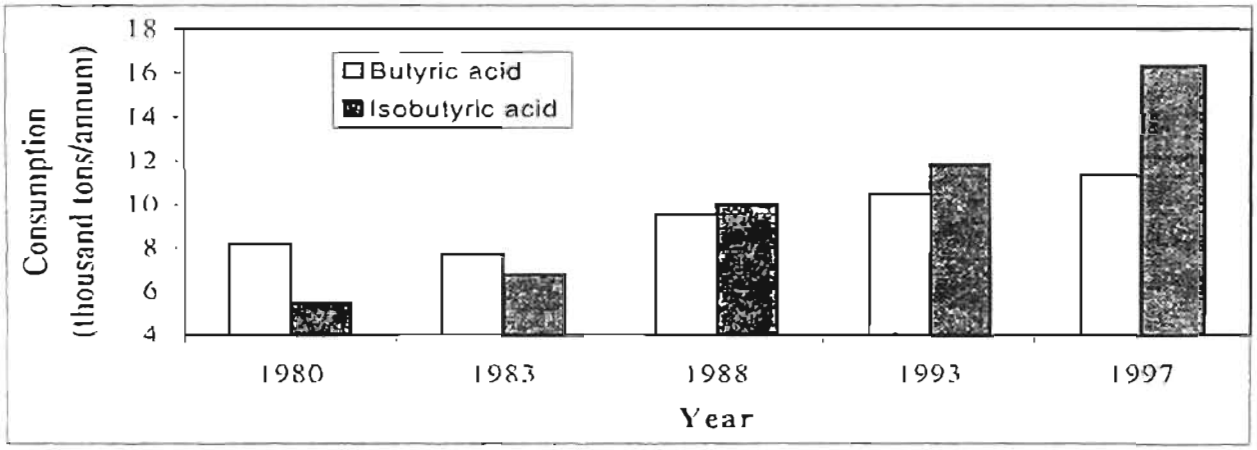

Figure 7-1: U.S consumption figures of the acids for the past years

These results show an average growth rate of 1.6 % and 4.6 % per annum for butyric acid and isobutyric acid respectively. Currently butyric acid and isobutyric acid are selling for 55 US c/lb (R9, 80/kg)* and 94 US c/lb (R16, 70/kg)* respectively on world markets (Bizarri et al [1999]).

* Calculated assuming R8, 00 to the dollar

These products are globally traded. Assuming that eighty percent of extractable volumes from the waste acid stream are possible, approximately 3200 tons of butyric acid and 1000 tons isobutyric acid could be produced annually. This will result in producing 13% of world's butyric acid and 2.5% of the world's isobutyric acid requirements. The projected revenue for these production figures amounts to approximately R47 million per annum.

7.2 Capital Cost Evaluation

One of the major costs in determining economic viability is the fixed capital investment cost. There are many different methods, which could determine these costs, all of which depend on the accuracy required by the estimate. Baasel [1990] and Timmerhaus et al [1981] discuss various techniques for estimating capital costs. For this particular project the factored estimate approach, with accuracy within 30%, was adopted. This method is based on knowledge of the major items of equipment required for separation and purification of the acids.

Equipment costs were determined using published cost data as given by Timmerhaus et al [1981]. These costs were also calculated using correlations by Mulet et al [1981]. Details of equipment costs are shown in Table C-1 of Appendix C with the calculated values lying within 10% literature (Timmerhaus at al [1981]). Because the costs obtained from literature were based on monetary value in the year 1979, Equation (7-1) was used to determine current day costs. A total of approximately R 1,524,000 was estimated for equipment costs.

$$\text{Present Cost} = \left(\frac{\text{index value at present time (1979)*}}{\text{index value at time original cost obtained (2001)*}} \right) \qquad (7\text{-}1)$$

* Marshall and Swift indices as supplied in Chemical Engineering [1979,2001].

Once equipment costs were determined, the fixed capital investment was calculated using the percentage of delivered equipment cost method as described by Timmerhaus et al [1981]. This method was suggested for preliminary cost estimation and only required equipment costs. Other items required in the total cost were determined as a percentage of the equipment costs. Table C-2 (Appendix C) shows a breakdown of the costs involved in estimating fixed capital investment. A total of approximately R 5,400,000 was estimated for fixed capital investment.

Due to the importance of capital costs in determining process feasibility, a second estimation technique (the Rapid Estimation Technique) was employed. This method suggested by Viola [1981], claims to be accurate to within 15% when compared to the factored estimate approach. Although the method was not used to determine economic viability, it is suggested to the reader because it requires the least amount of effort and time in determining capital costs. With knowledge of the major unit operations (Distillation and Crystallization), the plant capacity (10 000tpa), materials of construction (Stainless steel) and type of plant (solid-fluid plant) an estimate of R 5,000,000 was obtained. This value compares well against the value obtained by the factored estimate approach. It must be noted, however, that the rapid estimation technique has not yet been properly tested

7.3 Operating Cost Estimation

Operating costs are those that occur over the lifespan of the project and are directly associated with production. These costs usually consist of raw material costs, conversion costs (e.g. labour), and indirect expenses (e.g. finance charges). For this project raw material costs were not accounted for as the feed to the process is a waste stream that is currently being destroyed by incineration. Details of the operating costs are shown in Table C-3, Appendix C. A total of approximately R 1,700,000 per annum was estimated for operating costs.

7.4 Evaluation of Project Profitability

A fundamental objective of any company or business is that it operates profitably [Brennan, 1998]. Before capital is invested in a project, it is necessary to know how much profit can be obtained or whether it might be more advantageous to invest the capital in another form. There are as many ways to access project profitability as there are ways to determine capital costs. Timmerhaus et al [1981], Baasel [1990] and Brennan [1998] discuss these methods in detail. However, in this particular project, it is evidently clear (from the cash flow chart, Table C-4, Appendix C) that the income generated by the project exceeds the expenses and capital investment by a huge amount. This in turn results in high rate of returns and a payback period of less than one year for the investment required in implementing the project. It must, however, be noted that other factors such as risks involved in the project would also affect investment decisions. As this project is only in its

first phase, most of the risk can be associated with the author's inexperience in industry and the assumptions taken in the design stages of the project. This however should decrease once pilot plant work on the project has been completed.

CHAPTER
EIGHT

CONCLUSIONS & RECOMMENDATIONS

8.1 Conclusions

In an attempt to determine a suitable separation process for the recovery and purification of butyric acid and isobutyric acid from SASOL's waste acid stream vacuum distillation was chosen as a base case.

To evaluate the performance of distillation in recovering the acids, a flowsheeting program (*Hysys*) was used. For the proper use of the simulation program an appropriate thermodynamic model had to be selected. Therefore, vapour-liquid equilibrium (VLE) studies on the components present in the waste acid stream were conducted. VLE data for the binary systems propionic acid + butyric acid, isobutyric acid + butyric acid, butyric acid + isovaleric acid and butyric acid + hexanoic acid were experimentally determined in a dynamic VLE still. All systems were measured at 14kPa. All the measured systems, excluding butyric acid + hexanoic acid, were found to be thermodynamically consistent according to the direct test (Van Ness [1995]). The inconsistency for the binary system butyric acid + hexanoic acid was attributed to the formation of trimers in the vapour phase, which were not accounted for in the consistency tests. The measured VLE data was successfully correlated using the gamma-phi approach and was regressed to provide binary interaction coefficients for the NRTL model, which was then used in the *Hysys* process simulator to explore a range of design alternatives for distillation.

Results from the process simulator showed that recovery of the acids from the waste acid stream by distillation is indeed possible. Simulation results were analysed using Hengstebeck's method [1961] and showed that the simulation results could be regarded as a reflection of the "real world". Recovery of the valuable acids was confirmed in a subsequent batch distillation experiment, where greater than 90% of both acids (approximately 180ml butyric acid and 60ml isobutyric acid) were recovered from a 500ml sample of the waste acid stream in approximately six hours. A subsequent batch experiment concentrated the recovered acids into a distillate containing more than 95 % butyric acid and isobutyric acid combined. However, simulation results also showed that purification of butyric acid and isobutyric acid would require a distillation column with many stages and would thus not be feasible.

For purification of butyric acid and isobutyric acid freeze crystallization was selected as a base case. Examination of the predicted solid-liquid equilibrium curve for the binary system showed that butyric acid and isobutyric acid could be separated from each other by using two crystallizers at operating temperatures of $-20^{0}C$ and $-55^{0}C$ respectively. Simple freeze crystallization tests produced butyric acid with greater than 94% purity. However, isobutyric acid could not be purified due to limitations in the experimental operating conditions.

Market analysis of the acids showed that butyric acid and isobutyric acid are currently being globally traded at R9.80/kg and R16.70/kg respectively. Based on these figures and 80% extractable volumes a revenue of approximately R47 million was estimated for recovery and purification of the acids. A total of approximately R5.4 million was estimated for fixed capital. Operating costs for the project were also estimated at a total of approximately R1.7 million per annum. Using these estimated costs (accurate to within ± 30%), a cash flow statement was generated showing high rate of returns for this project and a payback period of less than one year.

8.2 Recommendations

Preliminary studies have shown that it is possible (and economically feasible) to recover and purify butyric acid and isobutyric acid from SASOL'S waste acid stream by distillation and crystallization. Although it may be necessary to experimentally verify the eutectic composition (as discussed in Chapter 6) for the crystallization operation, consideration should be given into pursuing pilot plant studies as the next phase of this project.

From the production figures presented in Chapter 7, it was noted that recovery and purification of 80% of the butyric acid and isobutyric acid present in the waste stream would result in producing 13% of the world's butyric acid and 2.5% of the world's isobutyric acid requirements. Due to the nature of the markets, production on this scale could decrease the current market prices of the acids, which is undesirable. Therefore, consideration may be given into treating a small amount of the waste acid stream initially and then steadily increasing the scale of production by using batch equipment. In this way, the current market prices of the acids may be maintained because batch equipment have the unique feature of separating a variety of feed mixtures, easily accommodating the frequent change in market demand.

Finally, studies have shown that the two unit operations, distillation and crystallization, can be simultaneously applied in a single piece of equipment. This is known as fractional crystallization and was very briefly discussed in Chapter 6. Because fractional crystallization is more efficient than the conventional manner of using two separate equipment for distillation and crystallization, it may also be worthwhile considering further studies on investigating fractional crystallization for this project.

REFRENCES

Abrams, D S, Prausnitz, J M, (1975), "Statistical Thermodynamics of Liquid Mixtures: A New Expression for the Excess Gibbs Energy of Partly or Completely Miscible Systems" *American Institute of Chemical Engineers Journal*, Vol. 21, 116-128.

Aly, G & Ashour, I, (1992), "Applicability of the Perturbed Hard Chain Equation of State for Simulation of Distillation Processes in the Oleochemical Industry Part 1: Separation of Fatty Acids", *Separation Science and Technology*, Vol. 27, No. 7, 955-974.

Baasel, W D, (1990), "Preliminary Chemical Engineering Plant Design", 2nd ed., Van Nostrand Reibhold, New York

Barolo, M, Botteon F, (1997), "Simple Method of Obtaining Pure Products by Batch Distillation", *American Institute of Chemical Engineers Journal*, Vol. 43, No. 10, 2601-2604.

Berry, D A & Ng, K M, (1997), "Synthesis of Crystallization-Distillation Hybrid Separation Processes", *American Institute of Chemical Engineers Journal*, Vol. 43, No. 7, 1751-1761.

Bernot, C, Doherty, M F, Malone, M F, (1991), "Feasibility and Separation Sequencing in Multicomponent Batch Distillation", *Chemical Engineering Science*, Vol. 46, No. 5, 1311-1326.

Bizzari, S N, Fenelon, S, Yamiki, M I, (1999), "Chemical Economics Handbook", SRI International, California.

Bogart, J P M, (1937), "The Design of Equipment for Fractional Batch Distillation", *Transactions of the American Institute of Chemical Engineers*, Vol. 33, 139-161.

Brennan, D, (1998), "Process Industry Economics", IchemE, Warwickshire.

Carlson, E C, (1996), "Don't Gamble with Physical Properties for Simulations", *Chemical Engineering Progress*, Vol. 92, 35-46.

Colburn, A P, (1941), as reported by Kister [1992].

References

Cran, J, (1981), "Improved factored method gives better preliminary cost estimates", *Chemical Engineering*, Vol. 88, No. 7, 65-79.

DECHEMA Data Base CD. (1999), "Pure Component Properties and Vapour-Liquid Equilibrium Data", Frankfurt.

Devyatikh, G G. (1981), as reported by Morari et al [1994].

Dye, S R & Ng, K M, (1995), "Fractional Crystallization: Design Alternatives and Tradeoffs", *American Institute of Chemical Engineers Journal*, Vol. 41, No. 11, 2427-2438.

Erbar, J H & Maddox, R N, (1961), as reported by Kister [1992].

Eduljee, H E, (1975), "Equations Replace Gilliland Plot", *Hydrocarbon Processing*, Vol. 54, No. 9, 120-122.

Ellerbe, R W, (1980), "Steam Distillation Basics", *Chemical Engineering Magazine, Separation Techniques 1: Liquid-Liquid Systems*, 12-19.

Fair, J R, Chapter 5, "Distillation", in Rousseau, R W, (1987), *Handbook of Separation Process Technology*, Wiley Interscience, New York.

Fenske, M R, (1932), "Fractionation of Straight-Run Pennsylvania Gasoline", *Industrial & Engineering Chemistry*, Vol. 28, 482-485.

Furlonge, H I, Pantelides, C C, Sorensen, (1999), "Optimal Operation of Multivessel Batch Distillation Columns", *American Institute of Chemical Engineers Journal*, Vol. 45, No. 7, 781-790.

Fredunslund, A, Gmehling, J, Rasmussen, P, (1977), "Vapor-Liquid Equilibrium using UNIFAC", Elsevier, Amsterdam.

Geankoplis, G J, (1997), "Transport Processes and Unit Operations", 3rd ed., Prentice Hall of India, New Delhi.

References

Gillet, R, Jeannesson P, Sefraoui H, Guérin, L M, Kirkiacharian, S, Jardillier, J C, Pieri, F, (1997), "Short Communication: Piperazine Derivatives of Butyric Acid as Differentiating Agents in Human Leukemic Cells", *Cancer Chemotherapy and Pharmacology Journal*, Vol. 41, No. 3, 252-255.

Gilliland, E R, (1940), "Multicomponent Rectification: Estimation of Number of Plates as a Function of Reflux Ratio", *Industrial & Engineering Chemistry*, Vol. 32, 1220-1223.

Giroul, F, Marocchino, A, Marrelli, L, (1981), "Vapour-Liquid Equilibria of the Formic Acid-Dimethylformamide System", *Journal of Chemical Engineering Data*, Vol. 26, 370-374.

Gmehling, J & Onken, U, (1977), "Vapour-Liquid Equilibrium Data Collection, Organic Hydroxy Compounds: Alcohols", Vol. 1, Part 2a, DECHEMA, Frankfurt/Main.

Hala, E, Pick, J, Fried, V, Vilim, O, (1967), "Vapor-Liquid Equilibrium", 2nd ed., Pergamon Press, Oxford.

Hart, M. (1991), "Organic Chemistry: A Short Course", 8th ed., Houghton Mifflin Company, Boston.

Harris, R A, (2001), "Monoethanolamine: Suitability as an Extractive Solvent", MSc. Thesis, University of Natal, South Africa.

Hayden, J G & O'Conell, J P, (1975), "A Generalized Method for Predicting Second Virial Coefficients", *Industrial and Engineering Chemistry Process Design and Development*, Vol. 14, 209-216.

Heist, J A, (1980), "Freeze Crystallization", *Chemical Engineering Magazine, Separation Techniques 1: Liquid-Liquid Systems*, 348-358.

Hengstebeck, R J, (1961), "Distillation-Principles and Design Procedures", Reinhold Publishing, New York.

References

Holland, C D. (1981), "Fundamentals of Multicomponent Distillation", McGraw-Hill Inc., New York.

Jakob, A, Joh, R, Rose, C, Gmehling, J. (1995), "Solid-Liquid Equilibria in Binary Mixtures of Organic Compounds", *Fluid Phase Equilibria*, Vol. 113, 117-126.

Joseph, M A. (2001), "Computer-Aided Measurement of Vapour-Liquid Equilibria in a Dynamic Still at Sub-Atmospheric Pressures, MSc. Thesis, University of Natal, South Africa.

Joseph, M A, Raal, J D, Ramjugernath, D, (2001), "Phase Equilibrium Properties of Binary Systems with Diacetyl from a Computer Controlled Vapour-Liquid Equilibrium Still", *Fluid Phase Equilibria*, Vol. 128, 157-176.

Keller, G E. (1987), "Separations: New Directions for an Old Field", *American Institute of Chemical Engineers Monograph Series*, Vol. 45, No. 7, 781-790.

Kertes, A S, Tamada, J A, King, C J, (1990), "Extraction of Carboxylic Acids with Amine Extractants", *Industrial & Engineering Chemistry Research*, Vol. 29, 1319-1326.

Kertes, A S & King, C J, (1986), as reported by Kertes et al [1990].

King, C J, (1971), "Separation Processes", McGraw-Hill Book Company, New York.

Kirkbridge, C G, (1944), as reported by Kister [1992].

Kister, H Z, (1992), "Distillation Design", McGraw Hill Inc., New York.

Kneisl, P, Zondlo, J W, Wallace, B W, (1989), "The Effect of Fluid Properties on Ebbulliometer Operation", *Fluid Phase Equilibria*, Vol. 46, 85-94.

Kojima, K & Tochigi, K, (1979), "Prediction of Vapor-Liquid Equilibria by the ASOG Method", Elsevier Scientific Publishing Company, Amsterdam.

References

Lipowicz, M. (1981), "Three-Phase Fractionation Yields Superpure Products", *Chemical Engineering*, Vol. 88, No. 9, 38-39.

McCabe, W L, Thiele, E W, (1925), "Graphical Design of Fractionating Columns", *Industrial & Engineering Chemistry*, Vol. 17, 605-611.

Morachevsky, A G & Zharov, V T, (1963), *Zhurnal Prikladnoi Khimii*, Vol. 36, p 2771 as reported by Gmehling & Onken [1977].

Morari, M, Meski, G A, Kiva, V N, Davidyan, A G, (1994), "Batch Distillation in a Column with a Middle Vessel", *Chemical Engineering Science*, Vol. 49, No. 18, 3033-3051.

Muir, R F & Howat, C S, (1982), "Predicting Solid-Liquid Equilibrium Data from Vapor-Liquid Data", *Chemical Engineering*, Vol. 89, No. 11, 89-92.

Mulet, A, Corropio, A B & Evans, L B, (1981), "Estimate Costs of Distillation and Absorption Towers via Correlation", *Chemical Engineering*, Vol. 88, No.26, 77-80,82.

Mullin, J W, (1961), "Crystallization", Butterworths, London.

Mutsuoka, M & Fukushima, H, (1986), as reported by Wynn [1992].

Nadgir, V M, & Liu, Y A, (1983), "Studies in Chemical Process Design and Synthesis: Part V: A Simple Heuristic Method for Systematic Synthesis of Initial Sequences for Multicomponent Separations", *American Institute of Chemical Engineers Journal*, Vol. 29, No. 6, 926-934.

Nath, R & Motard, R L, (1981), "Evolutionary Synthesis of Separation Processes", *American Institute of Chemical Engineers Journal*, Vol. 27, No 4, 578-592.

References

Nelson, R A, Olson, H J, Sandler, S I, (1983), "Sensitivity of Distillation Process Design and Operation to Vapour-Liquid Equilibrium Data", *Industrial and Engineering Chemistry, Process Design and Development*, Vol. 22, 547-552

Nothnagel, K H, Abrams, D S, Prausnitz, J M, (1973), "Generalized Correlation for Fugacity Coefficients in Mixtures at Moderate Pressures: Application of Chemical Theory of Vapour Imperfections", *Industrial and Engineering Chemistry Process Design and Development*, Vol. 12, No. 1, 25-35.

Null H R, Chapter 22, "Selection of a Separation Process", in Rousseau, R W, (1987), *Handbook of Separation Process Technology*, Wiley Interscience, New York.

Null, H R & Kruger, R E, (1980), "Phase Equilibrium in Process Design", Wiley-Interscience, New York.

Null, H R, (1980), "Energy Economy in Separation Processes", *Chemical Engineering Progress*, Vol. 76, 42-49.

Ott, B J, Goates, J R, Lamb, J D, (1972), "Solid-Liquid Phase Equilibria in Water + Ethylene Glycol", *Journal of Chemical Thermodynamics*, Vol. 4, 123-126.

Peridis, S, Magoulas, K, Tassios, D, (1993), "Sensitivity of Distillation Column to Uncertainties in Vapour-Liquid Equilibrium Information", *Separation Science and Technology*, Vol. 28, No. 9, 1753-1767.

Perry, R H & Green, D W, (1997), "Perry's Chemical Engineers' Handbook", 7th ed., McGraw-Hill, New York.

Prausnitz, J M, Anderson, T F, Grens, E A, Eckert, C A, Hseih, R, O'Connel, J P (1980), "Computer Calculations for Multicomponent Vapor-Liquid and Liquid-Liquid Equilibria", Prentice-Hall, Englewood Cliffs, NJ.

References

Prausnitz, J M, Lichtenthaler, R N, Gomes de Azevedo, E, (1986), "Molecular Thermodynamics of Fluid Phase Equilibria", 2nd ed., Prentice-Hall, Englewood Cliffs, NJ.

Price, C J, (1997), "Take Some Solid Steps to Improve Crystallization", *Chemical Engineering Progress*, Vol. 93, 34-43.

Raal, J D, Mühlbauer, A L, (1998), "Phase Equilibria: Measurement and Computation", Taylor and Francis, Bristol PA.

Reid, R C, Prausnitz, J M, Poling, B E, (1987), "The Properties of Gases and Liquids", 4th ed., McGraw-Hill Inc., New York.

Robinson, C S & Gilliland, E R, (1950), "Elements of Fractional Distillation", 4th ed., McGraw-Hill Book Company, New York.

Rose, L M, (1985), "Distillation Design in Practice", Elsevier Publishing Company, Amsterdam.

Rousseau, R W, (1987), "Handbook of Separation Process Technology", Wiley Interscience, New York.

Rousseau, R W & Moyers, C G, Chapter 11, "Crystallization Operations" in Rousseau, R W, (1987). *Handbook of Separation Process Technology*, Wiley Interscience, New York.

Russel, R A, (1983), "A Flexible and Reliable Method Solves Single-Tower and Crude-Distillation-Column Problems", *Chemical Engineering*, Vol. 90, No. 20, 53-59.

Safrit, B T, (1996), "Synthesis of Azeotropic Batch Distillation Systems", Ph.D. Thesis, Carnegie Mellon University.

Schrodt, V N, Somerfeld, J J, Martin, O M, Parisot, P E, Chew, H H, (1967), "Plant Scale Study of Controlled Cyclic Distillation", *Chemical Engineering Science*, Vol. 22, 759-767.

Seader, J D, Henley, E J, (1998), "Separation Process Principles", John Wiley & Sons, New York.

References

Seader, J D & Westerberg, A W, (1977), "A Combined Heuristic and Evolutionary Strategy for the Synthesis of Simple Separation Processes", *American Institute of Chemical Engineers Journal*, Vol. 23, No. 6, 951 - 954.

Sinnot, R K, (1993), "Coulson and Richardson's Chemical Engineering Design", 2nd ed., Vol. 6, Butterworth Hememann, Oxford.

Smoker & Rose, (1940), as reported by Perry & Green [1997].

Smith, J M & Van Ness, H C, (1987), "Introduction to Chemical Engineering Thermodynamics", 4th ed., McGraw Hill, Singapore.

Tamir, A & Wisniak, J, (1975), "Vapour-Liquid Equilibria in Associating Solutions", *Chemical Engineering Science*, Vol. 30, 335-342.

Tamir, A & Wisniak, J, (1976), "Association Effects in Ternary Vapour-Liquid Equilbria", *Chemical Engineering Science*, Vol. 31, 625-630.

Tamir, A & Wisniak, J, (1982), "Vapour-Liquid Equilibrium in the Systems Propyl Bromide-Acetic Acid, Propyl Bromide-Propionic Acid and Propyl Bromide-Acetic Acid-Propionic Acid", *Journal of Chemical Engineering Data*, Vol. 27, 430-435.

Tammann, G, (1989), as reported by Weissberger [1956].

Timmerhaus, K D & Peters, M S, (1981), "Plant Design and Economics for Chemical Engineers", 3rd ed., McGraw - Hill Inc., Singapore.

Treybal, R E, (1980), "Mass Transfer Operations", McGraw-Hill Inc., Auckland.

Underwood, A J V, (1948) as reported by Kister [1992].

Van Ness, H C, (1959), "Exact Forms of the Unrestricted Gibbs-Duhem Equation", *Chemical Engineering Science*, Vol. 10, 225-228.

References

Van Ness, H C, (1995), "Thermodynamics in the Treatment of Vapor/Liquid Equilibrium (VLE) Data", *Pure and Applied Chemistry*, Vol. 67, No. 6, 859-872.

Viola, J L, (1981), "Estimate capital costs via a new shortcut method", *Chemical Engineering*, Vol. 88, No.7, 80-86.

Walas, S M, (1985), "Phase Equilibria in Chemical Engineering", Butterworth Publishers, Boston.

Weast, R C, (1983), "Handbook of Chemistry and Physics", 64th ed., CRC Press, Boca Raton, Florida.

Weast, R C & Grasselli, J G, (1989), "Handbook of Data on Organic Compounds", 2nd ed . CRC Press, Boca Raton, Florida.

Weissberger, A, (1956), "Separation and Purification", Part I, Vol. 3, Interscience Publishers, New York.

Winn, F W, (1958) as reported by Kister [1992].

Wynn, N P, (1992), "Separate Organics by Melt Crystallization", *Chemical Engineering Progress*, Vol. 88, 52-60.

Yerazunis, S, Plowright, J D, Smola, F M, (1964), "Vapor-Liquid Equilibrium Determination by a New Apparatus", *Industrial and Engineering Chemistry*, Vol 34, 345-350.

APPENDIX A

A.1 Details of Solvents acid recovery plant

Simplified flowsheet of the Solvents acid recovery plant at SASOL'S plant in Secunda is shown in Figure A-1. The components present in the feed stream to the acid recovery process is shown in Table A-1.

Table A-1: Composition of acid water stream

Component	Composition (Mass %)
Acetic acid	0.930
Propionic acid	0.250
i-butyric acid	0.050
n-butyric acid	0.110
i-valeric acid	0.030
n-valeric acid	0.030
Hexanoic acid	0.015
Heptanoic acid	0.012
Non-acid chemicals	0.030
Methanol	0.025
Water	98.518

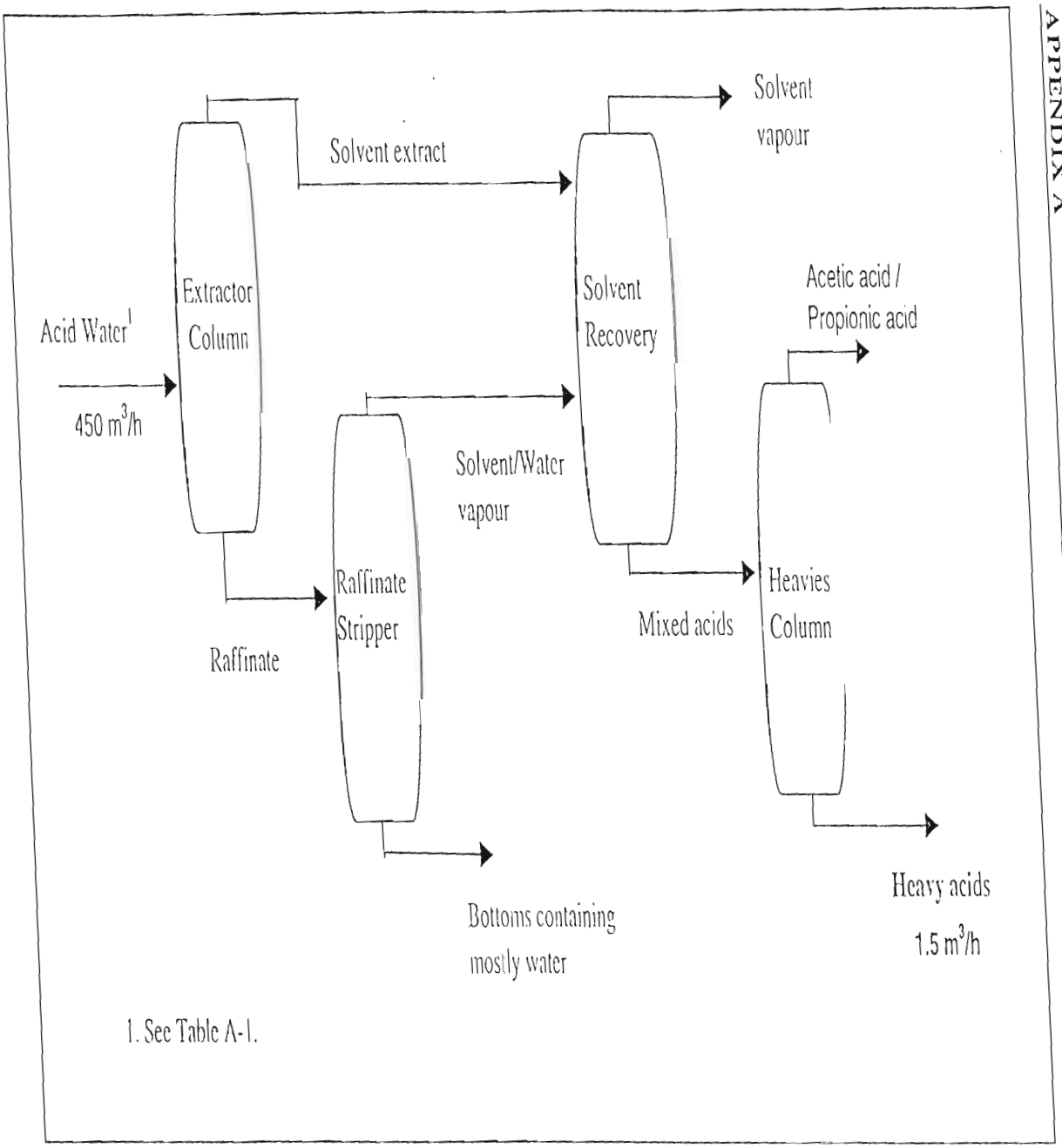

Figure A-1: Simplified flowsheet for acid recovery plant at Secunda

A.2 Physical propeties of components present in waste acid stream

Physical properties of all the components present in the waste acid stream are shown in Table A–2. All critical properties were obtained from Reid et al [1987]. Normal boiling points, densities freezing points and solubility were obtained from Weast [1983]. Dipole moments, accentricity and radius of gyration were obtained from Prausnitz et al [1980]. Physical properties for heptanoic acid, 2-cyclohexen-1-one, 3 heptene-2-one trans, phenyl butyrate, cyclopentyl acetate, cyclohexyl acetate were not available and was therefore estimated using the *Hysys* process simulator.

Table A-2: Properties of components present in waste acid stream

English Name (other name)	Chemical Formula	Molecular weight (g/mol)	Liquid Density (0C) (g/cm^3)	Normal Boiling Point (C)	Freezing Point (C)	Tc (K)	Pc(bar)	Vc(cm^3/mol)	Solubility*
1.Butyric Acid	$C_4H_8O_2$	88.11	0.9532 (25C)	164.05	-4.5	628	52.7	290	al,eth
2.Iso-butyric acid	$C_4H_8O_2$	88.11	0.9429 (25C)	154.75	-46.1	609	40.5	292	al,eth,w
3.iso-Valeric Acid (3-methyl-butyric acid)	$C_5H_{10}O_2$	102.13	0.9286 (25C)	176.55	-33.8	634	38.7	346	al,eth,ebl
4. Valeric Acid (Pentanoic Acid)	$C_5H_{10}O_2$	102.13	0.939 (20C)	185.5	-33.8	651	38.1	340	al,eth,w
5. Hexanoic Acid	$C_6H_{12}O_2$	116.16	0.923 (25C)	205.67	-2.0	667.05	33.5	389	al,eth
6. Heptanoic acid	$C_7H_{14}O_2$	130.19	0.918 (20C)	222.96	-7.5	418	30.83	451	ace,al,eth
7. 2-cyclohexen.. 1-one	C_6H_8O	96.13	0.9620 (25C)	170	-	631.58	24.91	533	ace,al
8. Propionic Acid	$C_3H_6O_2$	74.08	0.988 (25C)	141.14	-20.8	612	54	222	al,eth,w
9. 4 Butyrolactone	$C_4H_6O_2$	86.09	1.1286 (20C)	205.13	-	739	59.2	265	ace,al,bz,eth,w
10. Phenyl Acetate	$C_8H_8O_2$	136.15	1.073 (20C)	195.97	-	691.3	36.2	396	ace,al,eth
11.Phenyl propionate (3-phenyl propionic acid)	$C_9H_{10}O_2$	150.18	1.0467 (25C)	211	-	668.7	23.19	431	ace,al,eth
12. 3-heptene-2-one trans	$C_7H_{12}O$	112.07	0.8496 (20C)	62	-	602.3	31.73	415	al,eth

Table A-2...Continued

English Name (other name)	Chemical Formula	Molecular weight (g/mol)	Density [T(C)] (g/cm^3)	Normal Boiling Point (C)	Freezing Point (C)	Tc (K)	Pc(bar)	Vc(cm^3/mol)	Solubility*
13. Phenyl butyrate (3-phenyl butyric acid)	$C_{10}H_{12}O_2$	164.2	1.0382[15C]	225	-	743.85	30.82	511.5	al,eth
14. Cyclopentyl Acetate (Cyclopentanol acetate)	$C_7H_{12}O_2$	128.17	0.9522[15C]	51	-	586.64	31.24	423	-
15. Cyclohexyl Acetate	$C_8H_{14}O_2$	142.2	0.9698[20C]	173.21	-	608.16	28.14	485.5	al,eth
16. Cyclopentanone	C_5H_8O	84.12	0.9487[20C]	130.75	-	634.6	51.1	268	ace,al,eth,
17. Acetic acid	$C_2H_4O_2$	60.05	1.0437[25C]	117.86	-	592.7	57.9	171	ace,al,bz,w
18. 1M-2EBenzene	C_9H_{12}	120.19	0.8808[20C]	165.15	-	651	30.4	460	ace,al,eth,bz,

* ace = acetone
al = alcohol (generally ethyl alcohol)
bz = benzene
chl = chloroform
eth = ether (generally diethyl ether)
w = water

Table A-2...Continued

English Name (other name)	Radius of gyration (A)	Accentricity	Dipole moment (debye)
1.Butyric Acid	3.6	0.683	1.5
2.Iso-butyric acid	0.234	0.623	1.3
3.iso-Valeric Acid (3-methyl-butyric acid)	3.762	0.648	1
4. Valeric Acid (Pentanoic Acid)	3.965	0.614	0
5. Hexanoic Acid	4.4	0.67	1.2
6. Heptanoic acid	4.8	0.718	0
7. 2-cyclohexen.. 1-one	3.77	0.463	0
8. Propionic Acid	0.183	0.52	1.5
9. 4 Butyrolactone	3.1	0.369	4.03
10. Phenyl Acetate	4.36	0.43	1.9
11.Phenyl propionate (3-phenyl propionic acid)	4.765	0.551	0
12. 3-heptene-2-one.. trans	4.31	0.443	0

Table A-2...Continued

English Name (other name)	Radius of gyration (A)	Accentricity	Dipole moment (debye)
13. Phenyl butyrate (3-phenyl butyric acid)	5.45	0.587	0
14. Cyclopentyl Acetate (Cyclopentanol acetate)	4.703	0.555	0
15. Cyclohexyl Acetate	4.96	0.6	0
16. Cyclopentanone	0.26	0.35	3
17. Acetic acid	0.201	0.447	1.3
18. 1M-2EBenzene	0.26	0.294	0

APPENDIX B

B.1 The Criterion for phase equilibrium

Consider a closed system consisting of two phases, α and β, in equilibrium. Within this closed system, each of the individual phases is an open system, free to transfer mass to the other. Assuming that at equilibrium, the temperature and pressure are uniform throughout the closed system, the following equations can be written for each of the phases α and β:

$$d(nG)^{\alpha} = (nV)^{\alpha} dP - (nS)^{\alpha} dT + \sum \mu_i^{\alpha} dn_i^{\alpha} \tag{B-1}$$

$$d(nG)^{\beta} = (nV)^{\beta} dP - (nS)^{\beta} dT + \sum \mu_i^{\beta} dn_i^{\beta} \tag{B-2}$$

where μ_i is the chemical potential and it is defined in terms of the Gibbs energy as:

$$\mu_i = \left[\frac{\partial(nG)}{\partial n_i}\right]_{T,P,n_j} \tag{B-3}$$

Equations (B-1) and (B-2) may be added to give the total changes for the system.

$$d(nG) = (nV)dP - (nS)dT + \sum \mu_i^{\alpha} dn_i^{\alpha} + \sum \mu_i^{\beta} dn_i^{\beta} \tag{B-4}$$

In Equation (B-4), the total system properties were obtained using the following relation:

$$nM = (nM)^{\alpha} + (nM)^{\beta} \tag{B-5}$$

Since the two-phase system is closed, the following equation is valid:

$$d(nG) = (nV)dP - (nS)dT \tag{B-6}$$

Comparison of Equation (B-4) and (B-6) shows that at equilibrium:

$$\sum \mu_i^{\alpha} dn_i^{\alpha} + \sum \mu_i^{\beta} dn_i^{\beta} = 0 \tag{B-7}$$

Since the conservation of mass requires that $dn_i^{\alpha} = -dn_i^{\beta}$, Equation (B-7) reduces to:

$$\sum (\mu_i^{\alpha} - \mu_i^{\beta}) dn_i^{\alpha} = 0 \tag{B-8}$$

Since the quantities dn_i are independent and arbitrary, Equation (B-8) can only be satisfied if the term in the parenthesis is separately zeroed. Hence

$$\mu_i^{\alpha} = \mu_i^{\beta} \tag{B-9}$$

This result may be generalised to more than two phases by considering the phases by pairs. The general result for π phases with N chemical species is:

$$\mu_i^{\alpha} = \mu_i^{\beta} = \mu_i^{\pi} \; (i = 1, 2, \ldots, N) \tag{B-10}$$

An alternative and equally general criterion for equilibrium can be derived from the following equation:

$$d\overline{G_i} = RTd \ln f_i \qquad \text{(constant T)} \tag{B-11}$$

where f_i is the fugacity of species i in solution and $\overline{G_i}$ is the partial molar Gibbs energy which is given by:

$$\overline{G_i} = \left[\frac{\partial(nG)}{\partial n_i}\right]_{T,P,n_j} \tag{B-12}$$

Comparison of Equation (B-12) and (B-3) implies that $\mu_i = \overline{G_i}$. Thus Equation (B-11) becomes:

$$d\mu_i = RTd \ln f_i \qquad \text{(constant T)} \tag{B-13}$$

Integration of Equation (B-13) at constant temperature gives:

$$\mu_i = RT \ln f_i + \theta_i(T) \tag{B-14}$$

Since θ_i is dependent on temperature only and since and since all the phases are at the same temperature, substitution of Equation (B-14) into (B-10) yields:

$$f_i^{\alpha} = f_i^{\beta} = \ldots = f_i^{\pi} \qquad (i = 1,2,\ldots,N) \tag{B-15}$$

B.2 Program for calculation of fugacity coefficients

The following program was written in the Matlab programming language. The program that was used for the butyric acid (1) + valeric acid (2) system at 14Kpa is shown.

(The comments are denoted by " %")

```
% General Constants
R = 83.14; %Universal gas constant (cm^3 bar mol^-1K^-1)

% Properties of chemicals
mu2 = 1.0;  %Dipole moment (debyes)
mu1 = 1.5;
Tc1 = 627; %Critical Temperature (K)
Tc2 = 632;
Pc1 = 39.8;  %Critical Pressure (bar)
Pc2 =31.6;

% Calculation of Vapour Pressure (A, B, C constants for Antoine
Equation)
A2 = 7.6;
B2 = 2000;
C2 = -186.3;
A1 = 7.7;
B1 = 1999.98;
C1 = -177.3;
P1sat = exp.((A1-(B1./(C1+(T))))); % Vapour pressure (bar)
P2sat = exp.((A2-(B2./(C2+(T))))));


% Calculation of non-polar accentric factor
R1 = 3.60998; %Mean Radius of Gyration (Prausnitz et al. [1980])
R2 = 3.762;
wprime1 = 0.006026*R1 + 0.02096*R1^2 - 0.001366*R1^3;
wprime2 = 0.006026*R2 + 0.02096*R2^2 - 0.001366*R2^3;
wprime12 = 0.5*(wprime1 + wprime2);

% Prime Molecular size parameter for pure polar and associating pairs
sig1prime = (2.44 - wprime1)*(1.0133*Tc1/Pc1)^(1/3);
sig2prime = (2.44 - wprime2)*(1.0133*Tc2/Pc2)^(1/3);

%Calculation of Prime Characteristic Energy(e/k = ek)'-pure component
parameters
n1 = 4.5; %Association parameter (Prausnitz et al.[1980])
n2 = 4.5;
ekprime1 = Tc1*(0.748 + 0.91*wprime1 - 0.4*n1/(2 + 20*wprime1));
ekprime2 = Tc2*(0.748 + 0.91*wprime2 - 0.4*n2/(2 + 20*wprime2));

% Calculation of angle averaged polar effect for component 1
if mu1 < 1.45
   et1 = 0;
else
   et1 = 1.7941e7*mu1^4/((2.882 - 1.882*wprime1/(0.03 +
wprime1))*Tc1*sig1prime^6*ekprime1);
end
```

```
% Calculation of angle averaged polar effect for component 2
if mu2 < 1.45
   et2= 0;
else
   et2 = 1.7941e7*mu2^4/((2.882 - 1.882*wprime2/(0.03 +
wprime2))*Tc2*sig2prime^6*ekprime2);
end

%Calculation of Characteristic Energy (e/k = ek)-pure component
parameters
c11 = (16 + 400*wprime1)/(10 + 400*wprime1);
c12 = (16 + 400*wprime2)/(10 + 400*wprime2);
ek1 = ekprime1*(1 - et1*c11*(1 - et1*(1 + c11)*0.5));
ek2 = ekprime2*(1 - et2*c12*(1 - et2*(1 + c12)*0.5));

% Calculation of free contributions (nonpolar(Bfnp)& polar(Bfp)) to
second virial coefficient.
c21 = 3/(10 + 400*wprime1);
c22 = 3/(10 + 400*wprime2);
sig1 = sig1prime*(1 + et1*c21)^(1/3);
sig2 = sig2prime*(1 + et2*c22)^(1/3); %Molecular size parameter for
pure polar and associating
% pairs (A)
mu1r = 7243.8*mu1^2/(ek1*sig1^3);  %Reduced dipole moment (Debye)
mu2r = 7243.8*mu2^2/(ek2*sig2^3);
if mu1r < 0.04
   mu1rprime = mu1r;
elseif mu1r > 0.25
   mu1rprime = mu1r - 0.25;
else
   mu1rprime = 0;
end
if mu2r < 0.04
   mu2rprime = mu1r;
elseif mu2r > 0.25
   mu2rprime = mu2r - 0.25;
else
   mu2rprime = 0;
end

%Calculation of equivalent hard sphere volume of molecules (cm^3/mol)
bo1 = 1.26184*sig1^3;
bo2 = 1.26184*sig2^3;

%Calculation of reduced temperature (K)
Tr1 = 1./(ek1./T - 1.6*wprime1);
Tr2 = 1./(ek2./T - 1.6*wprime2);

%Calculation of Bfnp
B11fnp = bo1.*(0.94 - (1.47./Tr1) - (0.85./Tr1.^2) + (1.015./Tr1.^3));
B22fnp = bo2.*(0.94 - (1.47./Tr2) - (0.85./Tr2.^2) + (1.015./Tr2.^3));

%Calculation of bfp
B11fp = -bo1.*mu1rprime.*(0.75 - 3./Tr1 + 2.1./Tr1.^2 + 2.1./Tr1.^3);
B22fp = -bo2.*mu2rprime.*(0.75- 3./Tr2 + 2.1./Tr2.^2 + 2.1./Tr2.^3);
```

```
% Calculation of free contributions
B1f = B11fnp + B11fp;
B2f = B22fnp + B22fp;

% Calculation of true fugacity coefficient
truephi1 = exp.((P.*B1f)./(R.*T));
truephi2 = exp.((P.*B2f)./(R.*T));

%Calculation of Cross parameters
ek12prime = 0.7*(ek1*ek2)^(1/2) + 0.6/(1/ek1 + 1/ek2);
c112prime = (16 + 400*wprime12)/(10 + 400*wprime12);
sig12prime = (sig1*sig2)^0.5; % molecular size-Cross parameter'
if mu1 >= 2 & mu2 == 0
          et12prime =
(mu1^2*(ek2)^2/3*(sig2)^4)/((ek12prime)*(sig12prime)^6);
   elseif mu2 >= 2 & mu1 == 0
   et12prime = (mu1^2*(ek1)^2/3*(sig1)^4)/((ek12prime)*(sig12prime)^6);
else
   et12prime =0;
end
c212prime = 3/(10 + 400*wprime12);
sig12 = sig12prime*(1 - et12prime*c212prime)^(1/3);
ek12 = ek12prime*(1 + et12prime*c112prime);
mu12r = 7243.8*mu1*mu2/(ek12*sig12^3);
if mu12r < 0.04
   mu12rprime = mu12r;
elseif mu12r >= 0.25
   mu12rprime = mu12r - 0.25;
else
   mu12rprime = 0;
end
Tr12 = 1./(ek12./T - 1.6*wprime12);
bo12 = 1.26184*sig12^3;
B12fnp = bo12.*(0.94 - 1.47./Tr12 - 0.85./Tr12.^2 + 1.015./Tr12.^3);
B12fp = -bo12.*mu12rprime.*(0.75 - 3./Tr12 + 2.1./Tr12.^2 +
2.1./Tr12.^3);
B12f = B12fnp + B12fp;

%Calculation of effective enthalpy of formation of physically bound
pairs (ergs/molecule)
dH1 = 1.99 + 0.2*mu1r^2;
dH2 = 1.99 + 0.2*mu2r^2;
dH12 = 1.99 + 0.2*mu12r^2;

L1 = -0.3 - 0.05*mu1r;
L2 = -0.3 - 0.05*mu2r;
A12 = -0.3 - 0.05*mu12r;

B11mb = bo1*L1*exp(dH1./(T/ek1));  %cm^3/mol
B22mb = bo2*L2*exp(dH2./(T/ek2));
B12mb = bo12*A12*exp(dH12./(T/ek12));
```

```
%Calculation of Bchemical (Bc)
n12 =4.5; % association parameter (Prausnitz et al.[1980]).
if n1 < 4.5
   E1 = exp.(n1*(650/(ek1 + 300) - 4.27));
else
   E1 = exp.(n1*(42800/(ek1 + 22400) - 4.27));
end
if n2 < 4.5
   E2 = exp.(n2*(650/(ek2 + 300) - 4.27));
else
   E2 = exp.(n2*(42800/(ek2 + 22400) - 4.27));
end
if n12 < 4.5
   E12 = exp.(n12*(650/(ek12 + 300) - 4.27));
else
   E12 = exp.(n12*(42800/(ek12 + 22400) - 4.27));
End

B11c = bo1*E1*(1 - exp.(1500*n1./T)) ; %cm^3/mol
B22c = bo2*E2*(1 - exp.(1500*n2./T));
B12c = bo12*E12*(1 - exp.(1500*n12./T));
B12dimerized = B12c + B12mb;
B11dimerized = B11c + B11mb;
B22dimerized = B22c + B22mb;

% Calculation of equilibrium constants (Ki)
K1 = -B11dimerized./(R.*T);
K2 = -B22dimerized./(R.*T);
K12 = -2*B12dimerized./(R.*T);

%Experimental data required
%Butyric acid (1)+ valeric acid (2) system at 14kPa

%Pressure (bar)
P=0.14;

%Temperature (K)
T = 273.15+[122.1147, 121.0405, 119.4393, 115.9127, 114.1696, 112.7438.
111.778];

%Vapour mole fraction
v1 = [ 0.05097, 0.114251, 0.264827, 0.612579,0.759547, 0.856703,
0.925419 ];
v2 = 1-v1;


% Calculation of yi(apparent mole fraction) and zi(true mole fraction)
B12dimerized = -K12.*R.*T/2; % virial coefficient for dimerized
molecules
B11dimerized = -(K1.*R.*T)/1;
B22dimerized = -(K2.*R.*T)/1;
C12 = -(2.*B12dimerized).*(P./(R.*T)).*exp.((P./(R.*T)).*(B1f+B2f-
B12f));
C11 = -(1.*B11dimerized).*(P./(R.*T)).*exp.((P./(R.*T)).*(B1f));
C22 = -(1.*B22dimerized).*(P./(R.*T)).*exp.((P./(R.*T)).*(B1f));
C21 = C12;
```

```
P1m = (-1 + (1+(4.*K1.*P1sat)).^0.5)./(2.*K1); % vapor pressure for
apparent dimerization
P2m = (-1 + (1+(4.*K2.*P2sat)).^0.5)./(2.*K2);
if C11 <= 0.5 & C12 <= 0.5
   z1 = v1
   z2 = v2
elseif C12 > 0.5 & v1 > 0.5
   z2 = v2.*(1+(C12.*v1)).^-1;  % change equation for suite
   z1 = v1.*(1+(C12.*z2)).^-1;
else
   z1 = v1.*(1+(C12.*v2)).^-1;  % change equation for suite
   z2 = v2.*(1+(C12.*z1)).^-1;
end

z12 = C12.*z1.*z2;
z11 = C11.*z1.*z1;
z22 = C22.*z2.*z2;
z21 = z12;
gamma1 = z11 + z11 + z21;
gamma2 = z21 + z22 + z22;
z1r = (v1.*(1 + (0.5.*gamma1) + (0.5.*gamma2)))./(1+(2.*C11.*z1) +
(C21.*z2));
z2r = (v2.*(1 + (0.5.*gamma1) + (0.5.*gamma2)))./(1+(2.*C22.*z2) +
(C21.*z1));
error1 = abs(z1r-z1);
error2 = abs(z2r-z2);
while any(abs(error1) >0.0001 & abs(error2) > 0.0001);
   z1 = z1r;
   z2 = z2r;
   z12 = C12.*z1.*z2;
   z11 = C11.*z1.*z1;
   z22 = C22.*z2.*z2;
   z21 = z12;
   gamma1 = z11 + z11 + z21;
   gamma2 = z21 + z22 + z22;
   z1r = (v1.*(1 + (0.5.*gamma1) + (0.5.*gamma2)))./(1+(2.*C11.*z1) +
(C21.*z2));
   z2r = (v2.*(1 + (0.5.*gamma1) + (0.5.*gamma2)))./(1+(2.*C22.*z2) +
(C21.*z1));
   error1 = z1r-z1;
   error2 = z2r-z2;
end

% Calculation of fugacity coefficient
phi1 = z1r.*truephi1./v1;
phi2 = z2r.*truephi2./v2;
```

B.3 The UNIFAC method

For a binary system (1)-(2), the activity coefficient is determined as the sum of a residual and combinatorial activity coefficient:

$$\ln \gamma_1 = \ln \gamma_1^C + \ln \gamma_1^R \tag{B-16}$$

where the combinatorial term is expressed as follows:

$$\ln \gamma_1^C = \ln \frac{\Phi_1}{x_1} + \frac{Z}{2} q_1 \ln \frac{\theta_1}{\Phi_1} + l_1 - \frac{\Phi_1}{x_1}(x_1 l_1 + x_2 l_2) \tag{B-17}$$

The q, Φ, θ, and l values are calculated as follows:

$$r_i = \sum_k \nu_k^{(i)} R_k \tag{B-18}$$

$$q_i = \sum_k \nu_k^{(i)} Q_k \tag{B-19}$$

$$\Phi_i = \frac{r_i x_i}{\sum_j r_j x_j} \tag{B-20}$$

$$\theta_i = \frac{q_i x_i}{\sum_j q_j x_j} \tag{B-21}$$

Z = 10, and the R_k and Q_k values are group contribution values derived from literature tables (Fredenslund et al [1977] and Raal & Mühlbauer, [1998]).

The residual activity coefficient is calculated from equation (B-21):

$$\ln \gamma_i^R = \sum_k \nu_k^{(i)} (\ln \Gamma_k - \ln \Gamma_k^{(i)}) \tag{B-21}$$

where both Γ_k (contribution of solute group in the solution) and $\Gamma_k^{(i)}$ (contribution of solute groups in the pure-component environment) are calculated from equation (B-22):

$$\ln \Gamma_k = Q_k \left(1 - \ln \left(\sum_m \theta_m \psi_{mk} \right) - \sum_m \frac{\theta_m \psi_{km}}{\sum_n \theta_n \psi_{nm}} \right) \tag{B-23}$$

and θ, X ψ values are calculated as follows:

$$\theta_m = \frac{Q_m X_m}{\sum_n Q_n X_n} \tag{B-24}$$

$$X_m = \frac{\sum_n \nu_m^{(n)} x_n}{\sum_a \sum_p \nu_p^{(n)} x_n} \tag{B-25}$$

$$\psi_{mn} = \exp(a_{mn} / T) \tag{B-26}$$

a_{mn} is a group interaction parameter obtained from literature tables (Fredenslund et al. [1977] and Raal & Mühlbauer [1998]).

B.4 Calibration Curves

Calibration curves for the pressure transducer, temperature sensor and gas chromatographs were required to obtain actual readings.

B.4.1 Pressure Calibration

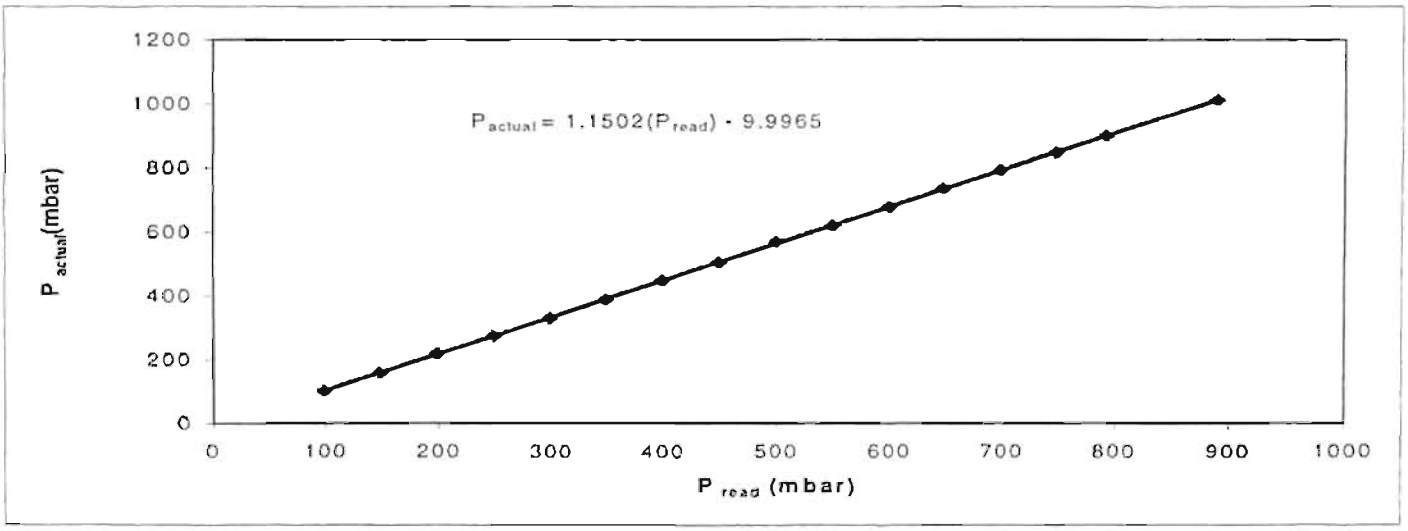

Figure B-1: Calibration curve for the Fisher pressure transducer

B.4.2 Temperature Calibration

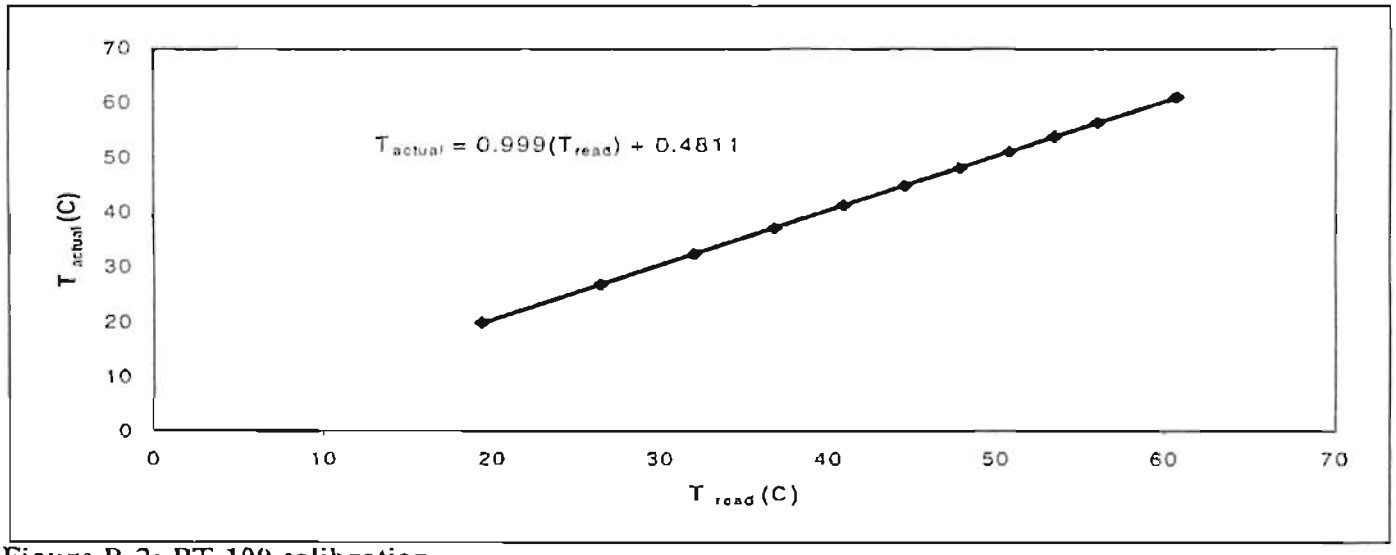

Figure B-2: PT-100 calibration

B.4.3 GC calibration curves

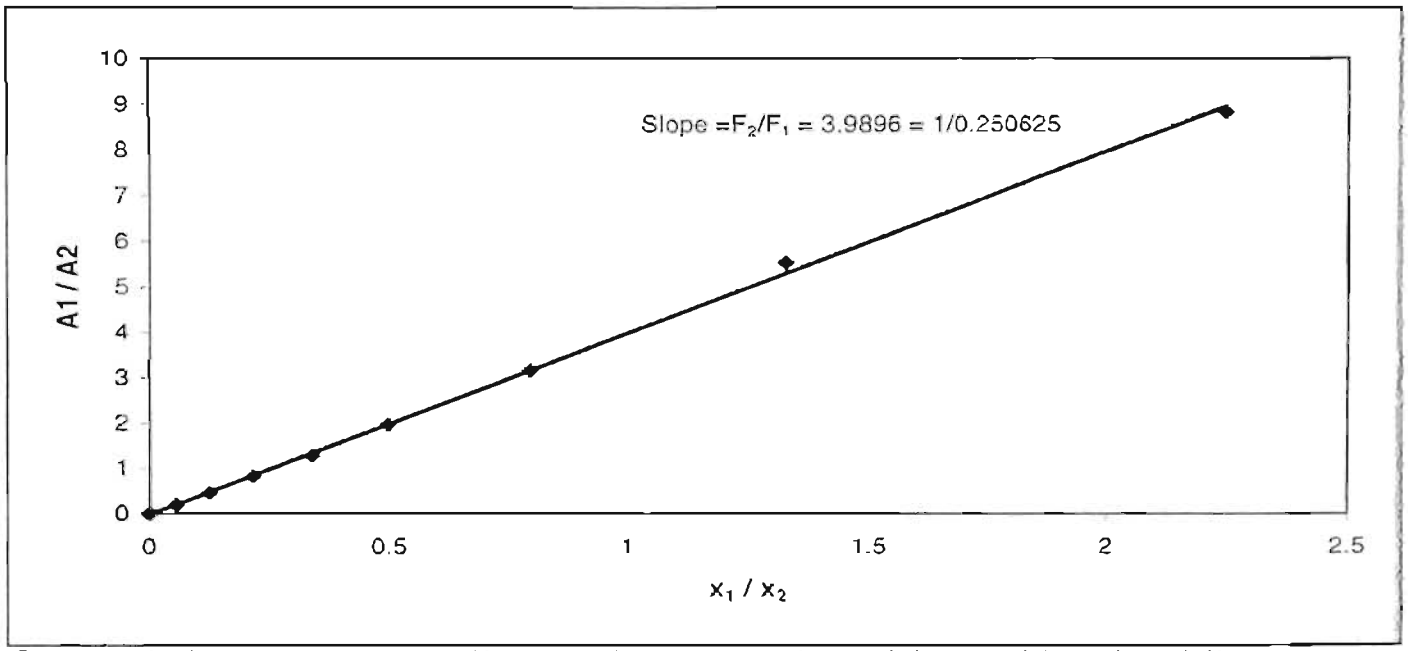

Figure B-3: Gas chromatograph (Shimadzu) calibration for cyclohexane (1) + ethanol (2)

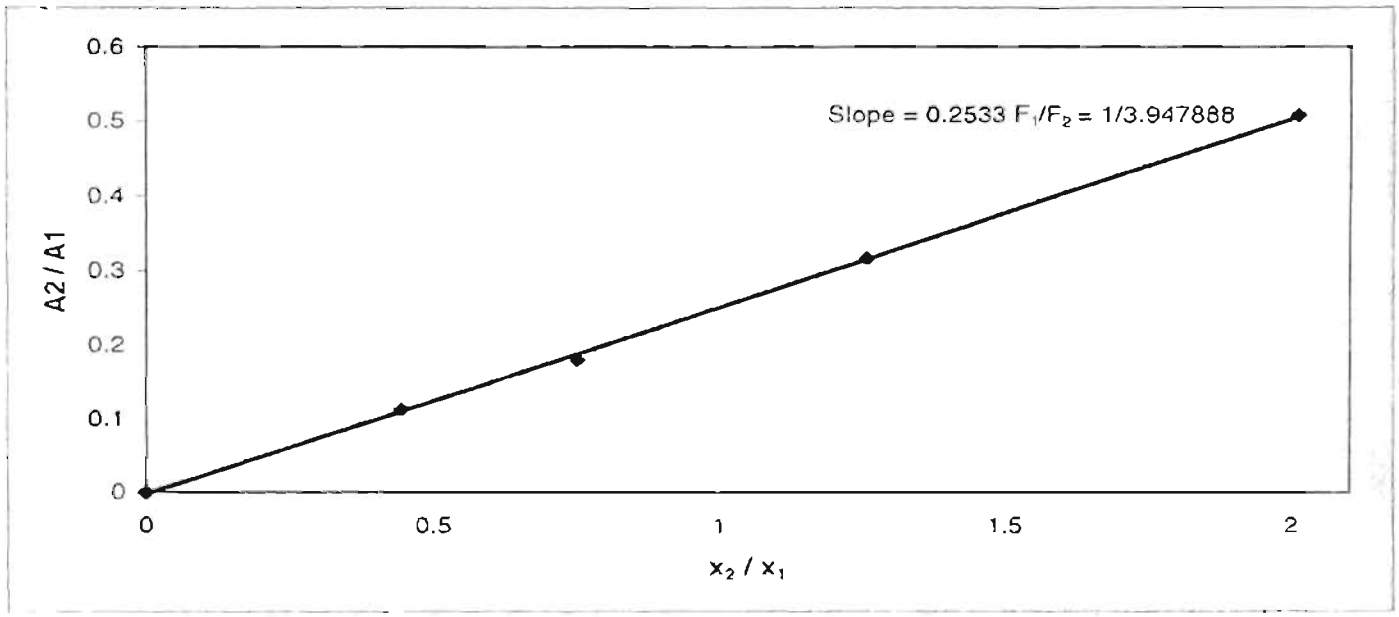

Figure B-4: Gas chromatograph (Shimadzu) calibration for cyclohexane (1) + ethanol (2)

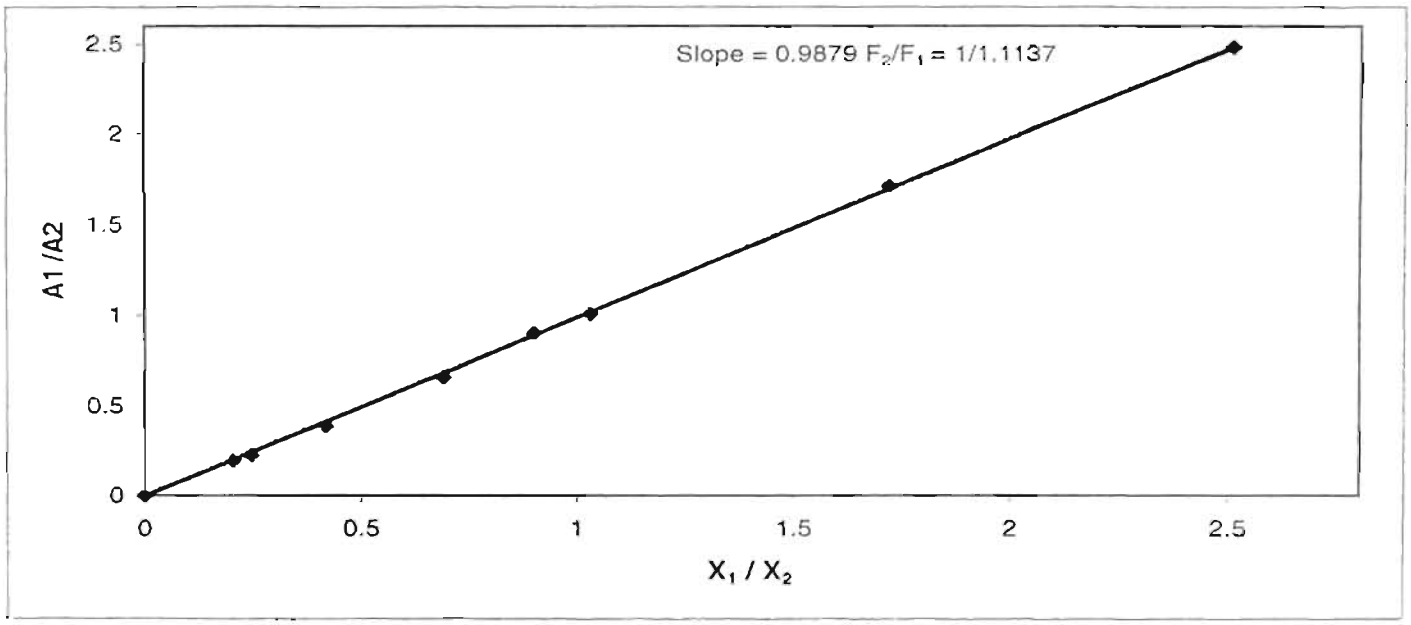

Figure B-5: Gas chromatograph (Varian 3000) calibration for propionic acid (1) + butyric acid (2)

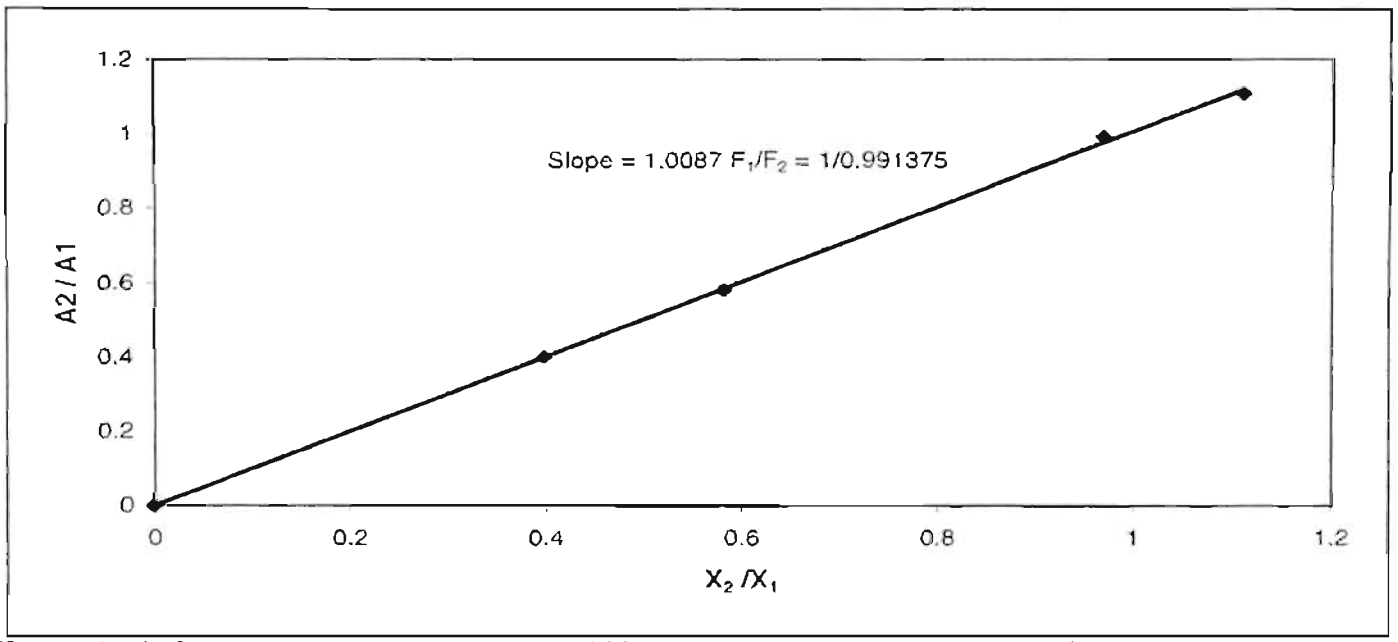

Figure B-6: Gas chromatograph (Varian 3000) calibration for propionic acid (1) + butyric acid (2)

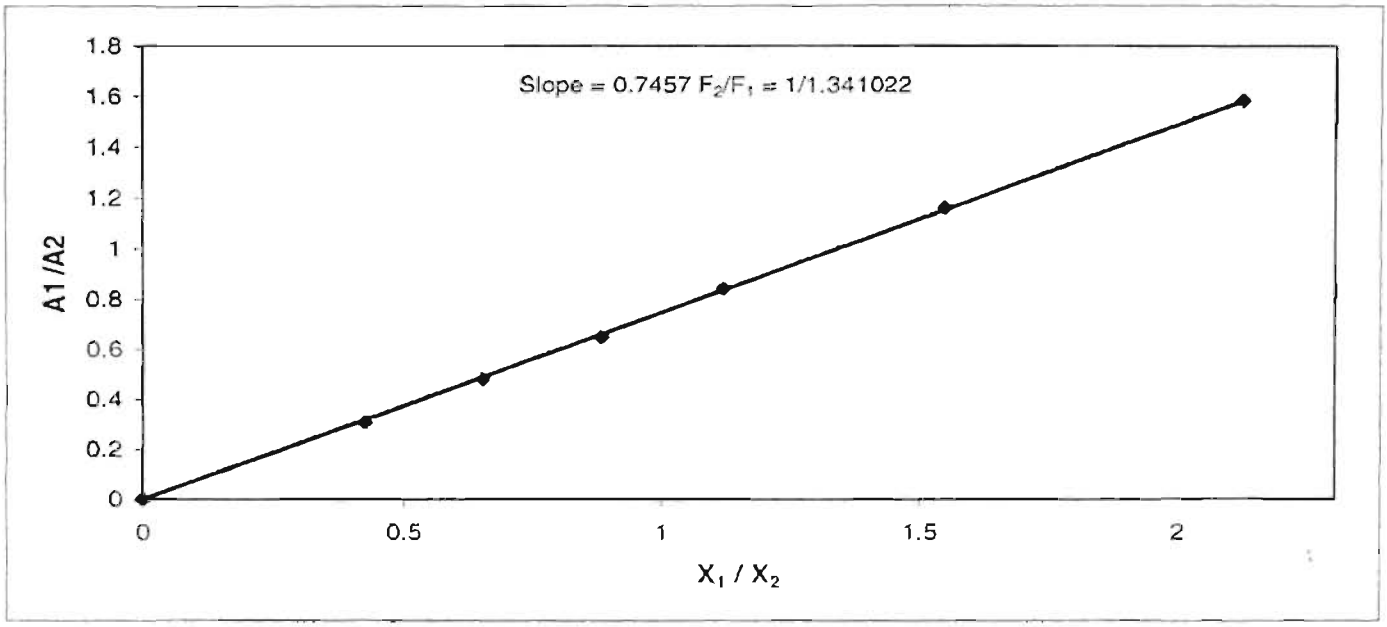

Figure B-7: Gas chromatograph (Varian 3000) calibration for butyric acid (1) + isovaleric acid (2)

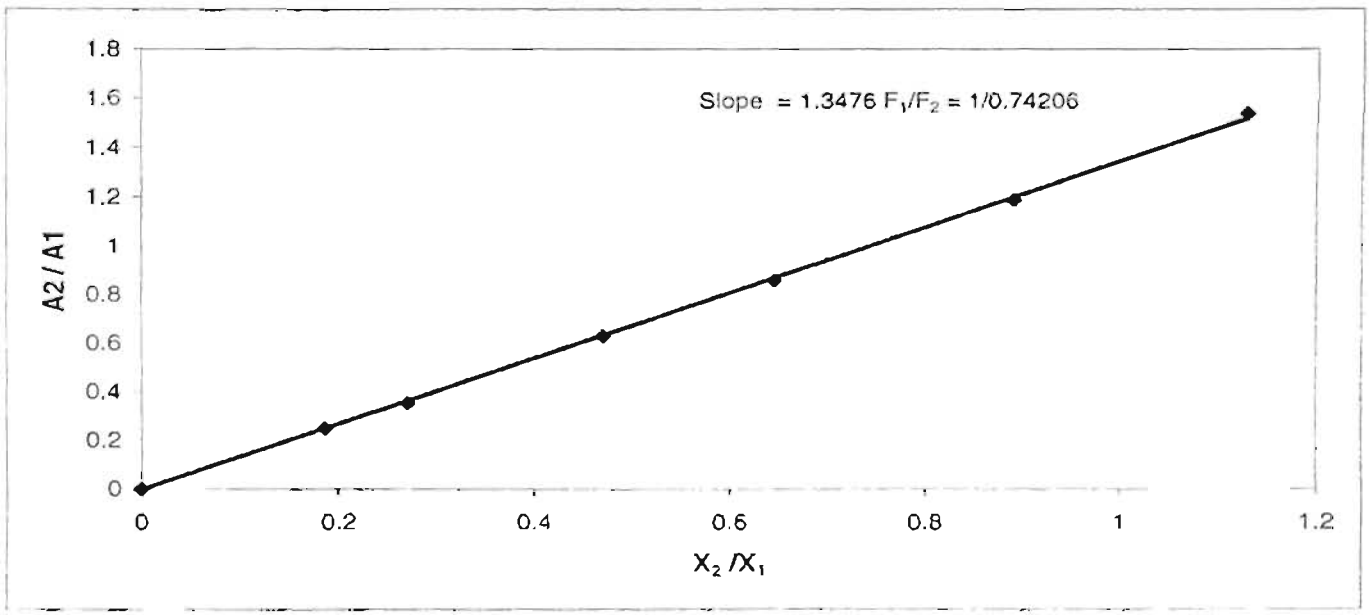

Figure B-8: Gas chromatograph (Varian 3000) calibration for butyric acid (1) + isovaleric acid (2)

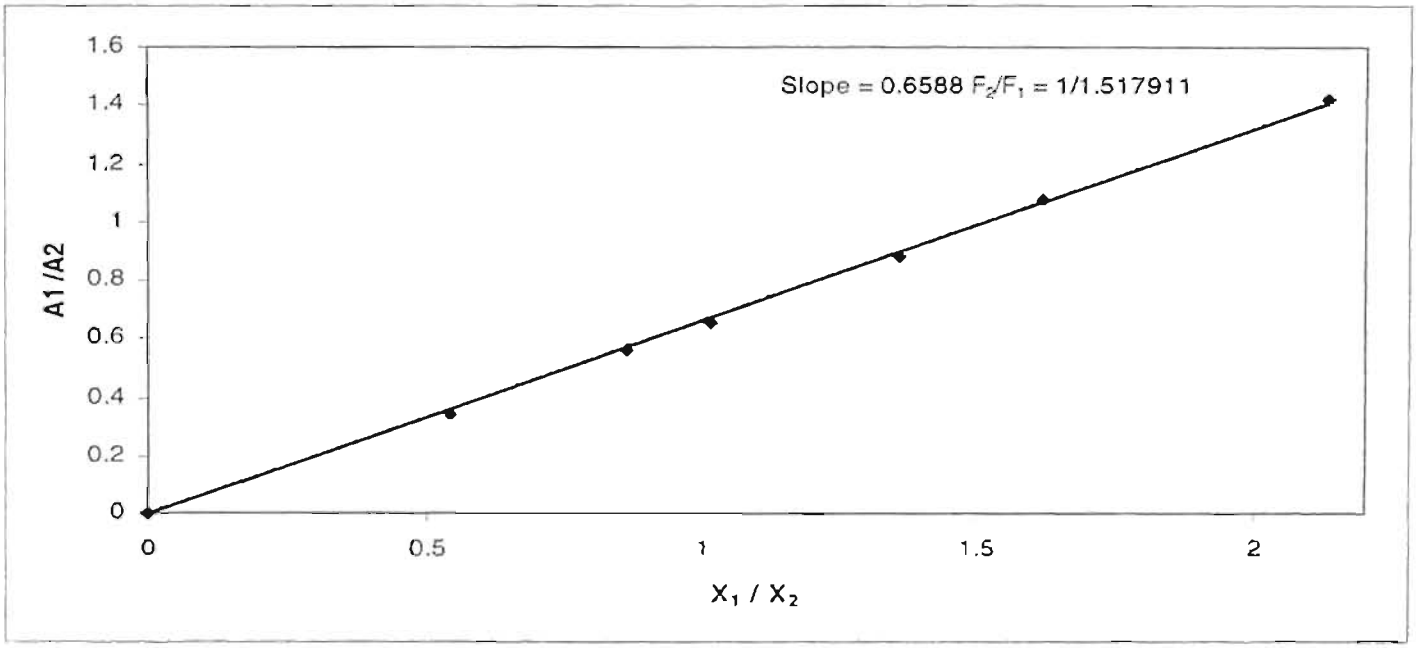

Figure B-9: Gas chromatograph (Varian 3000) calibration for butyric acid (1) + hexanoic acid (2)

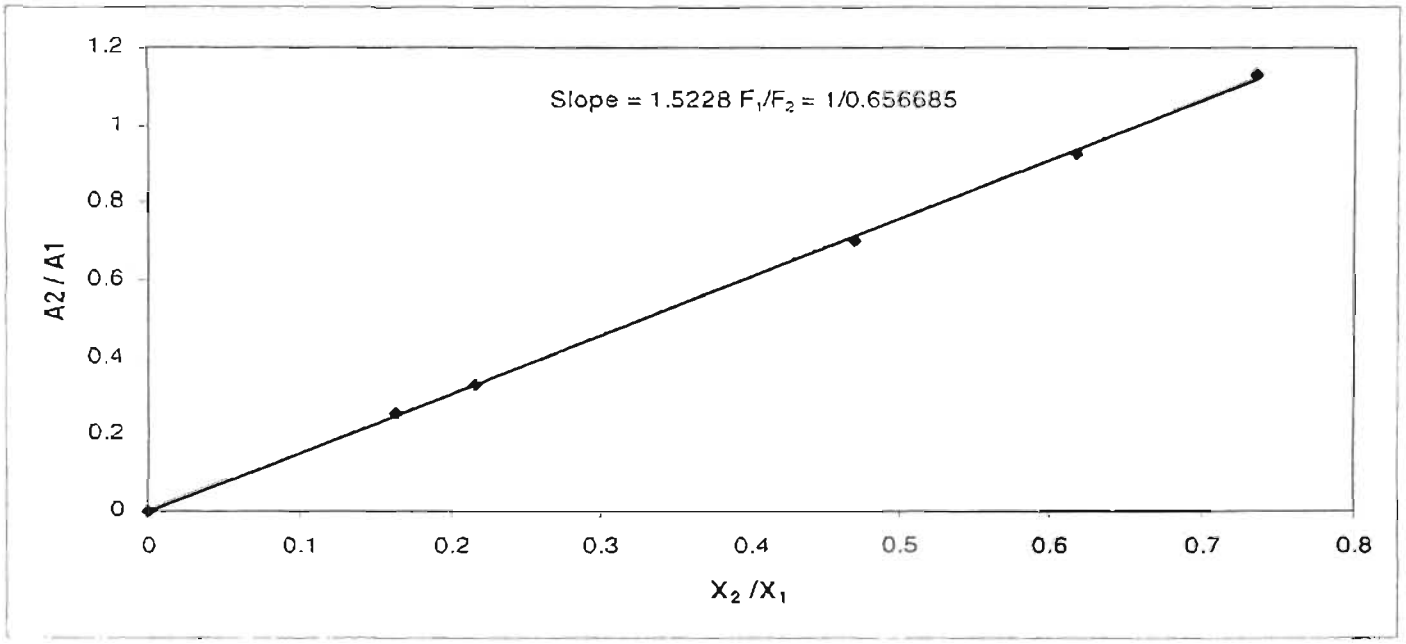

Figure B-10: Gas chromatograph (Varian 3000) calibration for butyric acid (1) + hexanoic acid (2)

B.5 Thermodynamic consistency tests

Thermodynamic consistency tests are based on the Gibbs-Duhem equation:

$$\sum x_i d\ln\gamma_i = \frac{V^E}{RT}dP - \frac{H^E}{RT^2}dT \qquad \text{(B-27)}$$

For a system to be thermodynamically consistent the VLE data must satisfy the Gibbs-Duhem equation. In this project the Direct test proposed by Van Ness [1995] was used. The test is formulated as follows:

The activity coefficient is related to the excess Gibbs energy (G^E) as:

$$\frac{G^E}{RT} = \sum x_i \ln\gamma_i \qquad \text{(B-28)}$$

For a binary system Equation (B-28) becomes:

$$g^* = x_1 \ln\gamma_1^* + x_2 \ln\gamma_2^* \qquad \text{(B-29)}$$

In the above equation $g = G^E/RT$ and the asterisk denotes experimental values.

Differentiation of Equation (B-29) yields:

$$\frac{dg^*}{dx_1} = \ln\frac{\gamma_1^*}{\gamma_2^*} + \varepsilon + x_1\frac{d\ln\gamma_1^*}{dx_1} + x_2\frac{d\ln\gamma_2^*}{dx_1} - \varepsilon \qquad \text{(B-30)}$$

where, for isothermal data,

$$\varepsilon = \frac{V^E}{RT}\frac{dP}{dx_1} \qquad \text{(B-31)}$$

or, for isobaric data,

$$\varepsilon = \frac{-H^E}{RT^2}\frac{dT}{dx_1} \qquad \text{(B-32)}$$

At this point an equation inter-relating the excess thermodynamic properties (G^E, V^E, and H^E) as derived by Van Ness [1959] is introduced:

$$d\left[n\left(\frac{G^E}{RT}\right)\right] = \frac{nV^E}{RT}dP - \frac{nH^E}{RT^2}dT + \sum \ln\gamma_i dn_i \qquad \text{(B-33)}$$

Applying equation (B-33) to one mole of a liquid phase containing species 1 and 2, the following equation results (written for only isothermal or only isobaric data):

$$\frac{dg}{dx_1} = \ln\frac{\gamma_1}{\gamma_2} + \varepsilon \qquad \text{(B-34)}$$

By subtracting equation (B-30) from equation (B-34), the following equation is obtained:

$$\frac{dg}{dx_1} - \frac{dg^*}{dx_1} = \ln\frac{\gamma_1}{\gamma_2} - \ln\frac{\gamma_1^*}{\gamma_2^*} - \left[x_1 \frac{d\ln\gamma_1^*}{dx_1} + x_2 \frac{d\ln\gamma_2^*}{dx_1} - \varepsilon \right] \qquad \text{(B-35)}$$

In terms of residuals, this equation becomes:

$$\frac{d(\delta g)}{dx_1} = \delta \ln\frac{\gamma_1}{\gamma_2} - \left[x_1 \frac{d\ln\gamma_1^*}{dx_1} + x_2 \frac{d\ln\gamma_2^*}{dx_1} - \varepsilon \right] \qquad \text{(B-36)}$$

If a data set, either isothermal or isobaric is reduced with $\sum(\delta g)^2$ as the objective function, then $d(\delta g)/dx_1$ is effectively zero, and

$$\delta \ln\frac{\gamma_1}{\gamma_2} = x_1 \frac{d\ln\gamma_1^*}{dx_1} + x_2 \frac{d\ln\gamma_2^*}{dx_1} - \varepsilon \qquad \text{(B-37)}$$

According to the Gibbs-Duhem equation, the right-hand side of equation (B-37) should be zero for consistent data. The residual on the left is therefore a direct measure of deviations from the Gibbs-Duhem equation. The extent to which values of this residual fail to scatter about zero measures the departure of the data from thermodynamic consistency. Thus the application of this test involves two basic steps. First the VLE data are reduced using $\sum(\delta g)^2$ as the objective function and second the residual $\delta \ln(\gamma_1/\gamma_2)$ is determined. Van Ness [1995] developed a consistency index [Table B-1] based on the root-mean square (RMS) value of $\delta \ln(\gamma_1/\gamma_2)$, which begins at one for highly consistent data and ends at ten for data of very poor quality. This replaces the totally inadequate "+/−" or "yes/no" designation presently employed by other tests to characterise the consistency of a data set.

Table B-1: Consistency index for direct test of Van Ness [1995]

Index	RMS $\delta\ln(\gamma_1/\gamma_2)$		Comments
1	>0	≤0.025	excellent
2	>0.025	≤0.050	very good
3	>0.050	≤0.075	good
4	>0.075	≤0.100	satisfactory
5	>0.100	≤0.125	poor
6	>0.125	≤0.150	very poor
7	>0.150	≤0.175	inconsistent data
8	>0.175	≤0.200	inconsistent data
9	>0.200	≤0.225	inconsistent data
10	>0.225		inconsistent data

APPENDIX C

C.1 Capital Cost Estimation

C.1.1. Equipment Costs

- Weight of Tower as calculated by method suggested by Kister [1992] = 3175 kg
- Area of Reboiler calculated by method suggested by Sinnot [1993] = 3.44 m^2
- Area of Condenser calculated by method suggested by Sinnot [1993] = 1.66 m^2
- Estimated capacity of Crystallizer = 3.00 m^3

Table C-1: Costing for Equipment obtained using published equipment data.

Item	Costs
- Continuos Distillation Column	
Cost of stainless steel tower, Timmerhaus et al [1981]	
(excluding trays + connections)	$40,000.00
Cost of stainless steel tower by correlation Mulet et al [1981]	
(excluding trays + connections)	$35,872.72
Cost of 25 stainless steel trays, Timmerhaus et al [1981]	$20,000.00
Cost of 25 stainless steel trays by correlation Mulet et al [1981]	$25,197.68
Cost for reboiler with above area, Timmerhaus et al [1981]	$2,000.00
Cost for condenser with above area, Timmerhaus et al [1981]	$1,500.00
Total Cost for Distillation Column (including reboiler and Condenser)	$64,570.40
- Batch Crystallizer	
Cost of Steel Crystallizer, Timmerhaus et al [1981] (x2)	$35,000.00
Total Equipment Costs[1979]	**$99,570.40**
-Conversion to Present Day Value	
1979 Cost index (1st quarter), Chemical Engineering [1979]	576.5
2001 Cost index (1st quarter), Chemical Engineering [2001]	1089.4
Total Equipment Costs[2001], @ R8.00 to the dollar	**R 1,524,064.45**

C.1.2. Fixed Capital Investment Costs

Table C-2: Estimation of Fixed Capital Investment as suggested by Timmerhaus et al [1980]

Item	% of Total	Costs
Direct Costs		
Purchased Equipment	28	R 1,524,064.45
Purchased Equipment Installation	11	R 594,385.14
Instrumentation + Controls(Installed)	4	R 198,128.38
Piping (Installed)	9	R 472,459.98
Electrical (Installed)	11	R 609,625.78
Service Facilities	6	R 304,812.89
Total Direct Costs		R 3,703,476.62
Indirect Costs		
Engineering and Supervision	8	R 457,219.34
Total Direct Costs + Indirect Costs		R 4,160,695.95
Contingency Costs	8	R 416,069.60
Fixed Capital Investment		R 4,576,765.55
Working Capital	15	R 823,817.80
Total Capital Investment		**R 5,400,583.35**

C.2 Operating Cost Estimation

Table C-3: Estimation of Operating Costs as suggested by Brennen [1998]

Products		Butyric Acid and Isobutyric Acid	
Plant Capacity	t/yr	10 000	
Total fixed Capital		R 5,400,583.35	
Product selling price			
Butyric Acid	R/t	R 7,260.00	
Isobutyric Acid	R/t	R 12,400.00	
Production Costs			Annual Cost
Raw Materials	Unit usage unit/yr.*	Unit Costs R/unit * *	
	0	0	0
Utilities	Unit usage, unit/yr. *	Unit Costs ,R/unit	
Steam	27512	15.3	R 421,108.07
Electricity	1965132	0.23	R 451,980.42
Cooling Water	222294413	0.0006	R 136,044.18
Total Utilities Cost			R 1,009,132.67
Labour	Number	Salary, R/yr.	
Operators	2	100 000	
General Labour	4	60 000	R 440,000.00
Insurance (1% of fixed capital)			R 54,005.83
Non-Manufacturing Costs			
Administration (includes packaging) (3% of production costs)			R 45,094.16
Selling Expenses (10% of production Costs)			R 150,313.85
Total Operating Costs			**R 1,698,546.51**

* Calculated from energy balances obtained by Hysys simulations

** Utility costs as given by Timmerhaus et al [1981]

C.3 Evaluation of Project Profitability

Table C-4: Cash Flow Statement

Code	Item / Time (yr.)	0	1	2	3
A	Capital Investment	-4,576,765.55			
B	Working Capital	-823,817.80			
C	Sales [1]		47,640,000.00	47,640,000.00	47,640,000.00
D	Operating Costs [2]		1,698,546.51	1,698,546.51	1,698,546.51
E = C-D	Net Income before Tax		45,941,453.49	45,941,453.49	45,941,453.49
F	Tax Allowances		1,601,867.94	1,373,029.66	1,144,191.39
G = E-F	Taxable income		44,339,585.54	44,568,423.82	44,797,262.10
H	Income Tax @ 35% p.a.		-15,518,854.94	-15,598,948.34	-15,679,041.73
I =0.35(F-E)	Tax saved on excess allow		0.00		
J =E+H+I	Net Income after tax		30,422,598.55	30,342,505.15	30,262,411.75
K= A+B+J	Net Cash Flow	-5,400,583.35	30,422,598.55	30,342,505.15	30,262,411.75

Table C-4...continued

Code	Item / Time (yr.)	4	5
A	Capital Investment		
B	Working Capital		
C	Sales	47,640,000.00	47,640,000.00
D	Operating Costs	1,698,546.51	1,698,546.51
E = C-D	Net Income before Tax	45,941,453.49	45,941,453.49
F	Tax Allowances		
G = E-F	Taxable income	45,941,453.49	45,941,453.49
H	Income Tax @ 35% p.a.	-16,079,508.72	-16,079,508.72
I =0.35(F-E)	Tax saved on excess allow		
J =E+H+I	Net Income after tax	29,861,944.77	29,861,944.77
K= A+B+J	Net Cash Flow	29,861,944.77	29,861,944.77
Payback Period		0.18	

Notes

1. Sales determined at 80% extractable volume. 4% inflation rate used to account for changes in selling price.
2. Operating Costs as determined in Table C-3. 3% internal inflation rate used to account for changes over five year period.